

# An optimal control model for COVID-19, zika, dengue, and chikungunya co-dynamics with reinfection

Andrew Omame<sup>1,2</sup>  | Mary Ele Isah<sup>2</sup> | Mujahid Abbas<sup>3,4</sup>

<sup>1</sup>Department of Mathematics, Federal University of Technology, Owerri, Nigeria

<sup>2</sup>Abdus Salam School of Mathematical Sciences, Government College University, Lahore, Pakistan

<sup>3</sup>Department of Mathematics, Government College University, Lahore, Pakistan

<sup>4</sup>Department of Medical Research, China Medical University Hospital, China Medical University, Taichung, Taiwan

## Correspondence

Andrew Omame, Department of Mathematics, Federal University of Technology, Owerri, Nigeria.  
Email: [omame2020@gmail.com](mailto:omame2020@gmail.com), [andrew.omame@futo.edu.ng](mailto:andrew.omame@futo.edu.ng)

## Funding information

None

## Abstract

The co-circulation of different emerging viral diseases is a big challenge from an epidemiological point of view. The similarity of symptoms, cases of virus co-infection, and cross-reaction can mislead in the diagnosis of the disease. In this article, a new mathematical model for COVID-19, zika, chikungunya, and dengue co-dynamics is developed and studied to assess the impact of COVID-19 on zika, dengue, and chikungunya dynamics and vice-versa. The local and global stability analyses are carried out. The model is shown to undergo a backward bifurcation under a certain condition. Global sensitivity analysis is also performed on the parameters of the model to determine the most dominant parameters. If the zika-related reproduction number  $\mathcal{R}_{0Z}$  is used as the response function, then important parameters are: the effective contact rate for vector-to-human transmission of zika ( $\beta_2^h$ , which is positively correlated), the human natural death rate ( $\vartheta^h$ , positively correlated), and the vector recruitment rate ( $\Psi^v$ , also positively correlated). In addition, using the class of individuals co-infected with COVID-19 and zika ( $I_{CZ}^h$ ) as response function, the most dominant parameters are: the effective contact rate for COVID-19 transmission ( $\beta_1$ , positively correlated), the effective contact rate for vector-to-human transmission of zika ( $\beta_2^h$ , positively correlated). To control the co-circulation of all the diseases adequately under an endemic setting, time dependent controls in the form of COVID-19, zika, dengue, and chikungunya preventions are incorporated into the model and analyzed using the Pontryagin's principle. The model is fitted to real COVID-19, zika, dengue, and chikungunya datasets for Espirito Santo (a city with the co-circulation of all the diseases), in Brazil and projections made for the cumulative cases of each of the diseases. Through simulations, it is shown that COVID-19 prevention could greatly reduce the burden of co-infections with zika, dengue, and chikungunya. The negative impact of the COVID-19 pandemic on the control of the arbovirus diseases is also highlighted. Furthermore, it is observed that prevention controls for zika, dengue, and chikungunya can significantly reduce the burden of co-infections with COVID-19.

## KEYWORDS

chikungunya, co-infection, COVID-19, dengue, optimal control, zika

## 1 | INTRODUCTION

Arbovirus diseases (ARBOD) transmitted by *Aedes aegypti* such as zika, dengue, and chikungunya and the concurrent circulation of these diseases are major public health concerns in tropical and subtropical regions. The coronavirus disease 2019 (COVID-19) caused by the “severe acute respiratory syndrome coronavirus” 2 (SARS-CoV-2) has posed more serious challenges in territories with overlapping epidemics, raising more demands for health care needs.<sup>1</sup> COVID-19 and ARBOD epidemics co-occurrence has become a matter of great concern to government and health agencies. Overlapping clinical and laboratory symptoms between COVID-19 and ARBOD pose another challenge during diagnosis. COVID-19, zika, dengue, and chikungunya can present identical clinical features at the early stages of infection.<sup>2</sup> Misdiagnosis cause inappropriate care and treatment of the right disease which could lead to worst clinical outcomes.<sup>1,3</sup> do Rosario and de Siqueira<sup>4</sup> have observed that arboviral infections can also have life-threatening implications, such as Guillain–Barré syndrome (GBS), encephalitis, myelitis, and others.

It is worth mentioning that arboviruses have a seasonal trend of incidence, which usually surge at the beginning of the year between March and April.<sup>5</sup> Interestingly, studies have confirmed that just after 2015–2016 zika epidemic in Brazil, the incidence of both zika and dengue infections has greatly reduced. Soon after this, the number of dengue cases kept on increasing significantly throughout 2019 and in the early period of 2020, accounting for over two million cases.<sup>6</sup> According to the Brazilian Ministry of Health, as of September 19, 2020, the number of probable cases of dengue, chikungunya and zika were 931,903, 71,698 and 6705, respectively (see Figure 1).<sup>7</sup> In 2019 alone, more than 780 dengue and over 90 chikungunya/zika related deaths were reported.<sup>8</sup> Surprisingly, there has been a great reduction in the number of arbovirus cases since March 2020 compared with 2019, due to gross under-reporting. The scenario coincided with the surge in SARS-CoV-2 cases in Brazil, which forced all health authorities to focus its full attention to test and deal with SARS-CoV-2. Thus, the reduction may be linked with the efforts carried out by the country’s authorities to cope with the COVID-19 pandemic.<sup>9</sup> The fact remains that, there has been an upsurge arboviral diseases (zika, dengue, and chikungunya) epidemic in Brazil. The COVID-19 pandemic has disturbed the diagnosis, treatment services, and vaccination campaigns for other diseases, thereby putting millions of lives at risk of infections.<sup>10</sup> In addition, the COVID-19 pandemic also caused lack of access to humanitarian aid and also an increased pressure on health systems in zika/dengue/chikungunya-endemic countries, making it impossible to handle two or more simultaneous outbreaks due to lack of capacity in personnel and supplies.<sup>11</sup>

Clinical studies affirming the co-circulation of SARS-CoV-2 and the arboviruses in different geographical regions abound in the literature.<sup>12–14</sup> For instance, da Silva et al.<sup>12</sup> investigated the simultaneous circulation of DENV, CHIKV, ZIKV and SARS-CoV-2 in Brazil. They pointed out that the emergence of SARS-CoV-2 has intensified the need of creation of more public health laboratories as important measure of arbovirus diagnosis and prevention. Furthermore, they noted that the co-circulation of SARS-CoV-2 and arboviral infections in Brazil required the intensity of disease control strategies and effective surveillance programs. The authors in Reference 13 carried out a population based study on 176 febrile patients to investigate co-infections between COVID-19 and some selected arboviral infections in Guerrero, Mexico between 2020 and 2021. Their report shows apparent concurrent co-infections between COVID-19 and some arbovirus diseases (dengue, zika and chikungunya) in Guerrero, Mexico and further reveals that COVID-19 and arbovirus diseases produced “overlapping clinical manifestations” (i.e., fever, headache, fatigue, and myalgia), thus complicating the severity of co-infections. Other geographical regions such as India, Thailand, and Singapore faced this overlap of COVID-19 and arbovirus diseases between September and November 2020.<sup>14</sup>

A lot of models have been developed for the control of COVID-19. Asamoah et al.<sup>15</sup> studied the stability analysis of COVID-19 and assessed the impact of environment using data from Ghana. Simulations of the optimal control model shows that reinfection is possible after recovery and that “the strategy that cleans environmental surfaces with home based detergents is the most cost-effective strategy in the control of COVID-19 infection.” Nkwayep et al.<sup>16</sup> investigated short term forecasts of COVID-19 pandemics in Cameroon. They showed that facemask usage alone was not sufficient to control coronavirus disease. However, the pandemic could be effectively contained if strategies such as face-mask usage by individuals in public and the social distancing rules are combined and effectively adhered to. Wang et al.<sup>17</sup> developed an SEIR model to estimate the epidemic trends in Wuhan, assuming the prevention and control measures were either sufficient or insufficient to control the epidemic. The authors in Reference 18 carried out an optimal control model for COVID-19 with comprehensive cost-effectiveness analysis. They showed that practicing “physical or social distancing” protocols are the most cost-saving and effective control intervention in Saudi Arabia in the absence of vaccination. Kucharski et al.<sup>19</sup> proposed a stochastic model with data on cases of COVID-19 in Wuhan and international cases to

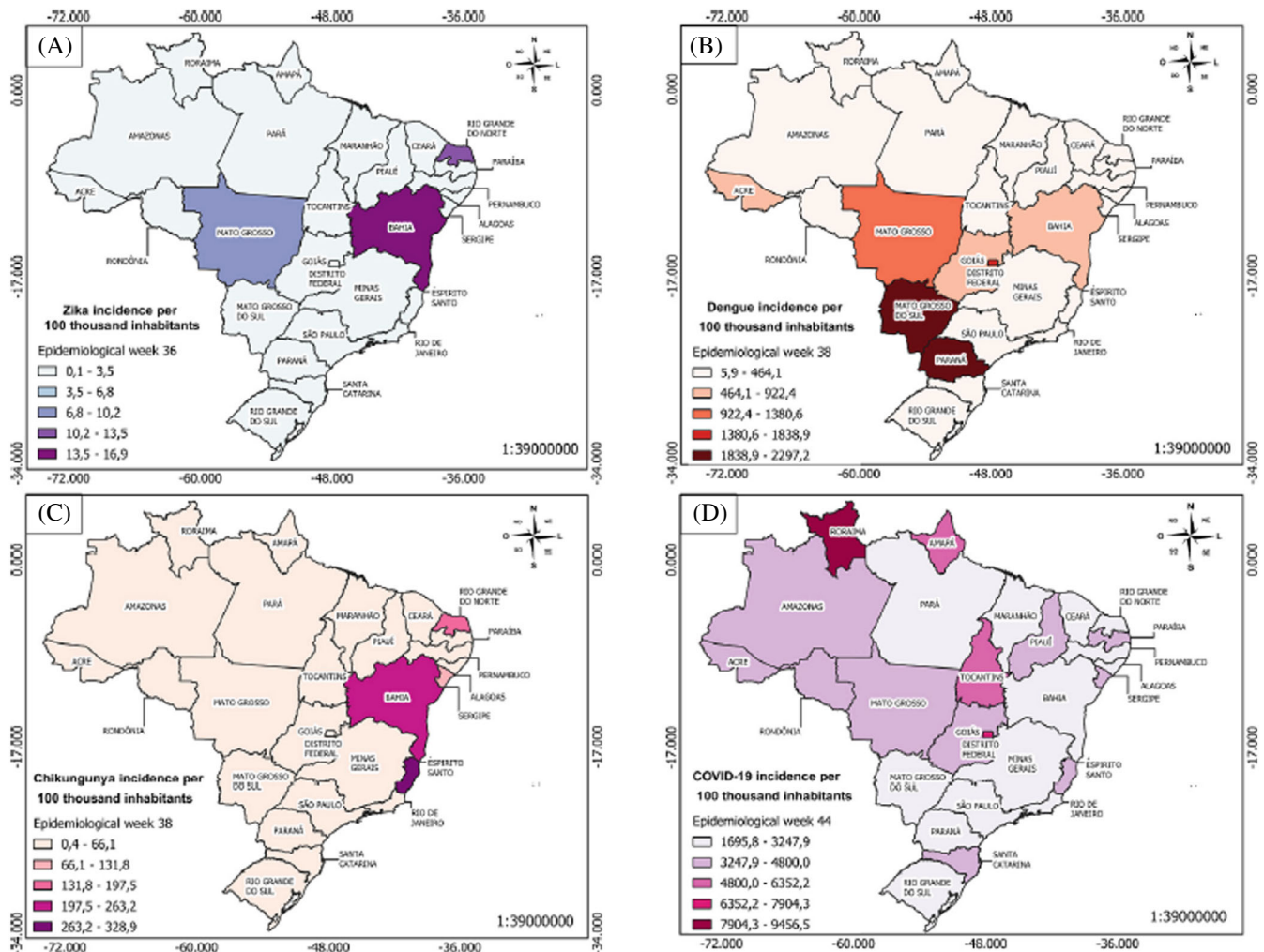


FIGURE 1 Incidence of (A) zika, (B) dengue, (C) chikungunya, and (D) COVID-19 in all Brazilian states. *Source:* References 7 and 12

estimate how the transmission varied over time between January and February in 2020. Ferguson et al.<sup>20</sup> pointed out that optimal control strategies such as home isolation of suspected cases, home quarantine of those living in the same household as suspected cases, and social distancing of the elderly and others at most risk of severe disease might greatly reduce peak healthcare demand and deaths. Maier and Brockmann<sup>21</sup> used a mathematical model to show that the distinctive subexponential increase of confirmed cases in mainland China could be explained as a direct consequence of containment policies that effectively reduce the population of susceptible individuals.

To understand the dynamics of co-interaction between diseases, a lot of models have been proposed in the literature.<sup>22-28</sup> The authors in Reference 22 considered a dynamical model for SARS-CoV-2 and zika virus, incorporating the assumption of incident co-infection with the two diseases. They showed that under this scenario, the qualitative behavior of the complete co-infection model is not driven by that of the sub-models. They also investigated the Lyapunov stability of both infection-free and endemic equilibria when the causes of backward bifurcation are removed from the model. Omame and Okuonghae<sup>23</sup> used optimal control to investigate the co-interaction of oncogenic human papillomavirus and tuberculosis. Using optimal control, Bonyah et al.<sup>24</sup> analyzed a co-dynamical model for dengue fever and zika virus. Numerical experiments on the model showed that, to effectively reduce the co-circulation of zika and dengue at the community level, the control measures must combine both prevention and treatment for each of the diseases concurrently. Furthermore, the authors in Reference 25 investigated COVID-19 and dengue co-infection model with optimal control, using Brazil as a case study. They showed that dengue-only preventive strategy or COVID-19 only preventive control would be sufficient to combat either of the diseases. Hezam<sup>26</sup> recently developed a novel dynamical optimal control model for COVID-19 and chikungunya outbreaks, using real data from Yemen. The results obtained confirm that the strategy, which provides resources to prevent the transmission of chikungunya and provides sufficient resources for

testing, applying average social distancing, and quarantining the affected individuals, has a significant impact in flattening the infection curves and is the most suitable strategy in Yemen. The authors in Reference 27 studied a model for the dynamics of dengue, zika, and chikungunya. They examined the impact of seasonality and local weather variability on the dynamics of the three diseases. Nwankwo and Okuonghae<sup>28</sup> studied a model for the co-dynamics of HIV and syphilis, and showed the importance of syphilis treatment in reducing HIV-syphilis co-infection.

Our contribution in this article is highlighted as follows:

1. A new mathematical model for COVID-19, zika, dengue, and chikungunya co-dynamics with optimal control analysis is proposed and the impact of COVID-19 on the dynamics and spread of arbovirus diseases and as well as on their co-infection is assessed.
2. The model is qualitatively analyzed for stability (local and global) as well as the occurrence of backward bifurcation.
3. Time dependent controls are incorporated into the model and analyzed with the help of the Pontryagin's principle.
4. Global sensitivity analysis is carried out to determine the parameters which are most influential on the dynamics of the diseases using the associated reproduction numbers and the co-infected classes as response functions.
5. The entire model is simulated to assess the impact of various control measures. We believe that this work will open some new avenues for further research in this direction.

## 2 | MODEL FORMULATION

At any time  $t$ , the total human population  $\mathcal{N}^h(t)$  consists of the following epidemiological states: susceptible humans  $S^h(t)$ , infectious humans with COVID-19  $I_C^h(t)$ , infectious humans with zika virus  $I_Z^h(t)$ , infectious humans with dengue virus  $I_D^h(t)$ , infectious humans with chikungunya  $I_K^h(t)$ , humans co-infected with COVID-19 and zika virus  $I_{CZ}^h(t)$ , humans co-infected with COVID-19 and dengue virus  $I_{CD}^h(t)$ , humans co-infected with COVID-19 and chikungunya  $I_{CK}^h(t)$ , with  $\mathcal{R}_C^h(t)$ ,  $\mathcal{R}_Z^h(t)$ ,  $\mathcal{R}_D^h(t)$ ,  $\mathcal{R}_K^h(t)$  denoting humans who have recovered from COVID-19, zika virus, dengue virus, and chikungunya, respectively. The total vector population, at any time  $t$ ,  $\mathcal{N}^v(t)$  consists of the following states:  $S^v(t)$ ,  $I_Z^v(t)$ ,  $I_D^v(t)$ ,  $I_K^v(t)$ , which denotes susceptible vectors, vectors infected with zika virus, those infected with dengue virus and those infected with chikungunya, respectively. Susceptible humans acquire COVID-19 at the rate  $\frac{\beta_1 I_C^h}{\mathcal{N}^h}$ . Individuals in this state also acquire zika either from infected vectors or from infected humans at the rate  $\frac{\beta_2(I_Z^h + I_{CZ}^h) + \beta_2^v I_Z^v}{\mathcal{N}^h}$ . Human-human-transmission of zika has been established in the literature.<sup>27</sup> Furthermore, susceptible humans acquire dengue virus or chikungunya virus at the rates  $\frac{\beta_3^v I_D^v}{\mathcal{N}^h}$  and  $\frac{\beta_4^v I_K^v}{\mathcal{N}^h}$ , respectively. Individuals in this group suffer natural death (just as those in other epidemiological groups) at the rate  $\vartheta^h$ . Humans who have recovered from COVID-19, zika, dengue, and chikungunya get reinfected and fall back to the respective infected classes. To avoid model complexity and because of insufficient biological evidences to show co-infection with all of the four diseases, it is only assumed co-infection between COVID-19 and each of the three diseases. This enables us adequately to assess the impact of COVID-19 on the dynamics of any of the three diseases and vice versa.

$$\begin{aligned} \frac{dS^h}{dt} &= \Psi^h - \left( \frac{\beta_1 I_C^h}{\mathcal{N}^h} + \frac{\beta_2(I_Z^h + I_{CZ}^h) + \beta_2^v I_Z^v}{\mathcal{N}^h} + \frac{\beta_3^v I_D^v}{\mathcal{N}^h} + \frac{\beta_4^v I_K^v}{\mathcal{N}^h} + \vartheta^h \right) S^h, \\ \frac{dI_C^h}{dt} &= \frac{\beta_1 I_C^h}{\mathcal{N}^h} (S^h + \mathcal{R}_C^h + \mathcal{R}_Z^h + \mathcal{R}_D^h + \mathcal{R}_K^h) - (\eta_C + \zeta_C + \vartheta^h) I_C^h - \frac{\beta_2(I_Z^h + I_{CZ}^h) + \beta_2^v I_Z^v}{\mathcal{N}^h} I_C^h - \frac{\beta_3^v I_D^v}{\mathcal{N}^h} I_C^h \\ &\quad - \frac{\beta_4^v I_K^v}{\mathcal{N}^h} I_C^h + \zeta_Z I_{CZ}^h + \zeta_D I_{CD}^h + \zeta_K I_{CK}^h, \\ \frac{dI_Z^h}{dt} &= \frac{\beta_2(I_Z^h + I_{CZ}^h) + \beta_2^v I_Z^v}{\mathcal{N}^h} (S^h + \mathcal{R}_C^h + \mathcal{R}_Z^h + \mathcal{R}_D^h + \mathcal{R}_K^h) - (\eta_Z + \zeta_Z + \vartheta^h) I_Z^h - \frac{\beta_1 I_C^h}{\mathcal{N}^h} I_Z^h + \zeta_C I_{CZ}^h, \\ \frac{dI_D^h}{dt} &= \frac{\beta_3^v I_D^v}{\mathcal{N}^h} (S^h + \mathcal{R}_C^h + \mathcal{R}_Z^h + \mathcal{R}_D^h + \mathcal{R}_K^h) - (\eta_D + \zeta_D + \vartheta^h) I_D^h - \frac{\beta_1 I_C^h}{\mathcal{N}^h} I_D^h + \zeta_C I_{CD}^h, \\ \frac{dI_K^h}{dt} &= \frac{\beta_4^v I_K^v}{\mathcal{N}^h} (S^h + \mathcal{R}_C^h + \mathcal{R}_Z^h + \mathcal{R}_D^h + \mathcal{R}_K^h) - (\eta_K + \zeta_K + \vartheta^h) I_K^h - \frac{\beta_1 I_C^h}{\mathcal{N}^h} I_K^h + \zeta_C I_{CK}^h, \\ \frac{dI_{CZ}^h}{dt} &= \frac{\beta_2(I_Z^h + I_{CZ}^h) + \beta_2^v I_Z^v}{\mathcal{N}^h} I_C^h + \frac{\beta_1 I_C^h}{\mathcal{N}^h} I_Z^h - (\eta_C + \eta_Z + \zeta_C + \zeta_Z + \vartheta^h) I_{CZ}^h, \end{aligned}$$

$$\begin{aligned}
\frac{dI_{CD}^h}{dt} &= \frac{\beta_3^h I_D^v}{\mathcal{N}^h} I_C^h + \frac{\beta_1^h I_C^h}{\mathcal{N}^h} I_D^h - (\eta_C + \eta_D + \zeta_C + \zeta_D + \vartheta^h) I_{CD}^h, \\
\frac{dI_{CK}^h}{dt} &= \frac{\beta_4^h I_K^v}{\mathcal{N}^h} I_C^h + \frac{\beta_1^h I_C^h}{\mathcal{N}^h} I_K^h - (\eta_C + \eta_K + \zeta_C + \zeta_K + \vartheta^h) I_{CK}^h, \\
\frac{dR_C^h}{dt} &= \zeta_C I_C^h - \left( \vartheta^h + \frac{\beta_1 I_C^h}{\mathcal{N}^h} + \frac{\beta_2(I_Z^h + I_{CZ}^h) + \beta_2^h I_Z^v}{\mathcal{N}^h} + \frac{\beta_3^h I_D^v}{\mathcal{N}^h} + \frac{\beta_4^h I_K^v}{\mathcal{N}^h} \right) R_C^h, \\
\frac{dR_Z^h}{dt} &= \zeta_Z I_Z^h - \left( \vartheta^h + \frac{\beta_1 I_C^h}{\mathcal{N}^h} + \frac{\beta_2(I_Z^h + I_{CZ}^h) + \beta_2^h I_Z^v}{\mathcal{N}^h} + \frac{\beta_3^h I_D^v}{\mathcal{N}^h} + \frac{\beta_4^h I_K^v}{\mathcal{N}^h} \right) R_Z^h, \\
\frac{dR_D^h}{dt} &= \zeta_D I_D^h - \left( \vartheta^h + \frac{\beta_1 I_C^h}{\mathcal{N}^h} + \frac{\beta_2(I_Z^h + I_{CZ}^h) + \beta_2^h I_Z^v}{\mathcal{N}^h} + \frac{\beta_3^h I_D^v}{\mathcal{N}^h} + \frac{\beta_4^h I_K^v}{\mathcal{N}^h} \right) R_D^h, \\
\frac{dR_K^h}{dt} &= \zeta_K I_K^h - \left( \vartheta^h + \frac{\beta_1 I_C^h}{\mathcal{N}^h} + \frac{\beta_2(I_Z^h + I_{CZ}^h) + \beta_2^h I_Z^v}{\mathcal{N}^h} + \frac{\beta_3^h I_D^v}{\mathcal{N}^h} + \frac{\beta_4^h I_K^v}{\mathcal{N}^h} \right) R_K^h, \\
\frac{dS^v}{dt} &= \Psi^v - \left( \frac{\beta_2^v(I_Z^h + I_{CZ}^h)}{\mathcal{N}^h} + \frac{\beta_3^v(I_D^h + I_{CD}^h)}{\mathcal{N}^h} + \frac{\beta_4^v(I_K^h + I_{CK}^h)}{\mathcal{N}^h} + \vartheta^v \right) S^v, \\
\frac{dI_Z^v}{dt} &= \frac{\beta_2^v(I_Z^h + I_{CZ}^h)}{\mathcal{N}^h} S^v - \vartheta^v I_Z^v, \\
\frac{dI_D^v}{dt} &= \frac{\beta_3^v(I_D^h + I_{CD}^h)}{\mathcal{N}^h} S^v - \vartheta^v I_D^v, \\
\frac{dI_K^v}{dt} &= \frac{\beta_4^v(I_K^h + I_{CK}^h)}{\mathcal{N}^h} S^v - \vartheta^v I_K^v.
\end{aligned} \tag{1}$$

### 3 | ANALYSIS OF THE MODEL

In this section, we qualitatively analyze the model (1) without controls. We begin with the following:

#### 3.1 | Positivity and boundedness of solutions

First, we show that the solutions of the system (1) are non-negative for all time  $t > 0$ .

**Theorem 1.** *The closed set  $\mathcal{Z} = \mathcal{Z}^h \times \mathcal{Z}^v$  with*

$$\begin{aligned}
\mathcal{Z}^h &= \{(S^h, I_C^h, I_Z^h, I_D^h, I_K^h, I_{CZ}^h, I_{CD}^h, I_{CK}^h, R_C^h, R_Z^h, R_D^h, R_K^h) \in \mathfrak{R}_+^{12} : \\
&\quad S^h + I_C^h + I_Z^h + I_D^h + I_K^h + I_{CZ}^h + I_{CD}^h + I_{CK}^h + R_C^h + R_Z^h + R_D^h + R_K^h \leq \frac{\Psi^h}{\vartheta^h}\}, \\
\mathcal{Z}^v &= \{(S^v, I_Z^v, I_D^v, I_K^v) \in \mathfrak{R}_+^4 : S^v + I_Z^v + I_D^v + I_K^v \leq \frac{\Psi^v}{\vartheta^v}\}
\end{aligned}$$

is positively invariant with respect to the model (1).

*Proof.* Adding all the equations corresponding to the human components of the system (1) gives

$$\frac{\mathcal{N}^h}{dt} = \Psi^h - \vartheta^h \mathcal{N}^h(t) - [\eta_C I_C^h + \eta_Z I_Z^h + \eta_K I_K^h + (\eta_C + \eta_Z) I_{CZ}^h + (\eta_C + \eta_D) I_{CD}^h + (\eta_C + \eta_K) I_{CK}^h]. \tag{2}$$

From (2), we have

$$\Psi^h - (\vartheta^h + 10\eta) \mathcal{N}^h \leq \frac{\mathcal{N}^h}{dt} \leq \Psi^h - \vartheta^h \mathcal{N}^h,$$

where  $\eta = \min\{\eta_C, \eta_Z, \eta_D, \eta_K\}$ .

The above inequality can be rewritten as

$$\frac{\mathcal{N}^h}{dt} \leq \Psi^h - \vartheta^h \mathcal{N}^h. \quad (3)$$

By applying the integrating factor method to the above inequality and on simplification, we obtain that

$$\mathcal{N}^h(t) \leq \frac{\Psi^h}{\vartheta^h} + \left( \mathcal{N}^h(0) - \frac{\Psi^h}{\vartheta^h} \right) e^{-\mu t}. \quad (4)$$

Therefore, the total human population,  $\mathcal{N}^h(t) \leq \frac{\Psi^h}{\vartheta^h}$  as  $t \rightarrow \infty$ . Similarly, it can be shown that  $\mathcal{N}^v(t) \leq \frac{\Psi^v}{\vartheta^v}$  as  $t \rightarrow \infty$ . Thus, the system (1) has the solution in  $\mathcal{Z}$  and hence the given system is positively invariant. ■

### 3.2 | The basic reproduction number of the model

The disease-free equilibrium (DFE) of the model (1) is obtained by setting the right-hand sides of the equations in the model (1) to zero and is given by

$$\begin{aligned} \psi_0 &= (S^{h*}, I_C^{h*}, I_Z^{h*}, I_D^{h*}, I_K^{h*}, I_{CZ}^{h*}, I_{CD}^{h*}, I_{CK}^{h*}, R_C^{h*}, R_Z^{h*}, R_D^{h*}, R_K^{h*}, S^{v*}, I_Z^{v*}, I_D^{v*}, I_K^{v*}) \\ &= \left( \frac{\Psi^h}{\vartheta^h}, 0, 0, 0, 0, 0, 0, 0, 0, 0, 0, 0, \frac{\Psi^v}{\vartheta^v}, 0, 0, 0 \right). \end{aligned}$$

The stability of the DFE is established by applying the next generation operator method<sup>32</sup> on the system (1). The transfer matrices are given by

$$F = \begin{pmatrix} \beta_1 & 0 & 0 & 0 & 0 & 0 & 0 & 0 & 0 & 0 \\ 0 & \beta_2 & 0 & 0 & \beta_2 & 0 & 0 & \beta_2^h & 0 & 0 \\ 0 & 0 & 0 & 0 & 0 & 0 & 0 & 0 & \beta_3^h & 0 \\ 0 & 0 & 0 & 0 & 0 & 0 & 0 & 0 & 0 & \beta_4^h \\ 0 & 0 & 0 & 0 & 0 & 0 & 0 & 0 & 0 & 0 \\ 0 & 0 & 0 & 0 & 0 & 0 & 0 & 0 & 0 & 0 \\ 0 & 0 & 0 & 0 & 0 & 0 & 0 & 0 & 0 & 0 \\ 0 & \frac{\beta_2^v S^{vv}}{\mathcal{N}^{hv}} & 0 & 0 & \frac{\beta_2^v S^{vv}}{\mathcal{N}^{hv}} & 0 & 0 & 0 & 0 & 0 \\ 0 & 0 & \frac{\beta_3^v S^{vv}}{\mathcal{N}^{hv}} & 0 & 0 & \frac{\beta_3^v S^{vv}}{\mathcal{N}^{hv}} & 0 & 0 & 0 & 0 \\ 0 & 0 & 0 & \frac{\beta_4^v S^{vv}}{\mathcal{N}^{hv}} & 0 & 0 & \frac{\beta_4^v S^{vv}}{\mathcal{N}^{hv}} & 0 & 0 & 0 \end{pmatrix}, \quad (5)$$

$$V = \begin{pmatrix} \mathcal{G}_1 & 0 & 0 & 0 & -\zeta_Z & -\zeta_D & -\zeta_K & 0 & 0 & 0 \\ 0 & \mathcal{G}_2 & 0 & 0 & -\zeta_C & 0 & 0 & 0 & 0 & 0 \\ 0 & 0 & \mathcal{G}_3 & 0 & 0 & -\zeta_C & 0 & 0 & 0 & 0 \\ 0 & 0 & 0 & \mathcal{G}_4 & 0 & 0 & -\zeta_C & 0 & 0 & 0 \\ 0 & 0 & 0 & 0 & \mathcal{G}_5 & 0 & 0 & 0 & 0 & 0 \\ 0 & 0 & 0 & 0 & 0 & \mathcal{G}_6 & 0 & 0 & 0 & 0 \\ 0 & 0 & 0 & 0 & 0 & 0 & \mathcal{G}_7 & 0 & 0 & 0 \\ 0 & 0 & 0 & 0 & 0 & 0 & 0 & \vartheta^v & 0 & 0 \\ 0 & 0 & 0 & 0 & 0 & 0 & 0 & 0 & \vartheta^v & 0 \\ 0 & 0 & 0 & 0 & 0 & 0 & 0 & 0 & 0 & \vartheta^v \end{pmatrix}, \quad (6)$$

where

$$\begin{aligned} \mathcal{G}_1 &= \eta_C + \zeta_C + \vartheta^h, & \mathcal{G}_2 &= \eta_Z + \zeta_Z + \vartheta^h, & \mathcal{G}_3 &= \eta_D + \zeta_D + \vartheta^h, & \mathcal{G}_4 &= \eta_K + \zeta_K + \vartheta^h, & \mathcal{G}_5 &= \eta_C + \eta_Z + \zeta_C + \zeta_Z + \vartheta^h, \\ \mathcal{G}_6 &= \eta_C + \eta_D + \zeta_C + \zeta_D + \vartheta^h, & \mathcal{G}_7 &= \eta_C + \eta_K + \zeta_C + \zeta_K + \vartheta^h. \end{aligned}$$

The basic reproduction number of the model (1) is given by  $\mathcal{R}_0 = \rho(FV^{-1}) = \max\{\mathcal{R}_{0C}, \mathcal{R}_{0Z}, \mathcal{R}_{0D}, \mathcal{R}_{0K}\}$ , where the associated reproduction number for COVID-19 denoted by  $\mathcal{R}_{0C}$  is given by

$$\mathcal{R}_{0C} = \frac{\beta_1}{G_1},$$

the associated reproduction number for zika denoted by  $\mathcal{R}_{0Z}$  is given by

$$\mathcal{R}_{0Z} = \frac{1}{2} \frac{\beta_2}{G_2} + \frac{1}{2} \sqrt{\left(\frac{\beta_2}{G_2}\right)^2 + \frac{4\beta_2^h \beta_2^v \Psi^v g^h}{\Psi^h g^{v2} G_2}}.$$

$\mathcal{R}_{0D}$  is the associated reproduction number for dengue which is given by

$$\mathcal{R}_{0D} = \sqrt{\frac{\beta_3^h \beta_3^v \Psi^v g^h}{\Psi^h g^{v2} G_3}},$$

and chikungunya associated reproduction number denoted by  $\mathcal{R}_{0K}$  is given by

$$\mathcal{R}_{0K} = \sqrt{\frac{\beta_4^h \beta_4^v \Psi^v g^h}{\Psi^h g^{v2} G_4}}.$$

If the reproduction number associated with the human-to-human zika transmission is  $\mathcal{R}_{0Z}^h = \frac{\beta_2}{G_2}$ , and the reproduction number associated with the vector-to-human-to-vector zika transmission is  $\mathcal{R}_{0Z}^v = \sqrt{\frac{\beta_2^h \beta_2^v \Psi^v g^h}{\Psi^h g^{v2} G_2}}$ , then the zika associated reproduction number can be rewritten as

$$\mathcal{R}_{0Z} = \frac{1}{2} \mathcal{R}_{0Z}^h + \frac{1}{2} \sqrt{(\mathcal{R}_{0Z}^h)^2 + 4(\mathcal{R}_{0Z}^v)^2}.$$

### 3.3 | Local asymptotic stability of the DFE of the model

**Theorem 2.** *The DFE,  $H_0$ , of the model (1) is locally asymptotically stable (LAS) if  $\mathcal{R}_0 < 1$ , and unstable if  $\mathcal{R}_0 > 1$ .*

*Proof.* The local stability of the model (1) is analyzed by the Jacobian matrix of the system (1) evaluated at the DFE,  $H_0$ , given by:

$$\begin{pmatrix} -g^h & -\beta_1 & -\beta_2 & 0 & 0 & -\beta_2 & 0 & 0 & 0 & 0 & 0 & 0 & 0 & -\beta_2^h & -\beta_3^h & -\beta_4^h \\ 0 & \beta_1 - G_1 & 0 & 0 & 0 & \zeta_Z & \zeta_D & \zeta_K & 0 & 0 & 0 & 0 & 0 & 0 & 0 & 0 \\ 0 & 0 & \beta_2 - G_2 & 0 & 0 & \beta_2 + \zeta_C & 0 & 0 & 0 & 0 & 0 & 0 & 0 & \beta_2^h & 0 & 0 \\ 0 & 0 & 0 & -G_3 & 0 & 0 & 0 & 0 & 0 & 0 & 0 & 0 & 0 & 0 & \beta_3^h & 0 \\ 0 & 0 & 0 & 0 & -G_4 & 0 & 0 & 0 & 0 & 0 & 0 & 0 & 0 & 0 & 0 & \beta_4^h \\ 0 & 0 & 0 & 0 & 0 & -G_5 & 0 & 0 & 0 & 0 & 0 & 0 & 0 & 0 & 0 & 0 \\ 0 & 0 & 0 & 0 & 0 & 0 & -G_6 & 0 & 0 & 0 & 0 & 0 & 0 & 0 & 0 & 0 \\ 0 & 0 & 0 & 0 & 0 & 0 & 0 & -G_7 & 0 & 0 & 0 & 0 & 0 & 0 & 0 & 0 \\ 0 & \zeta_C & 0 & 0 & 0 & 0 & 0 & 0 & -g^h & 0 & 0 & 0 & 0 & 0 & 0 & 0 \\ 0 & 0 & \zeta_Z & 0 & 0 & 0 & 0 & 0 & 0 & -g^h & 0 & 0 & 0 & 0 & 0 & 0 \\ 0 & 0 & 0 & \zeta_D & 0 & 0 & 0 & 0 & 0 & 0 & -g^h & 0 & 0 & 0 & 0 & 0 \\ 0 & 0 & 0 & 0 & \zeta_K & 0 & 0 & 0 & 0 & 0 & 0 & -g^h & 0 & 0 & 0 & 0 \\ 0 & 0 & -\frac{\beta_2^v S^{vv}}{\mathcal{N}^{hs}} & -\frac{\beta_3^v S^{vv}}{\mathcal{N}^{hs}} & -\frac{\beta_4^v S^{vv}}{\mathcal{N}^{hs}} & -\frac{\beta_2^v S^{vv}}{\mathcal{N}^{hs}} & -\frac{\beta_3^v S^{vv}}{\mathcal{N}^{hs}} & -\frac{\beta_4^v S^{vv}}{\mathcal{N}^{hs}} & 0 & 0 & 0 & 0 & -g^v & 0 & 0 & 0 \\ 0 & 0 & \frac{\beta_2^v S^{vv}}{\mathcal{N}^{hs}} & 0 & 0 & \frac{\beta_2^v S^{vv}}{\mathcal{N}^{hs}} & 0 & 0 & 0 & 0 & 0 & 0 & 0 & -g^v & 0 & 0 \\ 0 & 0 & 0 & \frac{\beta_3^v S^{vv}}{\mathcal{N}^{hs}} & 0 & 0 & \frac{\beta_3^v S^{vv}}{\mathcal{N}^{hs}} & 0 & 0 & 0 & 0 & 0 & 0 & 0 & -g^v & 0 \\ 0 & 0 & 0 & 0 & \frac{\beta_4^v S^{vv}}{\mathcal{N}^{hs}} & 0 & 0 & \frac{\beta_4^v S^{vv}}{\mathcal{N}^{hs}} & 0 & 0 & 0 & 0 & 0 & 0 & 0 & -g^v \end{pmatrix}. \tag{7}$$

The eigenvalues are given by

$$l_1 = -G_5, \quad l_2 = -G_6, \quad l_3 = -G_7, \quad l_4 = -g^v, \quad l_5 = -g^h \quad (\text{with multiplicity of } 5), \tag{8}$$

and the solutions of the equations

$$(\lambda + \mathcal{G}_1(1 - \mathcal{R}_{0C})) = 0, \quad \lambda^2 + \left( \mathcal{G}_2 + \vartheta^v - \frac{\beta_2 S^{v*}}{\mathcal{N}^h} \right) \lambda + \vartheta^v \mathcal{G}_2(1 - \mathcal{R}_{0Z}^h - \mathcal{R}_{0Z}^{v2}) = 0, \quad (9)$$

and

$$\lambda^2 + (\mathcal{G}_3 + \vartheta^v) \lambda + \vartheta^v \mathcal{G}_3(1 - \mathcal{R}_{0D}^2) = 0, \quad \lambda^2 + (\mathcal{G}_4 + \vartheta^v) \lambda + \vartheta^v \mathcal{G}_4(1 - \mathcal{R}_{0K}^2) = 0. \quad (10)$$

Applying the Routh–Hurwitz criterion, the three equations in (9) and (10) will have roots with negative real parts if and only if  $\mathcal{R}_{0C} < 1$ ,  $\mathcal{R}_{0Z} < 1$ ,  $\mathcal{R}_{0D} < 1$ , and  $\mathcal{R}_{0K} < 1$ , respectively. Thus, the DFE,  $\mathcal{H}_0$  is LAS if  $\mathcal{R}_0 = \max\{\mathcal{R}_{0C}, \mathcal{R}_{0Z}, \mathcal{R}_{0D}, \mathcal{R}_{0K}\} < 1$ . ■

### 3.4 | Global asymptotic stability of the DFE of the model

The approach illustrated in Reference 33 is used to investigate the global asymptotic stability of the DFE of the co-infection model. In this section, we give two conditions which guarantee the global asymptotic stability of the disease-free state. First, system (1) must be written in the form:

$$\begin{aligned} \frac{dY}{dt} &= P(Y, \Omega), \\ \frac{d\Omega}{dt} &= Q(Y, \Omega), Q(Y, 0) = \mathbf{0}, \end{aligned} \quad (11)$$

where  $Y = (S^h(t), \mathcal{R}_C^h(t), \mathcal{R}_Z^h(t), \mathcal{R}_D^h(t), \mathcal{R}_K^h(t), S^v(t)) \in \mathbb{R}^6$  represents the number of uninfected components of the model (1) and  $\Omega = (I_C^h(t), I_Z^h(t), I_D^h(t), I_K^h(t), I_{CZ}^h(t), I_{CD}^h(t), I_{CK}^h(t), I_Z^v(t), I_D^v(t), I_K^v(t)) \in \mathbb{R}^{10}$  represents the number of infected components of the model.  $\mathcal{H}_0 = (Y^*, \mathbf{0})$  is the DFE of system (1).

The conditions (i) and (ii) below must be satisfied in order to guarantee local asymptotic stability:

- (i) For  $\frac{dY}{dt} = P(Y, \mathbf{0})$ ,  $Y^*$  is globally asymptotically stable (GAS).
- (ii)  $Q(Y, \Omega) = B\Omega - \hat{Q}(Y, \Omega)Y$ ,  $Q(Y, \Omega) \geq 0$ , where  $B = D_\Omega Q(Y^*, \mathbf{0})$  is an M-matrix (the off-diagonal elements of  $B$  are nonnegative).

If system (1) satisfies the above two conditions then the following theorem holds:

**Theorem 3.** *The fixed point  $\mathcal{H}_0 = (Y^*, \mathbf{0})$  is a GAS equilibrium of (1) provided that  $\mathcal{R}_0 < 1$  and that assumptions (i) and (ii) are satisfied.*

*Proof.*

$$\frac{dY}{dt} = P(Y, \Omega) = \begin{pmatrix} \Psi^h - \left( \frac{\beta_1 I_C^h}{\mathcal{N}^h} + \frac{\beta_2(I_Z^h + I_{CZ}^h) + \beta_2^h I_Z^v}{\mathcal{N}^h} + \frac{\beta_3^h I_D^v}{\mathcal{N}^h} + \frac{\beta_4^h I_K^v}{\mathcal{N}^h} + \vartheta^h \right) S^h \\ \zeta_C I_C^h - \left( \vartheta^h + \frac{\beta_1 I_C^h}{\mathcal{N}^h} + \frac{\beta_2(I_Z^h + I_{CZ}^h) + \beta_2^h I_Z^v}{\mathcal{N}^h} + \frac{\beta_3^h I_D^v}{\mathcal{N}^h} + \frac{\beta_4^h I_K^v}{\mathcal{N}^h} \right) \mathcal{R}_C^h \\ \zeta_Z I_Z^h - \left( \vartheta^h + \frac{\beta_1 I_C^h}{\mathcal{N}^h} + \frac{\beta_2(I_Z^h + I_{CZ}^h) + \beta_2^h I_Z^v}{\mathcal{N}^h} + \frac{\beta_3^h I_D^v}{\mathcal{N}^h} + \frac{\beta_4^h I_K^v}{\mathcal{N}^h} \right) \mathcal{R}_Z^h \\ \zeta_D I_D^h - \left( \vartheta^h + \frac{\beta_1 I_C^h}{\mathcal{N}^h} + \frac{\beta_2(I_Z^h + I_{CZ}^h) + \beta_2^h I_Z^v}{\mathcal{N}^h} + \frac{\beta_3^h I_D^v}{\mathcal{N}^h} + \frac{\beta_4^h I_K^v}{\mathcal{N}^h} \right) \mathcal{R}_D^h \\ \zeta_K I_K^h - \left( \vartheta^h + \frac{\beta_1 I_C^h}{\mathcal{N}^h} + \frac{\beta_2(I_Z^h + I_{CZ}^h) + \beta_2^h I_Z^v}{\mathcal{N}^h} + \frac{\beta_3^h I_D^v}{\mathcal{N}^h} + \frac{\beta_4^h I_K^v}{\mathcal{N}^h} \right) \mathcal{R}_K^h \\ \Psi^v - \left( \frac{\beta_2^v(I_Z^h + I_{CZ}^h)}{\mathcal{N}^h} + \frac{\beta_3^v(I_D^h + I_{CD}^h)}{\mathcal{N}^h} + \frac{\beta_4^v(I_K^h + I_{CK}^h)}{\mathcal{N}^h} + \vartheta^v \right) S^v \end{pmatrix}, \quad (12)$$

$$P(Y, \mathbf{0}) = \begin{pmatrix} \Psi^h - \vartheta^h S^h \\ 0 \\ 0 \\ 0 \\ 0 \\ \Psi^v - \vartheta^v S^v \end{pmatrix}, \quad (13)$$

$Q(Y, \Omega)$

$$= \begin{pmatrix} \frac{\beta_1 I_C^h}{N^h} (S^h + R_C^h + R_Z^h + R_D^h + R_K^h) - (\eta_C + \zeta_C + \vartheta^h) I_C^h - \frac{\beta_2 (I_Z^h + I_{CZ}^h) + \beta_2^h I_Z^h}{N^h} I_C^h - \frac{\beta_3^h I_D^h}{N^h} I_C^h - \frac{\beta_4^h I_K^h}{N^h} I_C^h + \zeta_Z I_{CZ}^h + \zeta_D I_{CD}^h + \zeta_K I_{CK}^h \\ \frac{\beta_2 (I_Z^h + I_{CZ}^h) + \beta_2^h I_Z^h}{N^h} (S^h + R_C^h + R_Z^h + R_D^h + R_K^h) - (\eta_Z + \zeta_Z + \vartheta^h) I_Z^h - \frac{\beta_1 I_C^h}{N^h} I_Z^h + \zeta_C I_{CZ}^h \\ \frac{\beta_3^h I_D^h}{N^h} (S^h + R_C^h + R_Z^h + R_D^h + R_K^h) - (\eta_D + \zeta_D + \vartheta^h) I_D^h - \frac{\beta_1 I_C^h}{N^h} I_D^h + \zeta_C I_{CD}^h \\ \frac{\beta_4^h I_K^h}{N^h} (S^h + R_C^h + R_Z^h + R_D^h + R_K^h) - (\eta_K + \zeta_K + \vartheta^h) I_K^h - \frac{\beta_1 I_C^h}{N^h} I_K^h + \zeta_C I_{CK}^h \\ \frac{\beta_2 (I_Z^h + I_{CZ}^h) + \beta_2^h I_Z^h}{N^h} I_C^h + \frac{\beta_1 I_C^h}{N^h} I_Z^h - (\eta_C + \eta_Z + \zeta_C + \zeta_Z + \vartheta^h) I_{CZ}^h \\ \frac{\beta_3^h I_D^h}{N^h} I_C^h + \frac{\beta_1 I_C^h}{N^h} I_D^h - (\eta_C + \eta_D + \zeta_C + \zeta_D + \vartheta^h) I_{CD}^h \\ \frac{\beta_4^h I_K^h}{N^h} I_C^h + \frac{\beta_1 I_C^h}{N^h} I_K^h - (\eta_C + \eta_K + \zeta_C + \zeta_K + \vartheta^h) I_{CK}^h \\ \frac{\beta_2^v (I_Z^h + I_{CZ}^h)}{N^h} S^v - \vartheta^v I_Z^v \\ \frac{\beta_3^v (I_D^h + I_{CD}^h)}{N^h} S^v - \vartheta^v I_D^v \\ \frac{\beta_4^v (I_K^h + I_{CK}^h)}{N^h} S^v - \vartheta^v I_K^v \end{pmatrix}$$

$$B = D_\Omega Q(Y^*, \mathbf{0}) = \begin{pmatrix} \beta_1 - \mathcal{G}_1 & 0 & 0 & 0 & \zeta_Z & \zeta_D & \zeta_K & 0 & 0 & 0 \\ 0 & \beta_2 - \mathcal{G}_2 & 0 & 0 & \beta_2 + \zeta_C & 0 & 0 & \beta_2^h & 0 & 0 \\ 0 & 0 & -\mathcal{G}_3 & 0 & 0 & 0 & 0 & 0 & \beta_3^h & 0 \\ 0 & 0 & 0 & -\mathcal{G}_4 & 0 & 0 & 0 & 0 & 0 & \beta_4^h \\ 0 & 0 & 0 & 0 & -\mathcal{G}_5 & 0 & 0 & 0 & 0 & 0 \\ 0 & 0 & 0 & 0 & 0 & -\mathcal{G}_6 & 0 & 0 & 0 & 0 \\ 0 & 0 & 0 & 0 & 0 & 0 & -\mathcal{G}_7 & 0 & 0 & 0 \\ 0 & \frac{\beta_2^v S^{v*}}{N^h} & 0 & 0 & \frac{\beta_2^v S^{v*}}{N^h} & 0 & 0 & -\vartheta^v & 0 & 0 \\ 0 & 0 & \frac{\beta_3^v S^{v*}}{N^h} & 0 & 0 & \frac{\beta_3^v S^{v*}}{N^h} & 0 & 0 & -\vartheta^v & 0 \\ 0 & 0 & 0 & \frac{\beta_4^v S^{v*}}{N^h} & 0 & 0 & \frac{\beta_4^v S^{v*}}{N^h} & 0 & 0 & -\vartheta^v \end{pmatrix}$$

$$\hat{Q}(Y, \Omega) = B\Omega - Q(Y, \Omega) = \begin{pmatrix} \beta_1 \left( 1 - \frac{S^h + R_C^h + R_Z^h + R_D^h + R_K^h}{N^h} \right) + \frac{\beta_2 (I_Z^h + I_{CZ}^h) + \beta_2^h I_Z^h}{N^h} I_C^h + \frac{\beta_3^h I_D^h}{N^h} I_C^h + \frac{\beta_4^h I_K^h}{N^h} I_C^h \\ (\beta_2 (I_Z^h + I_{CZ}^h) + \beta_2^h I_Z^h) \left( 1 - \frac{S^h + R_C^h + R_Z^h + R_D^h + R_K^h}{N^h} \right) + \frac{\beta_1 I_C^h}{N^h} I_Z^h \\ \beta_3^h I_D^h \left( 1 - \frac{S^h + R_C^h + R_Z^h + R_D^h + R_K^h}{N^h} \right) + \frac{\beta_1 I_C^h}{N^h} I_D^h - \zeta_C I_{CD}^h \\ \beta_4^h I_K^h \left( 1 - \frac{S^h + R_C^h + R_Z^h + R_D^h + R_K^h}{N^h} \right) + \frac{\beta_1 I_C^h}{N^h} I_K^h - \zeta_C I_{CK}^h \\ - \frac{\beta_2 (I_Z^h + I_{CZ}^h) + \beta_2^h I_Z^h}{N^h} I_C^h - \frac{\beta_1 I_C^h}{N^h} I_Z^h \\ - \frac{\beta_3^h I_D^h}{N^h} I_C^h - \frac{\beta_1 I_C^h}{N^h} I_D^h \\ - \frac{\beta_4^h I_K^h}{N^h} I_C^h - \frac{\beta_1 I_C^h}{N^h} I_K^h \\ \beta_2^v (I_Z^h + I_{CZ}^h) \left( \frac{S^{v*}}{N^h} - \frac{S^v}{N^h} \right) \\ \beta_3^v (I_D^h + I_{CD}^h) \left( \frac{S^{v*}}{N^h} - \frac{S^v}{N^h} \right) \\ \beta_4^v (I_K^h + I_{CK}^h) \left( \frac{S^{v*}}{N^h} - \frac{S^v}{N^h} \right) \end{pmatrix}$$

It is observed that  $\hat{Q}(Y, \Omega) \not\geq \mathbf{0}$ . Hence, it follows from Reference 34 that the DFE is not GAS which shows the occurrence of a backward bifurcation in the system. We shall investigate this in the next section. ■

### 3.5 | Backward bifurcation analysis of the model

The phenomenon of backward bifurcation, which has been observed in several disease models, is typically characterized by the co-existence of a stable DFE and a stable endemic equilibrium when the associated reproduction number of the model is less than unity. The public health implication of the backward bifurcation phenomenon of model (1) is that, the

classical epidemiological requirement of having the reproduction number  $\mathcal{R}_0$  to be less than unity, although necessary, is no longer sufficient for the effective control of the diseases. In this section, the phenomenon of backward bifurcation in the model (1) is discussed. The following theorem is used to establish the presence of the backward bifurcation phenomenon for the model considered in this work.

**Theorem 4** (34). Consider the following system of ordinary differential equations with a parameter  $\phi$

$$\frac{dx}{dt} = f(x, \phi), \quad f : \mathbb{R}^n \times \mathbb{R} \rightarrow \mathbb{R} \text{ and } f \in C^2(\mathbb{R}^n \times \mathbb{R}), \tag{14}$$

where 0 is an equilibrium point of the system (i.e.,  $f(0, \phi) \equiv 0$  for all  $\phi$ ) and assume

- (A1)  $A = D_x f(0, 0) = \left( \frac{\partial f_i}{\partial x_j}(0, 0) \right)$ , which is the linearization matrix of the system (14) around the equilibrium 0 with  $\phi$  evaluated at 0, has simple eigenvalue equal to zero and other eigenvalues of  $A$  have negative real parts.
- (A2) Matrix  $A$  has a right eigenvector  $\varphi$  and a left eigenvector  $\delta$  (each corresponding to the zero eigenvalue).

Let  $f_k$  be the  $k$ th component of  $f$  and

$$a = \sum_{k,i,j=1}^n \delta_k \varphi_i \varphi_j \frac{\partial^2 f_k}{\partial x_i \partial x_j}(0, 0),$$

$$b = \sum_{k,i=1}^n \delta_k \varphi_i \frac{\partial^2 f_k}{\partial x_i \partial \phi}(0, 0).$$

The local dynamics of the system around 0 is completely determined by the sign of  $a$  and  $b$ .

- (i)  $a > 0, b > 0$ . When  $\phi < 0$  with  $|\phi| \ll 1$ , 0 is LAS and there exists a positive unstable equilibrium; when  $0 \leq \phi \ll 1$ , 0 is unstable and there exists a negative, LAS equilibrium.
- (ii)  $a < 0, b < 0$ . When  $\phi < 0$  with  $|\phi| \ll 1$ , 0 is unstable; when  $0 < \phi \ll 1$ , 0 is LAS equilibrium, and there exists a positive unstable equilibrium.
- (iii)  $a > 0, b < 0$ . When  $\phi < 0$  with  $|\phi| \ll 1$ , 0 is unstable and there exists an LAS negative equilibrium; when  $0 \leq \phi \ll 1$ , 0 is stable and a positive unstable equilibrium appears.
- (iv)  $a < 0, b > 0$ . When  $\phi$  changes from negative to positive, 0 changes its stability from stable to unstable. Correspondingly a negative unstable equilibrium becomes positive and LAS.

Particularly, if  $a > 0$  and  $b > 0$ , then a backward bifurcation occurs at  $\phi = 0$ .

For the model (1), we establish the results below:

**Theorem 5.** The model (1) exhibits backward bifurcation if the coefficient  $a$  defined below is positive

$$a = -\frac{2\beta_1\varphi_2\delta_2}{\mathcal{N}^{h*}}(\varphi_2 + \varphi_3 + \varphi_4 + \varphi_5) + \frac{2\beta_1[(\varphi_3\delta_6 + \varphi_4\delta_7 + \varphi_5\delta_8)\varphi_2 - (\varphi_3\delta_3 + \varphi_4\delta_4 + \varphi_5\delta_5)\varphi_2]}{\mathcal{N}^{h*}}$$

$$- \frac{2(\beta_2\varphi_3 + \beta_2^h\varphi_{14})\delta_3}{\mathcal{N}^{h*}}(\varphi_2 + \varphi_3 + \varphi_4 + \varphi_5) + \frac{2[(\beta_2\varphi_3 + \beta_2^h\varphi_{14})\varphi_2\delta_6 - (\beta_2\varphi_3 + \beta_2^h\varphi_{14})\varphi_2\delta_2]}{\mathcal{N}^{h*}}$$

$$- \frac{2\beta_3^h\varphi_{15}\delta_4}{\mathcal{N}^{h*}}(\varphi_2 + \varphi_3 + \varphi_4 + \varphi_5) + \frac{2[(\beta_3^h\varphi_{15}\delta_7 - \beta_3^h\varphi_{15}\delta_2)\varphi_2]}{\mathcal{N}^{h*}}$$

$$- \frac{2\beta_4^h\varphi_{16}\delta_5}{\mathcal{N}^{h*}}(\varphi_2 + \varphi_3 + \varphi_4 + \varphi_5) + \frac{2[(\beta_4^h\varphi_{16}\delta_8 - \beta_4^h\varphi_{16}\delta_2)\varphi_2]}{\mathcal{N}^{h*}}$$

$$- \frac{2(\beta_2^v\varphi_3\delta_{14} + \beta_3^v\varphi_4\delta_{15} + \beta_4^v\varphi_5\delta_{16})\mathcal{X}_{13}^*}{\mathcal{N}^{h*2}}(\varphi_1 + \varphi_2 + \varphi_3 + \varphi_4 + \varphi_5 + \varphi_9 + \varphi_{10} + \varphi_{11} + \varphi_{12} - \frac{\varphi_{13}\mathcal{N}^{h*}}{\mathcal{X}_{13}^*}).$$

*Proof.* Let

$$\mathcal{H}_e = (S^{h**}, I_C^{h**}, I_Z^{h**}, I_D^{h**}, I_K^{h**}, I_{CZ}^{h**}, I_{CD}^{h**}, I_{CK}^{h**}, \mathcal{R}_C^{h**}, \mathcal{R}_Z^{h**}, \mathcal{R}_D^{h**}, \mathcal{R}_K^{h**}, S^{v**}, I_Z^{v**}, I_D^{v**}, I_K^{v**})$$

denote an arbitrary endemic equilibrium of the model. We carry out the following change of variables as follows. Let

$$\begin{aligned} S^h &= x_1, I_C^h = x_2, I_Z^h = x_3, I_D^h = x_4, I_K^h = x_5, I_{CZ}^h = x_6, I_{CD}^h = x_7, I_{CK}^h = x_8, R_C^h = x_9, \\ R_Z^h &= x_{10}, R_D^h = x_{11}, R_K^h = x_{12}, S^v = x_{13}, I_Z^v = x_{14}, I_D^v = x_{15}, I_K^v = x_{16}, \end{aligned}$$

so that the model (1) can be represented in the form

$$\begin{aligned} \frac{dx_1}{dt} &= \Psi^h - \left( \frac{\beta_1 x_2}{\mathcal{N}^h} + \frac{\beta_2(x_3 + x_6) + \beta_2^h x_{14}}{\mathcal{N}^h} + \frac{\beta_3^h x_{15}}{\mathcal{N}^h} + \frac{\beta_4^h x_{16}}{\mathcal{N}^h} + \vartheta^h \right) x_1 : f_1, \\ \frac{dx_2}{dt} &= \frac{\beta_1 x_2}{\mathcal{N}^h} (x_1 + x_9 + x_{10} + x_{11} + x_{12}) - (\eta_C + \zeta_C + \vartheta^h) x_2 - \frac{\beta_2(x_3 + x_6) + \beta_2^h x_{14}}{\mathcal{N}^h} x_2 - \frac{\beta_3^h x_{15}}{\mathcal{N}^h} x_2 \\ &\quad - \frac{\beta_4^h x_{16}}{\mathcal{N}^h} x_2 + \zeta_Z x_6 + \zeta_D x_7 + \zeta_K x_8 : f_2, \\ \frac{dx_3}{dt} &= \frac{\beta_2(x_3 + x_6) + \beta_2^h x_{14}}{\mathcal{N}^h} (x_1 + x_9 + x_{10} + x_{11} + x_{12}) - (\eta_Z + \zeta_Z + \vartheta^h) x_3 - \frac{\beta_1 x_2}{\mathcal{N}^h} x_3 + \zeta_C x_6 : f_3, \\ \frac{dx_4}{dt} &= \frac{\beta_3^h x_{15}}{\mathcal{N}^h} (x_1 + x_9 + x_{10} + x_{11} + x_{12}) - (\eta_D + \zeta_D + \vartheta^h) x_4 - \frac{\beta_1 x_2}{\mathcal{N}^h} x_4 + \zeta_C x_7 : f_4, \\ \frac{dx_5}{dt} &= \frac{\beta_4^h x_{16}}{\mathcal{N}^h} (x_1 + x_9 + x_{10} + x_{11} + x_{12}) - (\eta_K + \zeta_K + \vartheta^h) x_5 - \frac{\beta_1 x_2}{\mathcal{N}^h} x_5 + \zeta_C x_8 : f_5, \\ \frac{dx_6}{dt} &= \frac{\beta_2(x_3 + x_6) + \beta_2^h x_{14}}{\mathcal{N}^h} x_2 + \frac{\beta_1 x_2}{\mathcal{N}^h} x_3 - (\eta_C + \eta_Z + \zeta_C + \zeta_Z + \vartheta^h) x_6 : f_6, \\ \frac{dx_7}{dt} &= \frac{\beta_3^h x_{15}}{\mathcal{N}^h} x_2 + \frac{\beta_1 x_2}{\mathcal{N}^h} x_4 - (\eta_C + \eta_D + \zeta_C + \zeta_D + \vartheta^h) x_7 : f_7, \\ \frac{dx_8}{dt} &= \frac{\beta_4^h x_{16}}{\mathcal{N}^h} x_2 + \frac{\beta_1 x_2}{\mathcal{N}^h} x_5 - (\eta_C + \eta_K + \zeta_C + \zeta_K + \vartheta^h) x_8 : f_8, \\ \frac{dx_9}{dt} &= \zeta_C x_2 - \left( \vartheta^h + \frac{\beta_1 x_2}{\mathcal{N}^h} + \frac{\beta_2(x_3 + x_6) + \beta_2^h x_{14}}{\mathcal{N}^h} + \frac{\beta_3^h x_{15}}{\mathcal{N}^h} + \frac{\beta_4^h x_{16}}{\mathcal{N}^h} \right) x_9 : f_9, \\ \frac{dx_{10}}{dt} &= \zeta_Z x_3 - \left( \vartheta^h + \frac{\beta_1 x_2}{\mathcal{N}^h} + \frac{\beta_2(x_3 + x_6) + \beta_2^h x_{14}}{\mathcal{N}^h} + \frac{\beta_3^h x_{15}}{\mathcal{N}^h} + \frac{\beta_4^h x_{16}}{\mathcal{N}^h} \right) x_{10} : f_{10}, \\ \frac{dx_{11}}{dt} &= \zeta_D x_4 - \left( \vartheta^h + \frac{\beta_1 x_2}{\mathcal{N}^h} + \frac{\beta_2(x_3 + x_6) + \beta_2^h x_{14}}{\mathcal{N}^h} + \frac{\beta_3^h x_{15}}{\mathcal{N}^h} + \frac{\beta_4^h x_{16}}{\mathcal{N}^h} \right) x_{11} : f_{11}, \\ \frac{dx_{12}}{dt} &= \zeta_K x_5 - \left( \vartheta^h + \frac{\beta_1 x_2}{\mathcal{N}^h} + \frac{\beta_2(x_3 + x_6) + \beta_2^h x_{14}}{\mathcal{N}^h} + \frac{\beta_3^h x_{15}}{\mathcal{N}^h} + \frac{\beta_4^h x_{16}}{\mathcal{N}^h} \right) x_{12} : f_{12}, \\ \frac{dx_{13}}{dt} &= \Psi^v - \left( \frac{\beta_2^v(x_3 + x_6)}{\mathcal{N}^h} + \frac{\beta_3^v(x_4 + x_7)}{\mathcal{N}^h} + \frac{\beta_4^v(x_5 + x_8)}{\mathcal{N}^h} + \vartheta^v \right) x_{13} : f_{13}, \\ \frac{dx_{14}}{dt} &= \frac{\beta_2^v(x_3 + x_6)}{\mathcal{N}^h} x_{13} - \vartheta^v x_{14} : f_{14}, \\ \frac{dx_{15}}{dt} &= \frac{\beta_3^v(x_4 + x_7)}{\mathcal{N}^h} x_{13} - \vartheta^v x_{15} : f_{15}, \\ \frac{dx_{16}}{dt} &= \frac{\beta_4^v(x_5 + x_8)}{\mathcal{N}^h} x_{13} - \vartheta^v x_{16} : f_{16}, \end{aligned} \tag{15}$$

where

$$\mathcal{N}^h = \sum_{i=1}^{12} x_i.$$

Consider the case when  $\mathcal{R}_0 = \max\{\mathcal{R}_{0C}, \mathcal{R}_{0Z}, \mathcal{R}_{0D}, \mathcal{R}_{0K}\} = 1$ . Without any loss of generality, suppose that  $\beta_3^h$  is chosen as a bifurcation parameter. Solving for  $\beta_3^h = \beta_3^{h*}$  from  $\mathcal{R}_{0D} = 1$  we have

$$\beta_3^h = \beta_3^{h*} = \frac{g^{v2} \mathcal{G}_3 \Psi^h}{\Psi^v g^h \beta_3^v}.$$

Evaluating the Jacobian of the system (15) at the DFE,  $J(\mathcal{H}_0)$ , and using the approach as given in Reference 34,  $J(\mathcal{H}_0)$  has a right eigenvector (linked with the zero eigenvalue of  $J(\mathcal{H}_0)$ ) given by  $\boldsymbol{\varphi} = [\varphi_1, \varphi_2, \varphi_3, \dots, \varphi_{16}]^T$ , where the components are

$$\begin{aligned} \varphi_1 &= -\frac{1}{g^h} [\beta_2 \varphi_3 + \beta_2^h \varphi_{14} + \beta_3^h \varphi_{15} + \beta_4^h \varphi_{16}] < 0, & \varphi_2 &= \varphi_2 > 0, & \varphi_3 &= \varphi_3 > 0, & \varphi_4 &= \frac{\beta_3^h}{g^v \mathcal{G}_3} > 0, \\ \varphi_5 &= \frac{\beta_4^h}{g^v \mathcal{G}_4} > 0, \varphi_6 = \varphi_7 = \varphi_8 = 0, & \varphi_9 &= \frac{\zeta_C \varphi_2}{g^h} > 0, & \varphi_{10} &= \frac{\zeta_Z \varphi_3}{g^h} > 0, & \varphi_{11} &= \frac{\zeta_D \beta_3^h}{g^v g^h \mathcal{G}_3} > 0, & \varphi_{12} &= \frac{\zeta_K \beta_4^h}{g^v g^h \mathcal{G}_4} > 0, \\ \varphi_{13} &= -\frac{1}{g^v} \left[ \frac{\beta_2^v \mathcal{S}^{v*}}{\mathcal{N}^{h*}} \varphi_3 + \frac{\beta_3^v \mathcal{S}^{v*}}{\mathcal{N}^{h*}} \varphi_4 + \frac{\beta_4^v \mathcal{S}^{v*}}{\mathcal{N}^{h*}} \varphi_5 \right] < 0, & \varphi_{14} &= \frac{\beta_2^v \mathcal{S}^{v*}}{g^v \mathcal{N}^{h*}} \varphi_3 > 0, & \varphi_{15} &= \frac{\mathcal{N}^{h*} \mathcal{G}_3}{\beta_3^h \beta_3^v \mathcal{S}^{v*}} > 0 & \varphi_{16} &= \frac{\mathcal{N}^{h*} \mathcal{G}_4}{\beta_4^h \beta_4^v \mathcal{S}^{v*}} > 0. \end{aligned}$$

The components of the left eigenvector of  $J(\mathcal{H}_0)|_{\beta_3^h = \beta_3^{h*}}$ ,  $\boldsymbol{\delta} = [\delta_1, \delta_2, \dots, \delta_{16}]$ , satisfying  $\boldsymbol{\varphi} \cdot \boldsymbol{\delta} = 1$  are

$$\begin{aligned} \delta_1 &= 0, & \delta_2 &= \delta_2 > 0, & \delta_3 &= \delta_3 > 0, & \delta_4 &= \frac{\beta_3^v \mathcal{S}^{v*}}{g^v \mathcal{G}_3 \mathcal{N}^{h*}} > 0, \\ \delta_5 &= \frac{\beta_4^v \mathcal{S}^{v*}}{g^v \mathcal{G}_4 \mathcal{N}^{h*}} > 0, & \delta_6 &= \frac{1}{\mathcal{G}_5} \left( (\beta_2 + \zeta_C) \delta_3 + \frac{\beta_2^h \beta_2^v \mathcal{S}^{v*}}{g^v \mathcal{N}^{h*}} \delta_3 \right) > 0 \\ \delta_7 &= \frac{\mathcal{G}_4}{\mathcal{G}_6 \beta_3^h} > 0, & \delta_8 &= \frac{\mathcal{G}_4}{\mathcal{G}_7 \beta_4^h} > 0, & \delta_9 &= \delta_{10} = \delta_{11} = \delta_{12} = \delta_{13} = 0, \\ \delta_{14} &= \frac{\beta_2^h}{g^v} \delta_3 > 0, & \delta_{15} &= \frac{\mathcal{N}^{h*} \mathcal{G}_3}{\beta_3^h \beta_3^v \mathcal{S}^{v*}} > 0 & \delta_{16} &= \frac{\mathcal{N}^{h*} \mathcal{G}_4}{\beta_4^h \beta_4^v \mathcal{S}^{v*}} > 0. \end{aligned}$$

The nonzero second partial derivatives of the functions  $f_i (i = 1, \dots, 16)$  are given in Appendix A.

From Theorem 4, and using the computed nonzero partial derivatives of  $f(x)$  (evaluated at the DFE,  $(\mathcal{H}_0)$ ), the associated bifurcation coefficients given below

$$a = \sum_{k,i,j=1}^{16} \delta_k \varphi_i \varphi_j \frac{\partial^2 f_k}{\partial x_i \partial x_j} (0, 0) \quad \text{and} \quad b = \sum_{k,i=1}^{16} \delta_k \varphi_i \frac{\partial^2 f_k}{\partial x_i \partial \beta_3^{h*}} (0, 0),$$

are computed by

$$\begin{aligned} a &= -\frac{2\beta_1 \varphi_2 \delta_2}{\mathcal{N}^{h*}} (\varphi_2 + \varphi_3 + \varphi_4 + \varphi_5) + \frac{2\beta_1 [(\varphi_3 \delta_6 + \varphi_4 \delta_7 + \varphi_5 \delta_8) \varphi_2 - (\varphi_3 \delta_3 + \varphi_4 \delta_4 + \varphi_5 \delta_5) \varphi_2]}{\mathcal{N}^{h*}} \\ &\quad - \frac{2(\beta_2 \varphi_3 + \beta_2^h \varphi_{14}) \delta_3}{\mathcal{N}^{h*}} (\varphi_2 + \varphi_3 + \varphi_4 + \varphi_5) + \frac{2[(\beta_2 \varphi_3 + \beta_2^h \varphi_{14}) \varphi_2 \delta_6 - (\beta_2 \varphi_3 + \beta_2^h \varphi_{14}) \varphi_2 \delta_2]}{\mathcal{N}^{h*}} \\ &\quad - \frac{2\beta_3^h \varphi_{15} \delta_4}{\mathcal{N}^{h*}} (\varphi_2 + \varphi_3 + \varphi_4 + \varphi_5) + \frac{2[(\beta_3^h \varphi_{15} \delta_7 - \beta_3^h \varphi_{15} \delta_2) \varphi_2]}{\mathcal{N}^{h*}} - \frac{2\beta_4^h \varphi_{16} \delta_5}{\mathcal{N}^{h*}} (\varphi_2 + \varphi_3 + \varphi_4 + \varphi_5) \\ &\quad + \frac{2[(\beta_4^h \varphi_{16} \delta_8 - \beta_4^h \varphi_{16} \delta_2) \varphi_2]}{\mathcal{N}^{h*}} - \frac{2(\beta_2^v \varphi_3 \delta_{14} + \beta_3^v \varphi_4 \delta_{15} + \beta_4^v \varphi_5 \delta_{16}) x_{13}^*}{\mathcal{N}^{h*2}} \\ &\quad \times \left( \varphi_1 + \varphi_2 + \varphi_3 + \varphi_4 + \varphi_5 + \varphi_9 + \varphi_{10} + \varphi_{11} + \varphi_{12} - \frac{\varphi_{13} \mathcal{N}^{h*}}{x_{13}^*} \right) \end{aligned} \tag{16}$$

and

$$b = \sum_{k,i=1}^{16} \delta_k \varphi_i \frac{\partial^2 f_k}{\partial x_i \partial \beta^*}(0, 0) = \varphi_{15} \delta_4 > 0.$$

The backward bifurcation coefficient  $b$  is strictly positive. It follows from Theorem 4 that the model (1) undergoes backward bifurcation when the coefficient  $a > 0$ . The epidemiological consequence of Theorem 5 gives that the classical requirement of having the reproduction number  $\mathcal{R}_0 = \max\{\mathcal{R}_{0C}, \mathcal{R}_{0Z}, \mathcal{R}_{0D}, \mathcal{R}_{0K}\}$  to be less than unity is necessary but no longer sufficient for the effective control of COVID-19, zika, dengue, and chikungunya in the population. Thus, the backward bifurcation property of the model (1) makes effective control of the diseases very difficult in the population. ■

#### 4 | OPTIMAL CONTROL ANALYSIS

We now define and incorporate time dependent controls into the model (1) as follows:  $u_1(t)$ : COVID-19 prevention control,  $u_2(t)$ : human-to-human transmission of zika prevention control,  $u_3(t)$ : human-to-vector (vector-to-human) transmission of zika prevention control,  $u_4(t)$ : dengue transmission prevention control, and  $u_5(t)$ : chikungunya transmission prevention control. Assume that the control functions,  $u_1(t), u_2(t), u_3(t), u_4(t)$ , and  $u_5(t)$  are bounded and Lebesgue integrable functions. The control  $u_1(t)$  represents the efforts geared toward preventing COVID-19 infections by susceptible humans (which include: vaccination, social distancing, face-mask usage in public, use of personal protective equipment [PPE], hand gloves by health workers, and so on). The control  $u_2(t)$  denotes efforts made to prevent human-to-human transmission of zika virus. As zika can be transmitted either from mother to child or by sexual route, this control seeks to reduce transmission by these means. The control function  $u_3(t)$  seeks to reduce vectorial transmission of zika virus. These efforts include minimizing contact between mosquitoes and humans by wearing light colored clothes, using bed nets and window screens. The control  $u_4(t)$  represents efforts to reduce vectorial transmission of dengue disease. These efforts also include minimizing contacts between humans and mosquitoes, using bed nets, and also getting dengue vaccination. Recently, the *Dengvaxia* vaccine has been approved for dengue prevention.<sup>35</sup> These efforts seek to enforce the administration of this vaccine to susceptible humans. Finally, the control function  $u_5(t)$  stands for efforts required for preventing chikungunya infection (which also includes use of bed nets, vector repellents, and ensuring clean and hygienic environments). The optimal control system examines scenarios where the number of infectious cases and the cost of implementing the controls  $u_1(t), u_2(t), u_3(t), u_4(t)$ , and  $u_5(t)$  are minimized subject to the state system (17). It is assumed that all the controls may not be 100% effective in averting infections. Thus, we bound them as follows:  $0 < u_1, u_2, u_3, u_4, u_5 \leq 0.9$ . However, policy makers and health agencies are advised to increase preventive efforts in the form sensitization and awareness campaigns geared toward keeping the efficacy of the controls at very high level, in order to adequately manage the co-circulation of all the diseases.

The optimal control model is thus given by:

$$\begin{aligned} \frac{dS^h}{dt} &= \Psi^h - \left( \frac{(1-u_1)\beta_1 I_C^h}{\mathcal{N}^h} + \frac{(1-u_2)\beta_2(I_Z^h + I_{CZ}^h)}{\mathcal{N}^h} + \frac{(1-u_3)\beta_2^h I_Z^v}{\mathcal{N}^h} + \frac{(1-u_4)\beta_3^h I_D^v}{\mathcal{N}^h} + \frac{(1-u_5)\beta_4^h I_K^v}{\mathcal{N}^h} + \vartheta^h \right) S^h, \\ \frac{dI_C^h}{dt} &= \frac{(1-u_1)\beta_1 I_C^h}{\mathcal{N}^h} (S^h + \mathcal{R}_C^h + \mathcal{R}_Z^h + \mathcal{R}_D^h + \mathcal{R}_K^h) \\ &\quad - (\eta_C + \zeta_C + \vartheta^h) I_C^h - \frac{(1-u_2)\beta_2(I_Z^h + I_{CZ}^h) + (1-u_3)\beta_2^h I_Z^v}{\mathcal{N}^h} I_C^h \\ &\quad - \frac{(1-u_4)\beta_3^h I_D^v}{\mathcal{N}^h} I_C^h - \frac{(1-u_5)\beta_4^h I_K^v}{\mathcal{N}^h} I_C^h + \zeta_Z I_{CZ}^h + \zeta_D I_{CD}^h + \zeta_K I_{CK}^h, \\ \frac{dI_Z^h}{dt} &= \frac{(1-u_2)\beta_2(I_Z^h + I_{CZ}^h) + (1-u_3)\beta_2^h I_Z^v}{\mathcal{N}^h} (S^h + \mathcal{R}_C^h + \mathcal{R}_Z^h + \mathcal{R}_D^h + \mathcal{R}_K^h) \\ &\quad - (\eta_Z + \zeta_Z + \vartheta^h) I_Z^h - \frac{(1-u_1)\beta_1 I_C^h}{\mathcal{N}^h} I_Z^h + \zeta_C I_{CZ}^h, \end{aligned}$$

$$\begin{aligned}
\frac{dI_D^h}{dt} &= \frac{(1-u_4)\beta_3^h I_D^v}{\mathcal{N}^h} (S^h + \mathcal{R}_C^h + \mathcal{R}_Z^h + \mathcal{R}_D^h + \mathcal{R}_K^h) - (\eta_D + \zeta_D + \vartheta^h) I_D^h - \frac{(1-u_1)\beta_1 I_C^h}{\mathcal{N}^h} I_D^h + \zeta_C I_{CD}^h, \\
\frac{dI_K^h}{dt} &= \frac{(1-u_5)\beta_4^h I_K^v}{\mathcal{N}^h} (S^h + \mathcal{R}_C^h + \mathcal{R}_Z^h + \mathcal{R}_D^h + \mathcal{R}_K^h) - (\eta_K + \zeta_K + \vartheta^h) I_K^h - \frac{(1-u_1)\beta_1 I_C^h}{\mathcal{N}^h} I_K^h + \zeta_C I_{CK}^h, \\
\frac{dI_{CZ}^h}{dt} &= \frac{(1-u_2)\beta_2(I_Z^h + I_{CZ}^h) + (1-u_3)\beta_2^h I_Z^v}{\mathcal{N}^h} I_C^h + \frac{(1-u_1)\beta_1 I_C^h}{\mathcal{N}^h} I_Z^h - (\eta_C + \eta_Z + \zeta_C + \zeta_Z + \vartheta^h) I_{CZ}^h, \\
\frac{dI_{CD}^h}{dt} &= \frac{(1-u_4)\beta_3^h I_D^v}{\mathcal{N}^h} I_C^h + \frac{(1-u_1)\beta_1 I_C^h}{\mathcal{N}^h} I_D^h - (\eta_C + \eta_D + \zeta_C + \zeta_D + \vartheta^h) I_{CD}^h, \\
\frac{dI_{CK}^h}{dt} &= \frac{(1-u_5)\beta_4^h I_K^v}{\mathcal{N}^h} I_C^h + \frac{(1-u_1)\beta_1 I_C^h}{\mathcal{N}^h} I_K^h - (\eta_C + \eta_K + \zeta_C + \zeta_K + \vartheta^h) I_{CK}^h, \\
\frac{d\mathcal{R}_C^h}{dt} &= \zeta_C I_C^h - \left( \vartheta^h + \frac{(1-u_1)\beta_1 I_C^h}{\mathcal{N}^h} + \frac{(1-u_2)\beta_2(I_Z^h + I_{CZ}^h) + (1-u_3)\beta_2^h I_Z^v}{\mathcal{N}^h} + \frac{(1-u_4)\beta_3^h I_D^v}{\mathcal{N}^h} + \frac{(1-u_5)\beta_4^h I_K^v}{\mathcal{N}^h} \right) \mathcal{R}_C^h, \\
\frac{d\mathcal{R}_Z^h}{dt} &= \zeta_Z I_Z^h - \left( \vartheta^h + \frac{(1-u_1)\beta_1 I_C^h}{\mathcal{N}^h} + \frac{(1-u_2)\beta_2(I_Z^h + I_{CZ}^h) + (1-u_3)\beta_2^h I_Z^v}{\mathcal{N}^h} + \frac{(1-u_4)\beta_3^h I_D^v}{\mathcal{N}^h} + \frac{(1-u_5)\beta_4^h I_K^v}{\mathcal{N}^h} \right) \mathcal{R}_Z^h, \\
\frac{d\mathcal{R}_D^h}{dt} &= \zeta_D I_D^h - \left( \vartheta^h + \frac{(1-u_1)\beta_1 I_C^h}{\mathcal{N}^h} + \frac{(1-u_2)\beta_2(I_Z^h + I_{CZ}^h) + (1-u_3)\beta_2^h I_Z^v}{\mathcal{N}^h} + \frac{(1-u_4)\beta_3^h I_D^v}{\mathcal{N}^h} + \frac{(1-u_5)\beta_4^h I_K^v}{\mathcal{N}^h} \right) \mathcal{R}_D^h, \\
\frac{d\mathcal{R}_K^h}{dt} &= \zeta_K I_K^h - \left( \vartheta^h + \frac{(1-u_1)\beta_1 I_C^h}{\mathcal{N}^h} + \frac{(1-u_2)\beta_2(I_Z^h + I_{CZ}^h) + (1-u_3)\beta_2^h I_Z^v}{\mathcal{N}^h} + \frac{(1-u_4)\beta_3^h I_D^v}{\mathcal{N}^h} + \frac{(1-u_5)\beta_4^h I_K^v}{\mathcal{N}^h} \right) \mathcal{R}_K^h, \quad (17) \\
\frac{dS^v}{dt} &= \Psi^v - \left( \frac{(1-u_3)\beta_2^v(I_Z^h + I_{CZ}^h)}{\mathcal{N}^h} + \frac{(1-u_4)\beta_3^v(I_D^h + I_{CD}^h)}{\mathcal{N}^h} + \frac{(1-u_5)\beta_4^v(I_K^h + I_{CK}^h)}{\mathcal{N}^h} + \vartheta^v \right) S^v, \\
\frac{dI_Z^v}{dt} &= \frac{(1-u_3)\beta_2^v(I_Z^h + I_{CZ}^h)}{\mathcal{N}^h} S^v - \vartheta^v I_Z^v, \\
\frac{dI_D^v}{dt} &= \frac{(1-u_4)\beta_3^v(I_D^h + I_{CD}^h)}{\mathcal{N}^h} S^v - \vartheta^v I_D^v, \\
\frac{dI_K^v}{dt} &= \frac{(1-u_5)\beta_4^v(I_K^h + I_{CK}^h)}{\mathcal{N}^h} S^v - \vartheta^v I_K^v,
\end{aligned}$$

subject to the initial conditions

$$\begin{aligned}
S_0^h &= S^h(0), \quad I_{c0}^h = I_C^h(0), \quad I_{z0}^h = I_Z^h(0), \quad I_{d0}^h = I_D^h(0) \\
I_{k0}^h &= I_K^h(0), \quad I_{cz0}^h = I_{CZ}^h(0), \quad I_{cd0}^h = I_{CD}^h(0), \\
I_{ck0}^h &= I_{CK}^h(0), \quad \mathcal{R}_{c0}^h = \mathcal{R}_C^h(0), \quad \mathcal{R}_{z0}^h = \mathcal{R}_Z^h(0), \quad \mathcal{R}_{d0}^h = \mathcal{R}_D^h(0), \\
\mathcal{R}_{k0}^h &= \mathcal{R}_K^h, \quad S_0^v = S^v(0), \quad I_{z0}^v = I_Z^v(0), \quad I_{d0}^v = I_D^v(0), \quad I_{k0}^v = I_K^v(0).
\end{aligned} \quad (18)$$

The cost of implementing all the control strategies is given by the following objective functional:

$$\begin{aligned}
& J[u_1, u_2, u_3, u_4, u_5] \\
&= \int_0^T [I_C^h(t) + I_Z^h(t) + I_D^h(t) + I_K^h(t) + I_{CZ}^h(t) + I_{CD}^h(t) + I_{CK}^h(t) + I_Z^v(t) + I_D^v(t) + I_K^v(t) \\
&\quad + \frac{\omega_1}{2} u_1^2 + \frac{\omega_2}{2} u_2^2 + \frac{\omega_3}{2} u_3^2 + \frac{\omega_4}{2} u_4^2 + \frac{\omega_5}{2} u_5^2] dt, \quad (19)
\end{aligned}$$

where  $T$  is the final time. The above nonlinear cost functional represents the total cost that includes the cost of COVID-19 and arboviruses preventive measures. We seek to find optimal controls denoted by  $u_1^*$ ,  $u_2^*$ ,  $u_3^*$ ,  $u_4^*$ ,  $u_5^*$  which minimizes the

cost functional, that is,

$$J(u_1^*, u_2^*, u_3^*, u_4^*, u_5^*) = \min\{J(u_1, u_2, u_3, u_4, u_5) | u_1, u_2, u_3, u_4, u_5 \in U\}, \tag{20}$$

where  $U = \{u_1, u_2, u_3, u_4, u_5\}$ , such that  $u_1, u_2, u_3, u_4, u_5$  are Lebesgue measurable with upper bounds  $u_1^b, u_2^b, u_3^b, u_4^b, u_5^b$  for  $t \in [0, T]$  is the control set. The Hamiltonian is given by:

$$\begin{aligned} \mathcal{H} = & I_C^h(t) + I_Z^h(t) + I_D^h(t) + I_K^h(t) + I_{CZ}^h(t) + I_{CD}^h(t) + I_{CK}^h(t) + I_{CZ}^v(t) + I_D^v(t) + I_K^v(t) \\ & + \frac{\omega_1}{2} u_1^2 + \frac{\omega_2}{2} u_2^2 + \frac{\omega_3}{2} u_3^2 + \frac{\omega_4}{2} u_4^2 + \frac{\omega_5}{2} u_5^2 \\ & + \varrho_1 \left( \Psi^h - \left( \frac{(1-u_1)\beta_1 I_C^h}{\mathcal{N}^h} + \frac{(1-u_2)\beta_2(I_Z^h + I_{CZ}^h)}{\mathcal{N}^h} + \frac{(1-u_3)\beta_2^h I_Z^v}{\mathcal{N}^h} + \frac{(1-u_4)\beta_3^h I_D^v}{\mathcal{N}^h} + \frac{(1-u_5)\beta_4^h I_K^v}{\mathcal{N}^h} + \vartheta^h \right) S^h \right) \\ & + \varrho_2 \left( \frac{(1-u_1)\beta_1 I_C^h}{\mathcal{N}^h} (S^h + \mathcal{R}_Z^h + \mathcal{R}_D^h + \mathcal{R}_K^h) - (\eta_C + \zeta_C + \vartheta^h) I_C^h - \frac{(1-u_2)\beta_2(I_Z^h + I_{CZ}^h) + (1-u_3)\beta_2^h I_Z^v}{\mathcal{N}^h} I_C^h \right. \\ & \left. - \frac{(1-u_4)\beta_3^h I_D^v}{\mathcal{N}^h} I_C^h - \frac{(1-u_5)\beta_4^h I_K^v}{\mathcal{N}^h} I_C^h + \zeta_Z I_{CZ}^h + \zeta_D I_{CD}^h + \zeta_K I_{CK}^h \right) \\ & + \varrho_3 \left( \frac{(1-u_2)\beta_2(I_Z^h + I_{CZ}^h) + (1-u_3)\beta_2^h I_Z^v}{\mathcal{N}^h} (S^h + \mathcal{R}_C^h + \mathcal{R}_D^h + \mathcal{R}_K^h) - (\eta_Z + \zeta_Z + \vartheta^h) I_Z^h - \frac{(1-u_1)\beta_1 I_C^h}{\mathcal{N}^h} I_Z^h + \zeta_C I_{CZ}^h \right) \\ & + \varrho_4 \left( \frac{(1-u_4)\beta_3^h I_D^v}{\mathcal{N}^h} (S^h + \mathcal{R}_C^h + \mathcal{R}_Z^h + \mathcal{R}_K^h) - (\eta_D + \zeta_D + \vartheta^h) I_D^h - \frac{(1-u_1)\beta_1 I_C^h}{\mathcal{N}^h} I_D^h + \zeta_C I_{CD}^h \right) \\ & + \varrho_5 \left( \frac{(1-u_5)\beta_4^h I_K^v}{\mathcal{N}^h} (S^h + \mathcal{R}_C^h + \mathcal{R}_Z^h + \mathcal{R}_D^h) - (\eta_K + \zeta_K + \vartheta^h) I_K^h - \frac{(1-u_1)\beta_1 I_C^h}{\mathcal{N}^h} I_K^h + \zeta_C I_{CK}^h \right) \\ & + \varrho_6 \left( \frac{(1-u_2)\beta_2(I_Z^h + I_{CZ}^h) + (1-u_3)\beta_2^h I_Z^v}{\mathcal{N}^h} I_C^h + \frac{(1-u_1)\beta_1 I_C^h}{\mathcal{N}^h} I_Z^h - (\eta_C + \eta_Z + \zeta_C + \zeta_Z + \vartheta^h) I_{CZ}^h \right) \\ & + \varrho_7 \left( \frac{(1-u_4)\beta_3^h I_D^v}{\mathcal{N}^h} I_C^h + \frac{(1-u_1)\beta_1 I_C^h}{\mathcal{N}^h} I_D^h - (\eta_C + \eta_D + \zeta_C + \zeta_D + \vartheta^h) I_{CD}^h \right) \\ & + \varrho_8 \left( \frac{(1-u_5)\beta_4^h I_K^v}{\mathcal{N}^h} I_C^h + \frac{(1-u_1)\beta_1 I_C^h}{\mathcal{N}^h} I_K^h - (\eta_C + \eta_K + \zeta_C + \zeta_K + \vartheta^h) I_{CK}^h \right) \\ & + \varrho_9 \left( \zeta_C I_C^h - \left( \vartheta^h + \frac{(1-u_1)\beta_1 I_C^h}{\mathcal{N}^h} + \frac{(1-u_2)\beta_2(I_Z^h + I_{CZ}^h) + (1-u_3)\beta_2^h I_Z^v}{\mathcal{N}^h} + \frac{(1-u_4)\beta_3^h I_D^v}{\mathcal{N}^h} + \frac{(1-u_5)\beta_4^h I_K^v}{\mathcal{N}^h} \right) \mathcal{R}_C^h \right) \\ & + \varrho_{10} \left( \zeta_Z I_Z^h - \left( \vartheta^h + \frac{(1-u_1)\beta_1 I_C^h}{\mathcal{N}^h} + \frac{(1-u_2)\beta_2(I_Z^h + I_{CZ}^h) + (1-u_3)\beta_2^h I_Z^v}{\mathcal{N}^h} + \frac{(1-u_4)\beta_3^h I_D^v}{\mathcal{N}^h} + \frac{(1-u_5)\beta_4^h I_K^v}{\mathcal{N}^h} \right) \mathcal{R}_Z^h \right) \\ & + \varrho_{11} \left( \zeta_D I_D^h - \left( \vartheta^h + \frac{(1-u_1)\beta_1 I_C^h}{\mathcal{N}^h} + \frac{(1-u_2)\beta_2(I_Z^h + I_{CZ}^h) + (1-u_3)\beta_2^h I_Z^v}{\mathcal{N}^h} + \frac{(1-u_4)\beta_3^h I_D^v}{\mathcal{N}^h} + \frac{(1-u_5)\beta_4^h I_K^v}{\mathcal{N}^h} \right) \mathcal{R}_D^h \right) \\ & + \varrho_{12} \left( \zeta_K I_K^h - \left( \vartheta^h + \frac{(1-u_1)\beta_1 I_C^h}{\mathcal{N}^h} + \frac{(1-u_2)\beta_2(I_Z^h + I_{CZ}^h) + (1-u_3)\beta_2^h I_Z^v}{\mathcal{N}^h} + \frac{(1-u_4)\beta_3^h I_D^v}{\mathcal{N}^h} + \frac{(1-u_5)\beta_4^h I_K^v}{\mathcal{N}^h} \right) \mathcal{R}_K^h \right) \tag{21} \\ & + \varrho_{13} \left( \Psi^v - \left( \frac{(1-u_3)\beta_2^v(I_Z^h + I_{CZ}^h)}{\mathcal{N}^h} + \frac{(1-u_4)\beta_3^v(I_D^h + I_{CD}^h)}{\mathcal{N}^h} + \frac{(1-u_5)\beta_4^v(I_K^h + I_{CK}^h)}{\mathcal{N}^h} + \vartheta^v \right) S^v \right) \\ & + \varrho_{14} \left( \frac{(1-u_3)\beta_2^v(I_Z^h + I_{CZ}^h)}{\mathcal{N}^h} S^v - \vartheta^v I_Z^v \right) \\ & + \varrho_{15} \left( \frac{(1-u_4)\beta_3^v(I_D^h + I_{CD}^h)}{\mathcal{N}^h} S^v - \vartheta^v I_D^v \right) \\ & + \varrho_{16} \left( \frac{(1-u_5)\beta_4^v(I_K^h + I_{CK}^h)}{\mathcal{N}^h} S^v - \vartheta^v I_K^v \right). \end{aligned}$$

## 4.1 | Existence of optimal control

We now establish the existence of control function that minimizes the cost functional  $J$ .

**Theorem 6.** Suppose  $J$  is defined on the control set  $U$  subject to system (17) with non-negative initial conditions at  $t = 0$ , then there exists an optimal control  $u^* = (u_1^*, u_2^*, u_3^*, u_4^*, u_5^*)$  such that  $J(u^*) = \min \{J(u_1, u_2, u_3, u_4, u_5) | u_1, u_2, u_3, u_4, u_5 \in U\}$ , if the following conditions are satisfied (see References 36 and 37):

- (i) The admissible control set  $U$  is convex and closed.
- (ii) The state system is bounded by a linear function in the state and control variables.
- (iii) The integrand of the objective functional in (19) is convex with respect to the controls.
- (iv) The Lagrangian is bounded below by  $\varpi_1 |u|^{\varpi_3} - \varpi_2$ , where  $\varpi_1 > 0$ ,  $\varpi_2 > 0$ ,  $\varpi_3 > 1$ .

*Proof.* See Appendix B. ■

**Theorem 7.** Suppose an optimal control problem for  $J$  over the set  $U$  is solved, then adjoint variables,  $\rho_1, \rho_2, \dots, \rho_{16}$  satisfy the adjoint equations

$$-\frac{\partial \rho_i}{\partial t} = \frac{\partial \mathcal{X}}{\partial i},$$

with transversality condition:

$$\rho_i(t_f) = 0, \quad \text{where } i = S^h, I_C^h, I_Z^h, I_D^h, I_K^h, I_{CZ}^h, I_{CD}^h, I_{CK}^h, R_C^h, R_Z^h, R_D^h, R_K^h, S^v, I_Z^v, I_D^v, I_K^v. \quad (22)$$

Furthermore,

$$\begin{aligned} u_1^* &= \min \{u_1^b, \max(0, \Phi_1)\}, \\ u_2^* &= \min \{u_2^b, \max(0, \Phi_2)\}, \\ u_3^* &= \min \{u_3^b, \max(0, \Phi_3)\}, \\ u_4^* &= \min \{u_4^b, \max(0, \Phi_4)\}, \\ u_5^* &= \min \{u_5^b, \max(0, \Phi_5)\} \end{aligned} \quad (23)$$

with

$$\begin{aligned} \Phi_1 &= \frac{\beta_1 I_D^h [S^h(\rho_2 - \rho_1) + R_C^h(\rho_2 - \rho_9) + R_Z^h(\rho_2 - \rho_{10}) + R_D^h(\rho_2 - \rho_{11}) + R_K^h(\rho_2 - \rho_{12}) + I_Z^h(\rho_6 - \rho_3) + \alpha_{11}]}{\omega_1 \mathcal{N}^h}, \\ \Phi_2 &= \frac{\beta_2 (I_Z^h + I_{CZ}^h) [S^h(\rho_3 - \rho_1) + R_C^h(\rho_3 - \rho_9) + R_Z^h(\rho_3 - \rho_{10}) + R_D^h(\rho_3 - \rho_{11}) + R_K^h(\rho_3 - \rho_{12}) + I_C^h(\rho_6 - \rho_2)]}{\omega_2 \mathcal{N}^h}, \\ \Phi_3 &= \frac{\beta_2^h I_Z^v [S^h(\rho_3 - \rho_1) + R_C^h(\rho_3 - \rho_9) + R_Z^h(\rho_3 - \rho_{10}) + R_D^h(\rho_3 - \rho_{11}) + R_K^h(\rho_3 - \rho_{12}) + I_C^h(\rho_6 - \rho_2)] + \alpha_{22}}{\omega_3 \mathcal{N}^h}, \\ \Phi_4 &= \frac{\beta_3^h I_D^v [S^h(\rho_4 - \rho_1) + R_C^h(\rho_4 - \rho_9) + R_D^h(\rho_4 - \rho_{11}) + R_K^h(\rho_4 - \rho_{12}) + R_Z^h(\rho_4 - \rho_{10}) + I_C^h(\rho_7 - \rho_2)] + \alpha_{33}}{\omega_4 \mathcal{N}^h}, \\ \Phi_5 &= \frac{\beta_4^h I_K^v [S^h(\rho_5 - \rho_1) + R_C^h(\rho_5 - \rho_9) + R_K^h(\rho_5 - \rho_{10}) + R_D^h(\rho_5 - \rho_{11}) + R_Z^h(\rho_5 - \rho_{10}) + I_C^h(\rho_8 - \rho_2)] + \alpha_{44}}{\omega_5 \mathcal{N}^h}, \\ \alpha_{11} &= I_D^h(\rho_7 - \rho_4) + I_K^h(\rho_8 - \rho_5), \quad \alpha_{22} = \beta_2^v (I_Z^h + I_{CZ}^h) [S^v(\rho_{14} - \rho_{13})], \quad \alpha_{33} = \beta_3^v (I_D^h + I_{CD}^h) [S^v(\rho_{15} - \rho_{13})], \\ \alpha_{44} &= \beta_4^v (I_K^h + I_{CK}^h) [S^v(\rho_{16} - \rho_{13})] \end{aligned}$$

*Proof of Theorem 7.* Consider  $U^* = (u_1^*, u_2^*, u_3^*, u_4^*, u_5^*)$  and  $S^{h*}, I_C^{h*}, I_Z^{h*}, I_D^{h*}, I_K^{h*}, I_{CZ}^{h*}, I_{CD}^{h*}, I_{CK}^{h*}, R_C^{h*}, R_Z^{h*}, R_D^{h*}, R_K^{h*}, S^{v*}, I_Z^{v*}, I_D^{v*}, I_K^{v*}$  being the associated solutions. Using Pontryagin's maximum principle<sup>38</sup> is applied, there exist adjoint variables such that:

$$\begin{aligned}
 -\frac{d\varrho_1}{dt} &= \frac{\partial \mathcal{X}}{\partial S^h}, & \varrho_1(t_f) &= 0, & -\frac{d\varrho_2}{dt} &= \frac{\partial \mathcal{X}}{\partial I_C^h}, & \varrho_2(t_f) &= 0, & -\frac{d\varrho_3}{dt} &= \frac{\partial \mathcal{X}}{\partial I_Z^h}, & \varrho_3(t_f) &= 0, \\
 -\frac{d\varrho_4}{dt} &= \frac{\partial \mathcal{X}}{\partial I_D^h}, & \varrho_4(t_f) &= 0, & -\frac{d\varrho_5}{dt} &= \frac{\partial \mathcal{X}}{\partial I_K^h}, & \varrho_5(t_f) &= 0, & -\frac{d\varrho_6}{dt} &= \frac{\partial \mathcal{X}}{\partial I_{CZ}^h}, & \varrho_6(t_f) &= 0, \\
 -\frac{d\varrho_7}{dt} &= \frac{\partial \mathcal{X}}{\partial I_{CD}^h}, & \varrho_7(t_f) &= 0, & -\frac{d\varrho_8}{dt} &= \frac{\partial \mathcal{X}}{\partial I_{CK}^h}, & \varrho_8(t_f) &= 0, & -\frac{d\varrho_9}{dt} &= \frac{\partial \mathcal{X}}{\partial R_C^h}, & \varrho_9(t_f) &= 0, \\
 -\frac{d\varrho_{10}}{dt} &= \frac{\partial \mathcal{X}}{\partial R_Z^h}, & \varrho_{10}(t_f) &= 0, & -\frac{d\varrho_{11}}{dt} &= \frac{\partial \mathcal{X}}{\partial R_D^h}, & \varrho_{11}(t_f) &= 0, & -\frac{d\varrho_{12}}{dt} &= \frac{\partial \mathcal{X}}{\partial R_K^h}, & \varrho_{12}(t_f) &= 0, \\
 \frac{d\varrho_{13}}{dt} &= \frac{\partial \mathcal{X}}{\partial S^v}, & \varrho_{13}(t_f) &= 0, & -\frac{d\varrho_{14}}{dt} &= \frac{\partial \mathcal{X}}{\partial I_Z^v}, & \varrho_{14}(t_f) &= 0, & -\frac{d\varrho_{15}}{dt} &= \frac{\partial \mathcal{X}}{\partial I_D^v}, & \varrho_{15}(t_f) &= 0, \\
 -\frac{d\varrho_{16}}{dt} &= \frac{\partial \mathcal{X}}{\partial I_K^v}, & \varrho_{16}(t_f) &= 0.
 \end{aligned} \tag{24}$$

On the interior of the set, where  $0 < u_j < 1 \forall (j = 1, \dots, 5)$ , we have

$$\begin{aligned}
 0 &= \frac{\partial \mathcal{X}}{\partial u_1} = \omega_1 \mathcal{N}^h u_1^* - \beta_1 I_D^h [S^h(\varrho_2 - \varrho_1) + R_C^h(\varrho_2 - \varrho_9) + R_Z^h(\varrho_2 - \varrho_{10}) + R_D^h(\varrho_2 - \varrho_{11}) + R_K^h(\varrho_2 - \varrho_{12}) \\
 &\quad + I_Z^h(\varrho_6 - \varrho_3) + I_D^h(\varrho_7 - \varrho_4) + I_K^h(\varrho_8 - \varrho_5)], \\
 0 &= \frac{\partial \mathcal{X}}{\partial u_2} = \omega_2 \mathcal{N}^h u_2^* - \beta_2 (I_Z^h + I_{CZ}^h) [S^h(\varrho_3 - \varrho_1) + R_C^h(\varrho_3 - \varrho_9) + R_Z^h(\varrho_3 - \varrho_{10}) + R_D^h(\varrho_3 - \varrho_{11}) \\
 &\quad + R_K^h(\varrho_3 - \varrho_{12}) + I_C^h(\varrho_6 - \varrho_2)], \\
 0 &= \frac{\partial \mathcal{X}}{\partial u_3} = \omega_3 \mathcal{N}^h u_3^* - \beta_2^h I_Z^v [S^h(\varrho_3 - \varrho_1) + R_C^h(\varrho_3 - \varrho_9) + R_Z^h(\varrho_3 - \varrho_{10}) + R_D^h(\varrho_3 - \varrho_{11}) + R_K^h(\varrho_3 - \varrho_{12}) + I_C^h(\varrho_6 - \varrho_2)] \\
 &\quad + \beta_2^v (I_Z^h + I_{CZ}^h) [S^v(\varrho_{14} - \varrho_{13})], \\
 0 &= \frac{\partial \mathcal{X}}{\partial u_4} = \omega_4 \mathcal{N}^h u_4^* - \beta_3^h I_D^v [S^h(\varrho_4 - \varrho_1) + R_C^h(\varrho_4 - \varrho_9) + R_D^h(\varrho_4 - \varrho_{11}) + R_K^h(\varrho_4 - \varrho_{12}) + R_Z^h(\varrho_4 - \varrho_{10}) \\
 &\quad + I_C^h(\varrho_7 - \varrho_2)] + \beta_3^v (I_D^h + I_{CD}^h) [S^v(\varrho_{15} - \varrho_{13})], \\
 0 &= \frac{\partial \mathcal{X}}{\partial u_5} = \omega_5 \mathcal{N}^h u_5^* - \beta_4^h I_K^v [S^h(\varrho_5 - \varrho_1) + R_C^h(\varrho_5 - \varrho_9) + R_K^h(\varrho_5 - \varrho_{10}) + R_D^h(\varrho_5 - \varrho_{11}) \\
 &\quad + R_Z^h(\varrho_5 - \varrho_{10}) + I_C^h(\varrho_8 - \varrho_2)] + \beta_4^v (I_K^h + I_{CK}^h) [S^v(\varrho_{16} - \varrho_{13})].
 \end{aligned} \tag{25}$$

Therefore,

$$\begin{aligned}
 u_1^* &= \frac{\beta_1 I_D^h [S^h(\varrho_2 - \varrho_1) + R_C^h(\varrho_2 - \varrho_9) + R_Z^h(\varrho_2 - \varrho_{10}) + R_D^h(\varrho_2 - \varrho_{11}) + R_K^h(\varrho_2 - \varrho_{12}) + I_Z^h(\varrho_6 - \varrho_3) + \alpha_{11}]}{\omega_1 \mathcal{N}^h}, \\
 u_2^* &= \frac{\beta_2 (I_Z^h + I_{CZ}^h) [S^h(\varrho_3 - \varrho_1) + R_C^h(\varrho_3 - \varrho_9) + R_Z^h(\varrho_3 - \varrho_{10}) + R_D^h(\varrho_3 - \varrho_{11}) + R_K^h(\varrho_3 - \varrho_{12}) + I_C^h(\varrho_6 - \varrho_2)]}{\omega_2 \mathcal{N}^h}, \\
 u_3^* &= \frac{\beta_2^h I_Z^v [S^h(\varrho_3 - \varrho_1) + R_C^h(\varrho_3 - \varrho_9) + R_Z^h(\varrho_3 - \varrho_{10}) + R_D^h(\varrho_3 - \varrho_{11}) + R_K^h(\varrho_3 - \varrho_{12}) + I_C^h(\varrho_6 - \varrho_2)] + \alpha_{22}}{\omega_3 \mathcal{N}^h}, \\
 u_4^* &= \frac{\beta_3^h I_D^v [S^h(\varrho_4 - \varrho_1) + R_C^h(\varrho_4 - \varrho_9) + R_D^h(\varrho_4 - \varrho_{11}) + R_K^h(\varrho_4 - \varrho_{12}) + R_Z^h(\varrho_4 - \varrho_{10}) + I_C^h(\varrho_7 - \varrho_2)] + \alpha_{33}}{\omega_4 \mathcal{N}^h}, \\
 u_5^* &= \frac{\beta_4^h I_K^v [S^h(\varrho_5 - \varrho_1) + R_C^h(\varrho_5 - \varrho_9) + R_K^h(\varrho_5 - \varrho_{10}) + R_D^h(\varrho_5 - \varrho_{11}) + R_Z^h(\varrho_5 - \varrho_{10}) + I_C^h(\varrho_8 - \varrho_2)] + \alpha_{44}}{\omega_5 \mathcal{N}^h},
 \end{aligned} \tag{26}$$

where

$$\begin{aligned}
 \alpha_{11} &= I_D^h(\varrho_7 - \varrho_4) + I_K^h(\varrho_8 - \varrho_5), & \alpha_{22} &= \beta_2^v (I_Z^h + I_{CZ}^h) [S^v(\varrho_{14} - \varrho_{13})], & \alpha_{33} &= \beta_3^v (I_D^h + I_{CD}^h) [S^v(\varrho_{15} - \varrho_{13})], \\
 \alpha_{44} &= \beta_4^v (I_K^h + I_{CK}^h) [S^v(\varrho_{16} - \varrho_{13})].
 \end{aligned}$$

Using the bounds on the controls, the characterization (23) can be derived and we conclude that,

$$\begin{aligned} u_1^* &= \min \{u_1^b, \max(0, \Phi_1)\}, \\ u_2^* &= \min \{u_2^b, \max(0, \Phi_2)\}, \\ u_3^* &= \min \{u_3^b, \max(0, \Phi_3)\}, \\ u_4^* &= \min \{u_4^b, \max(0, \Phi_4)\}, \\ u_5^* &= \min \{u_5^b, \max(0, \Phi_5)\}, \end{aligned} \quad (27)$$

with

$$\begin{aligned} \Phi_1 &= \frac{\beta_1 I_D^h [S^h(\rho_2 - \rho_1) + \mathcal{R}_C^h(\rho_2 - \rho_9) + \mathcal{R}_Z^h(\rho_2 - \rho_{10}) + \mathcal{R}_D^h(\rho_2 - \rho_{11}) + \mathcal{R}_K^h(\rho_2 - \rho_{12}) + I_Z^h(\rho_6 - \rho_3) + \alpha_{11}]}{\omega_1 \mathcal{N}^h}, \\ \Phi_2 &= \frac{\beta_2 (I_Z^h + I_{CZ}^h) [S^h(\rho_3 - \rho_1) + \mathcal{R}_C^h(\rho_3 - \rho_9) + \mathcal{R}_Z^h(\rho_3 - \rho_{10}) + \mathcal{R}_D^h(\rho_3 - \rho_{11}) + \mathcal{R}_K^h(\rho_3 - \rho_{12}) + I_C^h(\rho_6 - \rho_2)]}{\omega_2 \mathcal{N}^h}, \\ \Phi_3 &= \frac{\beta_3^h I_Z^v [S^h(\rho_3 - \rho_1) + \mathcal{R}_C^h(\rho_3 - \rho_9) + \mathcal{R}_Z^h(\rho_3 - \rho_{10}) + \mathcal{R}_D^h(\rho_3 - \rho_{11}) + \mathcal{R}_K^h(\rho_3 - \rho_{12}) + I_C^h(\rho_6 - \rho_2)] + \alpha_{22}}{\omega_3 \mathcal{N}^h}, \\ \Phi_4 &= \frac{\beta_3^h I_D^v [S^h(\rho_4 - \rho_1) + \mathcal{R}_C^h(\rho_4 - \rho_9) + \mathcal{R}_D^h(\rho_4 - \rho_{11}) + \mathcal{R}_K^h(\rho_4 - \rho_{12}) + \mathcal{R}_Z^h(\rho_4 - \rho_{10}) + I_C^h(\rho_7 - \rho_2)] + \alpha_{33}}{\omega_4 \mathcal{N}^h}, \\ \Phi_5 &= \frac{\beta_4^h I_K^v [S^h(\rho_5 - \rho_1) + \mathcal{R}_C^h(\rho_5 - \rho_9) + \mathcal{R}_K^h(\rho_5 - \rho_{10}) + \mathcal{R}_D^h(\rho_5 - \rho_{11}) + \mathcal{R}_Z^h(\rho_5 - \rho_{10}) + I_C^h(\rho_8 - \rho_2)] + \alpha_{44}}{\omega_5 \mathcal{N}^h}. \end{aligned}$$

■

## 5 | NUMERICAL SIMULATIONS

Simulations carried out on the control system (17), adjoint equations (24), and characterizations of the control (23) are run in MATLAB using the forward backward sweep method in Reference 39. The method requires an initial value on the optimal control  $u^*$ . The initial conditions in (18) is used to solve the state system forward in time using the MATLAB built-in ODE45 routine. Next, the adjoint system is solved using the transversality condition (22) and the approximated solution of the state system. Then, the values of the control variables are computed using the control characterization in (23), and the control set  $u^*$  is updated via a convex combination of previous and current values of the control characterization. The process is repeated until the state variables, adjoint and control values converge. The quadratic cost functions  $\frac{1}{2}\omega_1 u_1^2$ ,  $\frac{1}{2}\omega_2 u_2^2$ ,  $\frac{1}{2}\omega_3 u_3^2$ ,  $\frac{1}{2}\omega_4 u_4^2$ , and  $\frac{1}{2}\omega_5 u_5^2$  are applied over the time. It is worth mentioning that the choice of the weights is of theoretical sense to illustrate the control strategies implemented in this article. The weight constants are assumed as follows:  $\omega_1 = 0.15$ ,  $\omega_2 = 0.08$ ,  $\omega_3 = 0.10$ ,  $\omega_4 = 0.12$ , and  $\omega_5 = 0.10$ . The cost of implementing preventive controls against COVID-19 (PPE, hand gloves, vaccination, and face-mask usage) is assumed greater than the cost of preventive strategies for the arboviruses (zika, dengue, and chikungunya). Also, the cost of preventive efforts against human to human transmission of zika virus is assumed to be less than the cost of implementing preventive controls against vectorial transmission. The sexual transmission of zika is very rare, and we have assumed it will involve less cost as compared to the use of bed nets, window screens and repellents for prevention of vectorial transmission. Also, the weight constant associated with dengue transmission is assumed higher than the other two arboviruses (as it involves the cost of dengue vaccination).

### 5.1 | Uncertainty and sensitivity analysis

Due to uncertainties which may arise in parameters estimation, sensitivity analysis is carried out in this section, following the approach in Reference 40. As shown in Figure 2A, when the COVID-19 associated reproduction number  $\mathcal{R}_{0C}$  is used as a response function, the effective contact rate for COVID-19 transmission ( $\beta_1$ , positively correlated) and the COVID-19 recovery rate ( $\zeta_C$ ), dominates the dynamics of the disease. Using the zika-related reproduction number

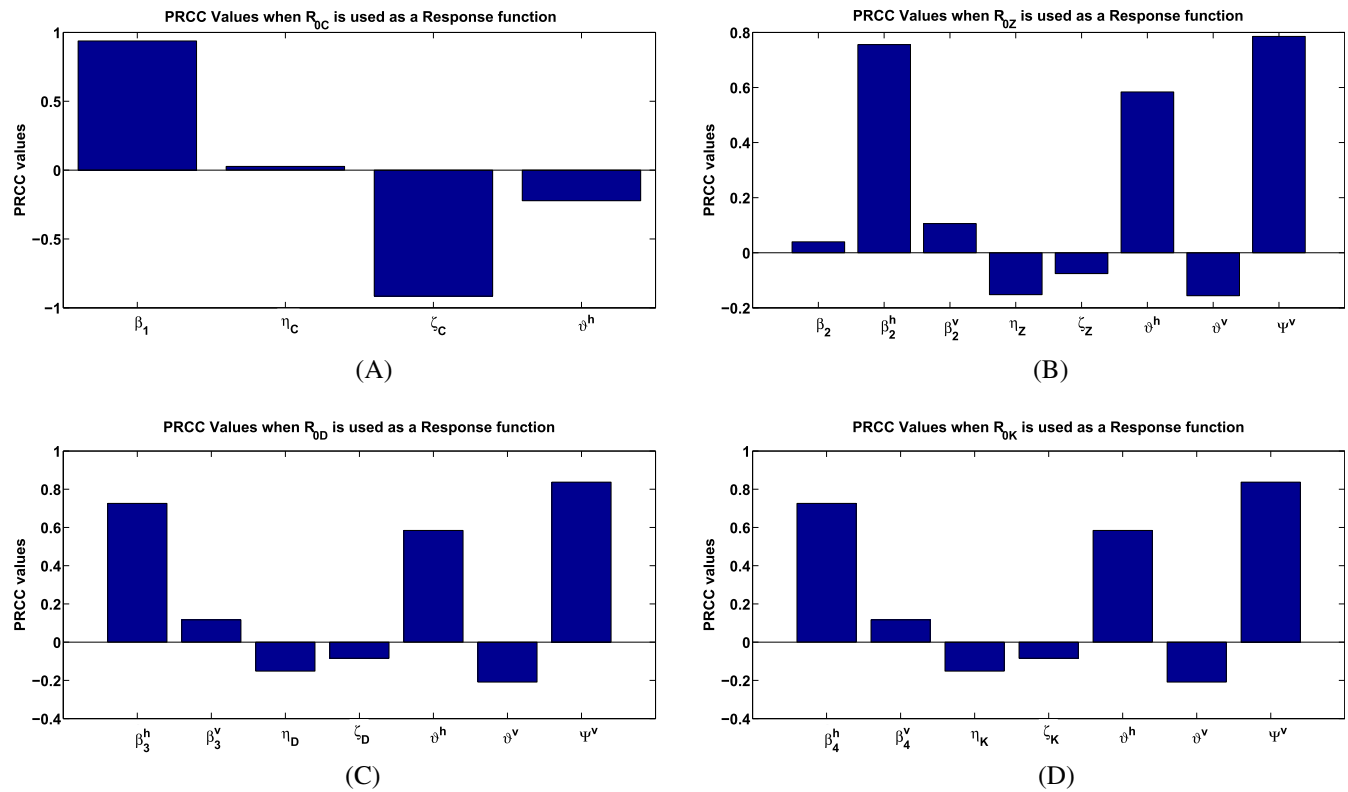


**FIGURE 2** PRCC values when the COVID-19 (A), zika (B), dengue (C), and chikungunya (D) associated reproduction numbers are used as response functions. Parameter values are given in Table 1.

$\mathcal{R}_{OZ}$ , as the response function, the important parameters are: the effective contact rate for vector-to-human transmission of zika ( $\beta_2^h$ , which is positively correlated), the human natural death rate ( $\vartheta^h$ , positively correlated) and the vector recruitment rate ( $\Psi^v$ ). Although the human-to-human transmission rate for zika ( $\beta_2$ ) is positively correlated, its impact is very negligible, as observed in Figure 2B. Similarly, using the dengue and chikungunya related reproduction numbers as input functions, as depicted in Figure 2C,D, the most dominant parameters are the transmission rates ( $\beta_3^h$  ( $\beta_4^h$ ) positively correlated), human natural death rate ( $\vartheta^h$ ) and vector recruitment rate ( $\Psi^v$ ) (both, positively correlated). Also, using the class of individuals co-infected with COVID-19 and zika ( $I_{CZ}^h$ ) as response function, the most dominant parameters are: the effective contact rate for COVID-19 transmission ( $\beta_1$ , positively correlated), the effective contact rate for vector-to-human transmission of zika ( $\beta_2^h$ , positively correlated). Other important parameters driving the dynamics of infections in this class are COVID-19 recovery rate ( $\zeta_C$ , negatively correlated) and the zika recovery rate ( $\zeta_Z$ ). Although the human-to-human transmission rate for zika ( $\beta_2$ ) is positively correlated, its impact on this epidemiological class is also very negligible, as observed in Figure 3A. Furthermore, when the class of individuals co-infected with COVID-19 and dengue and COVID-19 and chikungunya,  $I_{CD}^h$  ( $I_{CK}^h$ ), are used as inputs, the two most dominant parameters are the effective contact rates for COVID-19 and dengue (zika) transmissions, respectively. This is observed in Figure 3B,C.

## 5.2 | Initial conditions and model fitting

The population of Espiritio Santo State in Brazil is estimated to be 4,108,508.<sup>30</sup> The initial conditions are set as follows:  $S^h(0) = 3,600,000$ ;  $I_C^h(0) = 180,620$ ;  $I_Z^h(0) = 24$ ;  $I_D^h(0) = 251$ ;  $I_K^h(0) = 85$ ;  $I_{CZ}^h(0) = 100$ ;  $I_{CD}^h(0) = 100$ ;  $I_{CK}^h(0) = 100$ ;  $\mathcal{R}_C^h(0) = 100$ ;  $\mathcal{R}_Z^h(0) = 100$ ;  $\mathcal{R}_D^h(0) = 100$ ;  $\mathcal{R}_K^h(0) = 100$ ;  $S^v(0) = 48,000$ ;  $I_Z^v(0) = 600$ ;  $I_D^v(0) = 1000$ ;  $I_K^v(0) = 1000$ .

The fittings of the model to the cumulative COVID-19, zika, dengue, and chikungunya cases, respectively (Table 2),<sup>41,42</sup> were done using the *fmincon* function in the Optimization Toolbox of MATLAB.<sup>43</sup> The *fmincon*'s optimization routine

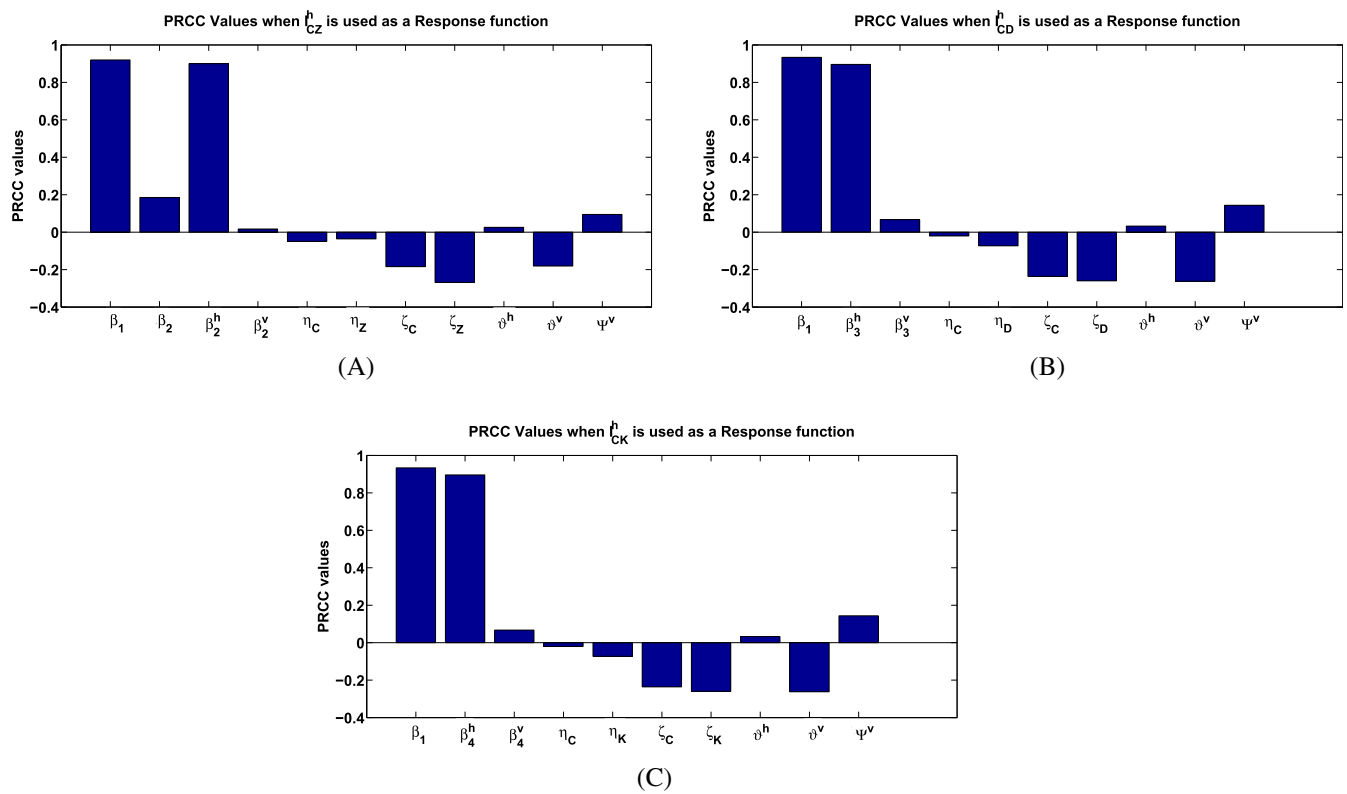


**FIGURE 3** PRCC values when the co-infected epidemiological classes:  $I_{CZ}^h$  (A),  $I_{CD}^h$  (B), and  $I_{CK}^h$  (C), are used as response functions. Parameter values are given in Table 1.

**TABLE 1** Description of parameters in the model (1)

Parameter	Description	Value	References
$\Psi^v$	Vector recruitment rate	20,000 per day	29
$\Psi^h$	Human recruitment rate	$\frac{4,108,508}{74.9 \times 365}$ per day	30
$\beta_1$	Contact rate for COVID-19 infection	0.5642	Fitted
$\beta_2$	Zika infection contact rate (sexual transmission)	0.0296	Fitted
$\beta_2^h$	Zika infection contact rate (vector human)	0.0529	Fitted
$\beta_3^h$	Dengue infection contact rate (vector human)	0.3427	Fitted
$\beta_4^h$	Chikungunya infection contact rate (vector human)	0.1137	Fitted
$\beta_2^v$	Zika infection contact rate (human to vector)	0.60 – 0.75	27
$\beta_3^v$	Dengue infection contact rate (human to vector)	0.60 – 0.75	27
$\beta_4^v$	Chikungunya infection contact rate (human to vector)	0.60 – 0.75	27
$\theta^h$	Human natural death rate	$\frac{1}{74.9 \times 365}$ per day	31
$\theta^v$	Vector removal rate	$\frac{1}{21}$ per day	29
$\eta_C, \eta_Z, \eta_D, \eta_K$	COVID-19, zika, dengue, and chikungunya disease-induced death rates, respectively	0.05	Assumed
$\zeta_C$	COVID-19 recovery rate	0.45	Assumed
$\zeta_Z, \zeta_D, \zeta_K$	Zika, dengue, chikungunya recovery rates	0.09–0.15	27
$R_{0C}$	COVID-19 associated reproduction number	1.1283	Fitted
$R_{0Z}$	Zika associated reproduction number	0.7429	Fitted
$R_{0D}$	Dengue associated reproduction number	1.18817	Fitted
$R_{0K}$	Chikungunya associated reproduction number	1.1586	Fitted

**TABLE 2** Number of cases of SARS-COV-2, zika, dengue, and chikungunya, per epidemiological week in Espirito Santo State, Brazil from January 3, 2021 to April 17, 2021

Week	Period	COVID-19	Zika	Dengue	Chikungunya
1	03/01/2021–09/01/2021	180,620	24	251	85
2	10/01/2021–16/01/2021	179,134	31	238	95
3	17/01/2021–23/01/2021	177,939	28	250	105
4	24/01/2021–30/01/2021	161,190	32	267	102
5	31/01/2021–06/02/2021	140,813	22	235	72
6	07/02/2021–13/02/2021	132,170	23	195	63
7	14/02/2021–20/02/2021	118,948	31	206	63
8	21/02/2021–27/02/2021	117,321	19	238	58
9	28/02/2021–06/03/2021	123,501	28	277	101
10	07/03/2021–13/03/2021	131,566	25	310	97
11	14/03/2021–20/03/2021	151,517	26	373	100
12	21/03/2021–27/03/2021	189,768	25	358	99
13	28/03/2021–03/04/2021	218,909	31	306	99
14	04/04/2021–10/04/2021	223,309	31	454	93
15	11/04/2021–17/04/2021	217,807	31	401	99

Source: References 41 and 42.

syntax:  $x = \text{fmincon}(@\text{modelfun}, x0, A, b, Aeq, beq, lb, ub, \text{nonlcon}, \text{options})$ , starts at  $x0$  (the initial guesses) and finds an optimum  $x$  to the function described in  $@\text{modelfun}$  that fits the model to a given dataset, subject to the nonlinear inequalities  $c(x)$  or equalities  $ceq(x)$  defined in  $\text{nonlcon}$ , and also subject to the linear inequalities  $Ax \leq b$  and linear equalities  $Aeqx = beq$ , defined in  $A, b, Aeq, beq$ , respectively.  $x0$  can be a scalar, vector, or matrix.  $lb$  and  $ub$  are the bounds on the parameters to be estimated. The optimization parameters and error tolerance are specified in options. The method utilizes the least squares method, which is very efficient and reliable.<sup>44</sup> The method seeks to fit the observed datasets,  $Y_i$ , with the estimated values,  $X_i$ , such that; the sum of squares of errors between the observed and fitted curve is minimal.<sup>44</sup> The sum of squares error, SSE, is illustrated mathematically as:

$$\text{SSE} = \sum_{i=1}^k (Y_i - X_i)^2.$$

The results of the fittings are presented in Figure 4A–D. The period of the fitting covered 15 weeks, from January 3, 2021 to April 17, 2021 (*the period when there is a surge in the seasonal trend of the arboviruses*). The figures show that our proposed model fits well to the datasets. Furthermore, the projections of the cumulative COVID-19, zika, dengue, and chikungunya cases presented in Figure 5A–D also validates the fittings, and reveals when all infection curves flatten.

In the subsequent sections, we shall investigate the impact of various control strategies on the co-dynamics of all the diseases.

### 5.3 | Strategy A: Impact of COVID-19 prevention control ( $u_1 \neq 0$ )

The simulations of the optimal control system (17) when the only COVID-19 prevention strategy ( $u_1 \neq 0$ ) is implemented, are depicted in Figures 6A–D and 7A–C, respectively. The motivation for the choice of this scenario is what was obtainable during the COVID-19 pandemic. At this time, so much attention was given to the control of COVID-19, with very little or no efforts to curtail the co-circulation of the arboviruses. On implementation of this

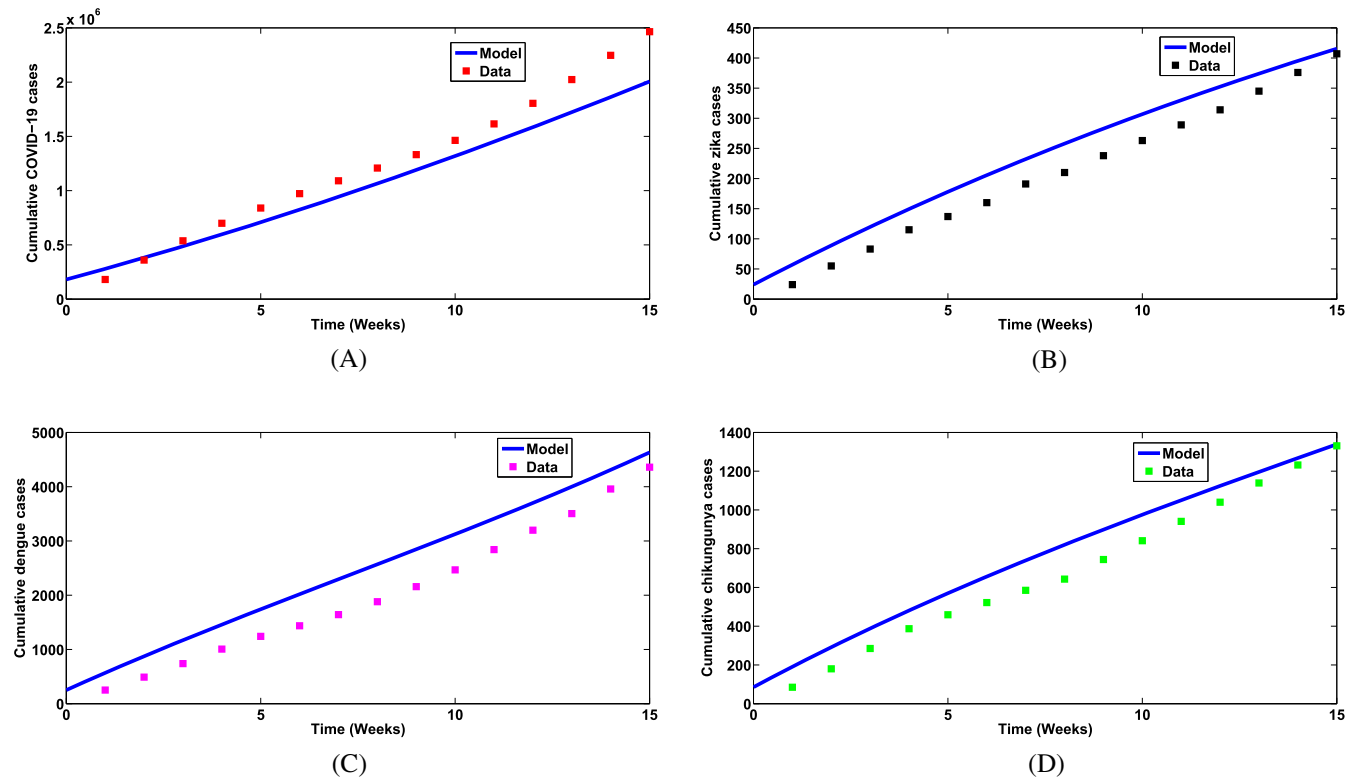


FIGURE 4 Model fittings using the cumulative (A) COVID-19, (B) zika, (C) dengue, and (D) chikungunya cases, respectively

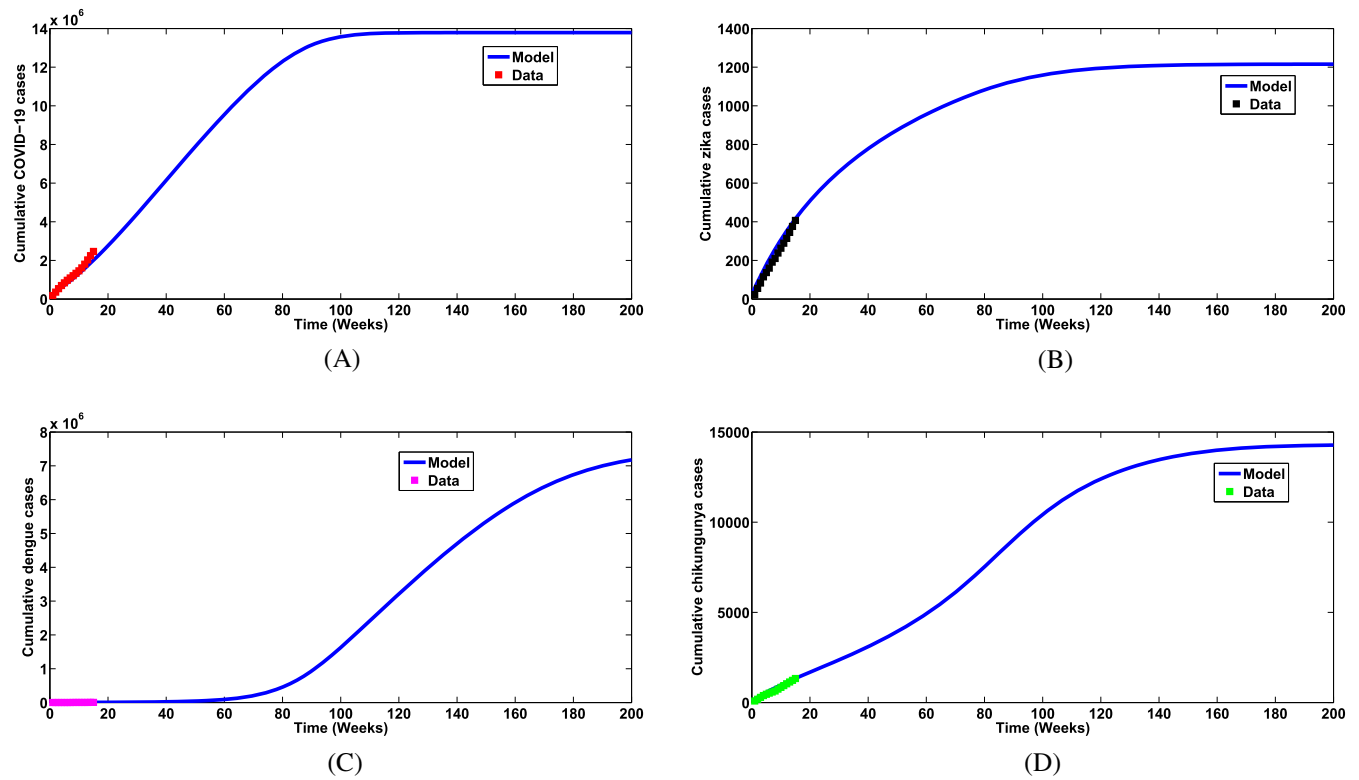
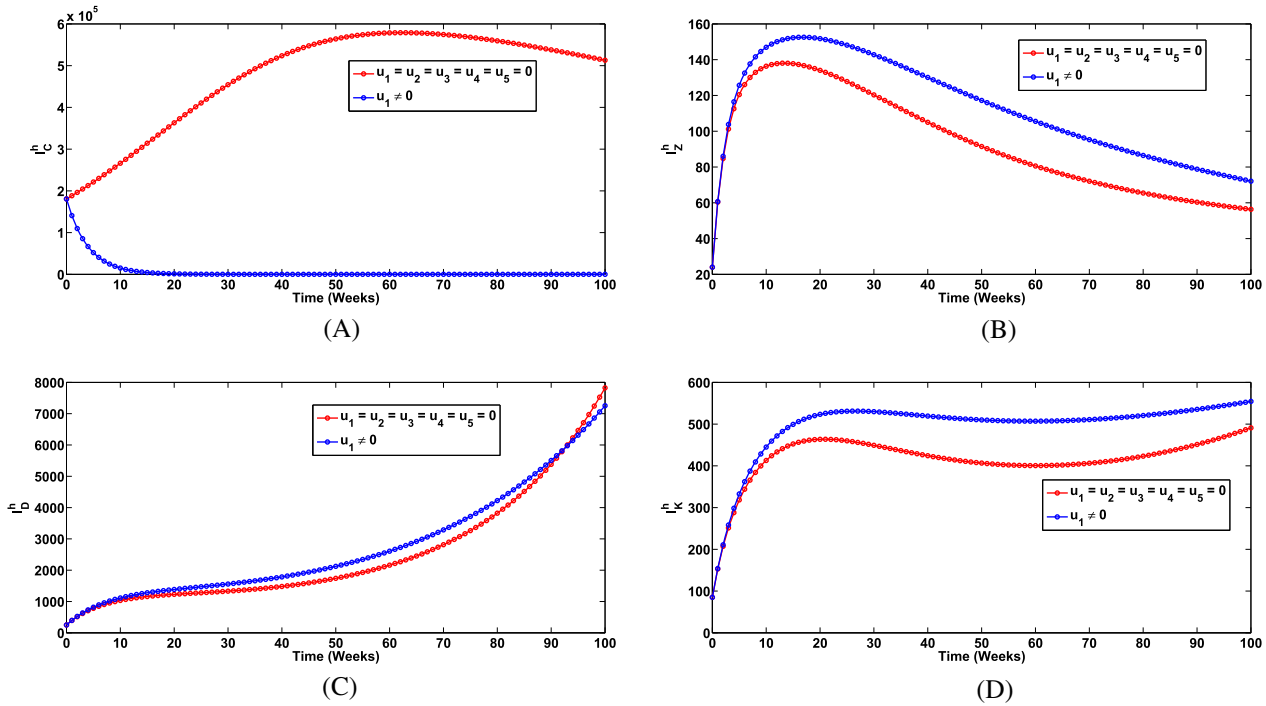


FIGURE 5 Projections using the cumulative (A) COVID-19, (B) zika, (C) dengue, and (D) chikungunya cases, respectively



**FIGURE 6** Impact of COVID-19 prevention strategy on individuals in various epidemiological classes: (A)  $I_C^h$  (B)  $I_Z^h$ , (C)  $I_D^h$ , and (D)  $I_K^h$ . Here,  $\beta_1 = 0.6150$ ,  $\beta_2 = 0.0866$ ,  $\beta_2^h = 0.0403$ ,  $\beta_3^h = 0.3029$ ,  $\beta_4^h = 0.1103$ ,  $\beta_2^v = 0.75$ ,  $\beta_3^v = 0.75$ ,  $\beta_4^v = 0.75$ , so that  $\mathcal{R}_0 = \max\{\mathcal{R}_{0C}, \mathcal{R}_{0Z}, \mathcal{R}_{0D}, \mathcal{R}_{0K}\} = 1.7693 > 1$

intervention strategy, for  $\beta_1 = 0.6150$ ,  $\beta_2 = 0.0866$ ,  $\beta_2^h = 0.0403$ ,  $\beta_3^h = 0.3029$ ,  $\beta_4^h = 0.1103$ ,  $\beta_2^v = 0.75$ ,  $\beta_3^v = 0.75$ ,  $\beta_4^v = 0.75$ , so that  $\mathcal{R}_0 = \max\{\mathcal{R}_{0C}, \mathcal{R}_{0Z}, \mathcal{R}_{0D}, \mathcal{R}_{0K}\} = 1.7693 > 1$ , we notice a significant decrease in the total number of individuals infected with COVID-19, as expected (shown in Figure 6A). However, this strategy has a marginal or detrimental impact on the control of zika, dengue, and chikungunya, as can be observed in Figure 6B–D. This is not surprising. The COVID-19 pandemic greatly disturbed the diagnosis, treatment, and preventive services for other diseases, such as the arboviruses, thereby putting millions of lives at risk of other infections.<sup>10</sup> Interestingly, this strategy also has significant impact on co-infected cases in Espirito Santo. It is observed that, significant co-infected cases of COVID-19 and zika are averted by this control strategy (as depicted in Figure 7A). Equally, this strategy prevented several new cases of COVID-19 and dengue co-infections, as observed in Figure 7B. In addition, we observe the prevention of over 300 cases of COVID-19 and chikungunya co-infections in the population (noticed in Figure 7C). COVID-19 prevention has also been reported to have a positive population level impact on COVID-19 and dengue co-infection cases.<sup>25</sup> In addition, Lorenz et al.<sup>5</sup> reported that social distancing rule, in order to contain COVID-19-may greatly reduce the risk of co-infection with other arboviruses in Brazil. Hence, it is not surprising that COVID-19 prevention greatly help bring down the co-infected cases, as observed in our simulations. The control profile for this strategy is shown in Figure 7D, where it is observed that the control was at its peak for more than half of the simulation period.

### 5.4 | Strategy B: Impact of zika prevention controls ( $u_2 \neq 0, u_3 \neq 0$ )

The simulations of the optimal control system (17) when the strategy that prevents zika transmission (via human and vectors) ( $u_2 \neq 0, u_3 \neq 0$ ) is implemented, are depicted in Figure 8A–C, respectively. Here, the aim is to assess the population level impact of this strategy. Implementing this intervention strategy, for  $\beta_1 = 0.6150$ ,  $\beta_2 = 0.0866$ ,  $\beta_2^h = 0.0403$ ,  $\beta_3^h = 0.3029$ ,  $\beta_4^h = 0.1103$ ,  $\beta_2^v = 0.75$ ,  $\beta_3^v = 0.75$ ,  $\beta_4^v = 0.75$ , so that  $\mathcal{R}_0 = \max\{\mathcal{R}_{0C}, \mathcal{R}_{0Z}, \mathcal{R}_{0D}, \mathcal{R}_{0K}\} = 1.7693 > 1$ , reveals a significant decrease in the total number of individuals infected with zika virus, as expected (shown in Figure 8A). Also, this

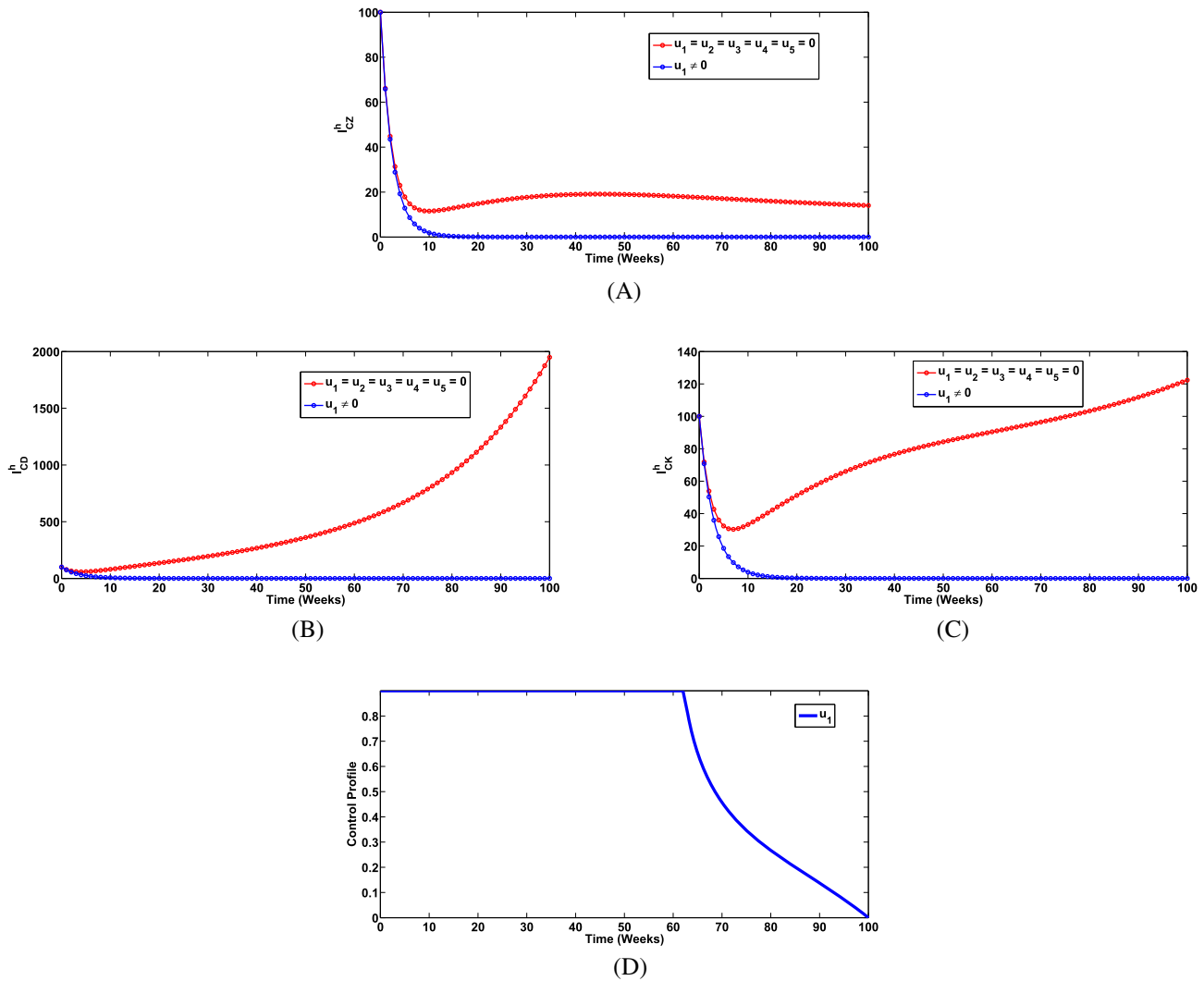


**FIGURE 7** Impact of COVID-19 prevention strategy on individuals in various epidemiological classes: (A)  $I_{CZ}^h$ , (B)  $I_{CD}^h$ , and (C)  $I_{CK}^h$ . (D) Control profile for  $u_1$ . Here,  $\beta_1 = 0.6150$ ,  $\beta_2 = 0.0866$ ,  $\beta_2^h = 0.0403$ ,  $\beta_3^h = 0.3029$ ,  $\beta_4^h = 0.1103$ ,  $\beta_2^v = 0.75$ ,  $\beta_3^v = 0.75$ ,  $\beta_4^v = 0.75$ , so that  $\mathcal{R}_0 = \max\{\mathcal{R}_{0C}, \mathcal{R}_{0Z}, \mathcal{R}_{0D}, \mathcal{R}_{0K}\} = 1.7693 > 1$ .

strategy has high positive population level impact on co-infected cases, observed in Figure 8B. We notice that, significant co-infected cases of COVID-19 and zika are averted by this control strategy. Equally, this strategy caused great reduction in infected vector populations as observed in Figure 8C. The control profiles for this strategy are depicted in Figure 8D,E. It is seen that the control against vector-human-human-to-vector transmission of zika has more efficacy than the control against the human to human transmission of zika. This is most likely due to the low value of the contact rate for human to human transmission, as noticed in Table 1, obtained from the fitting. Sexual transmission of zika has been relatively low compared to vector-human transmission. Thus, more efforts should be channeled toward controlling the vectors that spread the disease.

### 5.5 | Strategy C: Impact of dengue prevention control ( $u_4 \neq 0$ )

The simulations of system (17) when the strategy that prevents dengue transmission ( $u_4 \neq 0$ ) is implemented, are depicted in Figure 9A–C, respectively. Here also, the aim is to assess the population level impact of this strategy. Implementing this intervention strategy, for  $\beta_1 = 0.6150$ ,  $\beta_2 = 0.0866$ ,  $\beta_2^h = 0.0403$ ,  $\beta_3^h = 0.3029$ ,  $\beta_4^h = 0.1103$ ,  $\beta_2^v = 0.75$ ,  $\beta_3^v = 0.75$ ,  $\beta_4^v = 0.75$ , so that  $\mathcal{R}_0 = \max\{\mathcal{R}_{0C}, \mathcal{R}_{0Z}, \mathcal{R}_{0D}, \mathcal{R}_{0K}\} = 1.7693 > 1$ , reveals a significant decrease in the

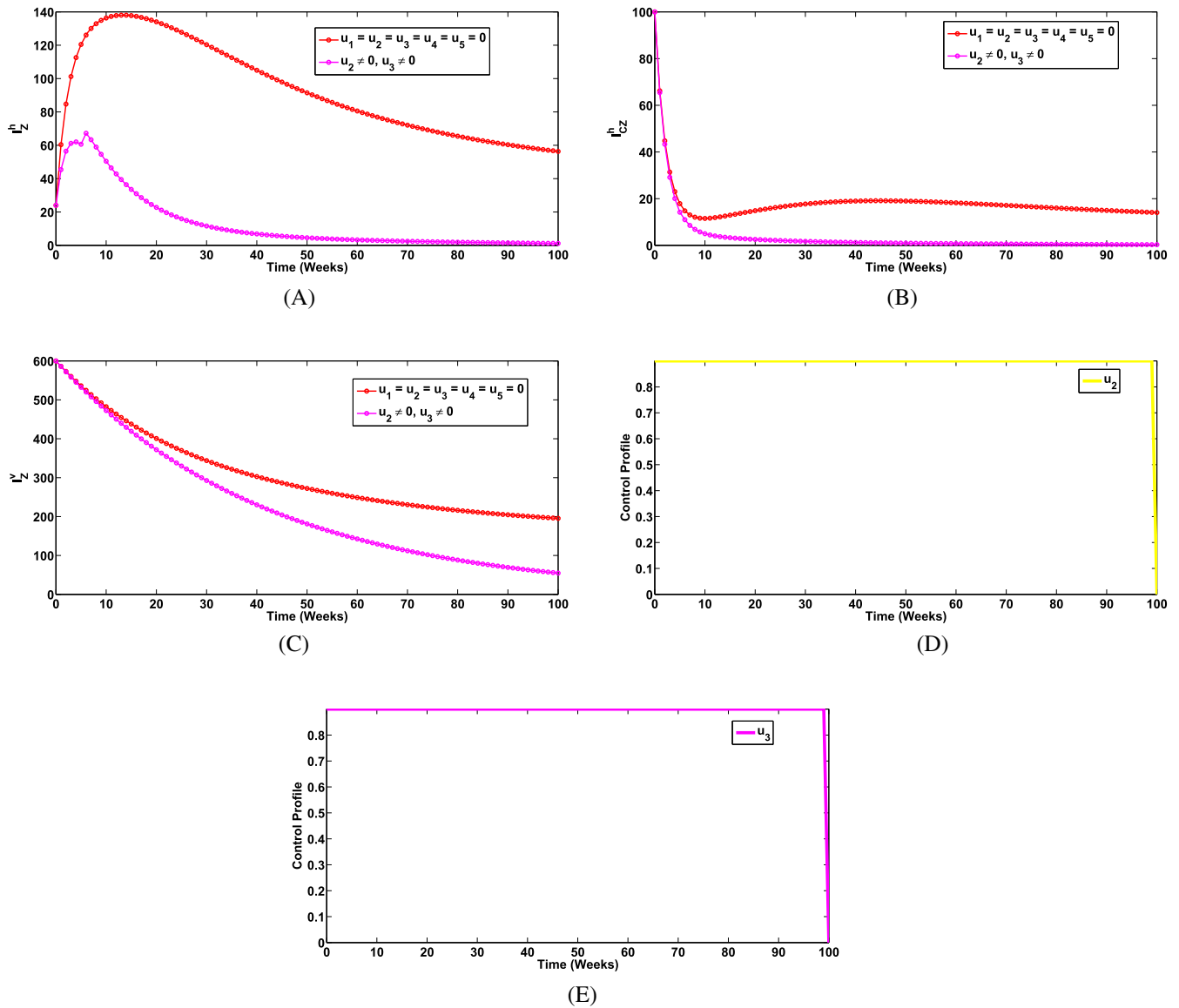


**FIGURE 8** Impact of zika prevention strategies on individuals in various epidemiological classes: (A)  $I_Z^h$ , (B)  $I_{CZ}^h$ . Impact of zika prevention strategies on vectors in epidemiological class: (C)  $I_Z^v$ . Control profile for (D)  $u_2$  and (E)  $u_3$ . Here,  $\beta_1 = 0.6150, \beta_2 = 0.0866, \beta_2^h = 0.0403, \beta_3^h = 0.3029, \beta_4^h = 0.1103, \beta_2^v = 0.75, \beta_3^v = 0.75, \beta_4^v = 0.75$ , so that  $\mathcal{R}_0 = \max\{\mathcal{R}_{OC}, \mathcal{R}_{OZ}, \mathcal{R}_{OD}, \mathcal{R}_{OK}\} = 1.7693 > 1$ .

total number of individuals infected with dengue virus, as expected (shown in Figure 9A). More so, this strategy has high positive population level impact on co-infected cases, seen in Figure 9B. It is also observed that, significant co-infected cases of COVID-19 and dengue are averted by this control strategy. Furthermore, this strategy caused great reduction in infected vector populations as observed in Figure 9C. The control profile for this strategy is depicted in Figure 9D. It is observed that, the control strategy against dengue transmission has significant impact.

**5.6 | Strategy D: Impact of chikungunya prevention control ( $u_5 \neq 0$ )**

Simulations of the model (17) when only chikungunya prevention control ( $u_5 \neq 0$ ) is administered, are presented in Figure 10A–C, respectively. The objective here is to assess the level of new infections this strategy

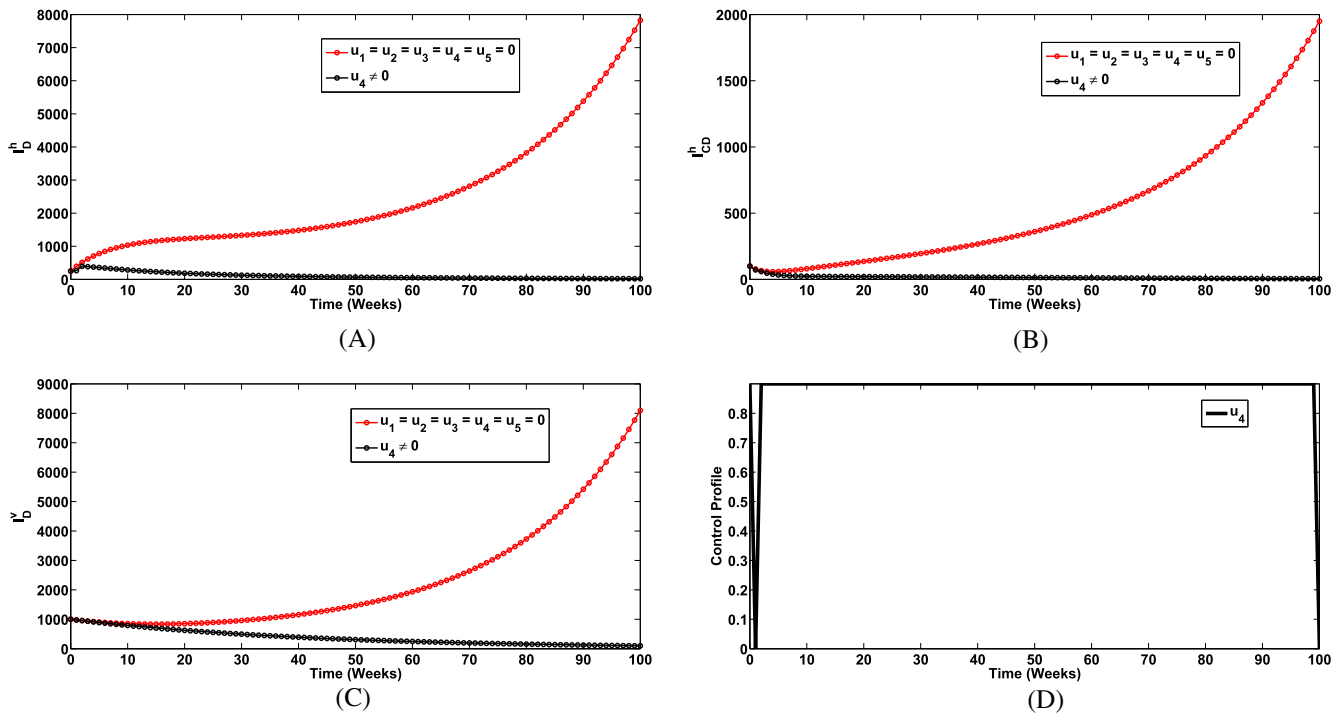


**FIGURE 9** Impact of dengue prevention strategies on individuals in various epidemiological classes: (A)  $I_D^h$ , (B)  $I_{CD}^h$ . Impact of dengue prevention strategies on vectors in epidemiological class: (C)  $I_D^v$ . (D) Control profile for  $u_4$ . Here,  $\beta_1 = 0.6150, \beta_2 = 0.0866, \beta_2^h = 0.0403, \beta_3^h = 0.3029, \beta_4^h = 0.1103, \beta_2^v = 0.75, \beta_3^v = 0.75, \beta_4^v = 0.75$ , so that  $\mathcal{R}_0 = \max\{\mathcal{R}_{OC}, \mathcal{R}_{OZ}, \mathcal{R}_{OD}, \mathcal{R}_{OK}\} = 1.7693 > 1$ .

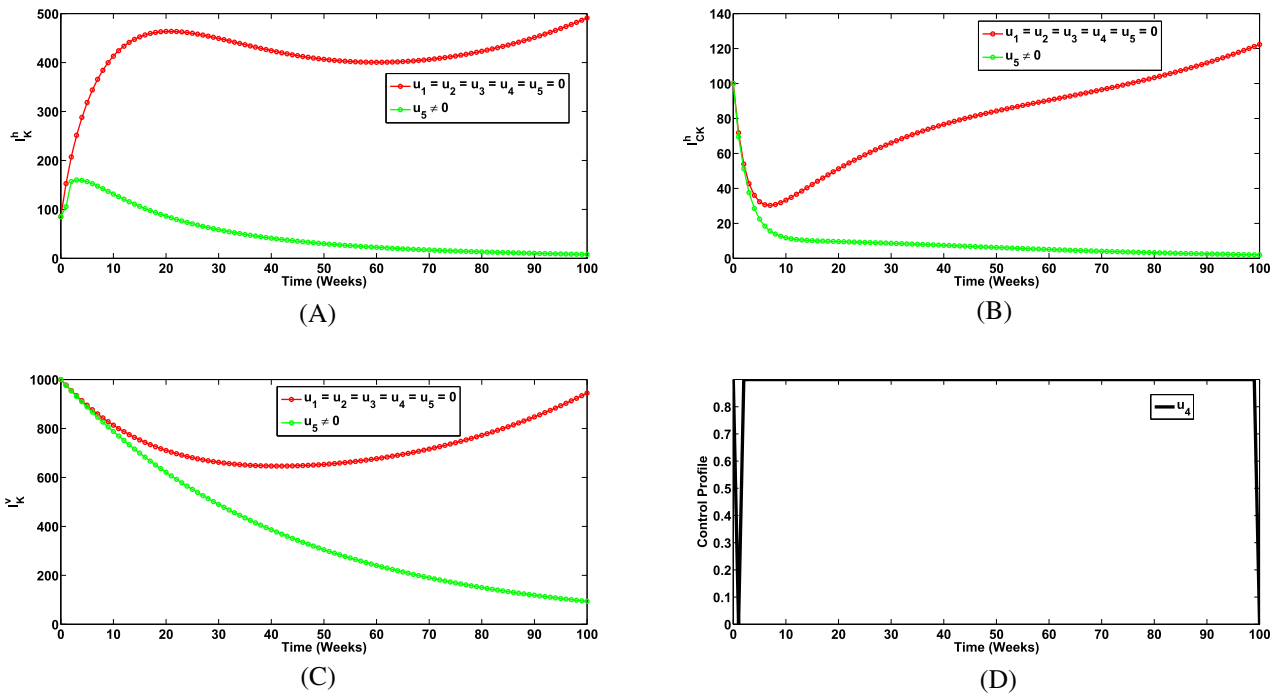


**FIGURE 10** Impact of chikungunya prevention strategy on individuals in various epidemiological classes: (A)  $I_K^h$ , (B)  $I_{CK}^h$ . Impact of chikungunya prevention strategy on vectors in epidemiological class: (C)  $I_K^v$ . (D) Control profile for  $u_5$ . Here,  $\beta_1 = 0.6150, \beta_2 = 0.0866, \beta_2^h = 0.0403, \beta_3^h = 0.3029, \beta_4^h = 0.1103, \beta_2^v = 0.75, \beta_3^v = 0.75, \beta_4^v = 0.75$ , so that  $\mathcal{R}_0 = \max\{\mathcal{R}_{OC}, \mathcal{R}_{OZ}, \mathcal{R}_{OD}, \mathcal{R}_{OK}\} = 1.7693 > 1$ .

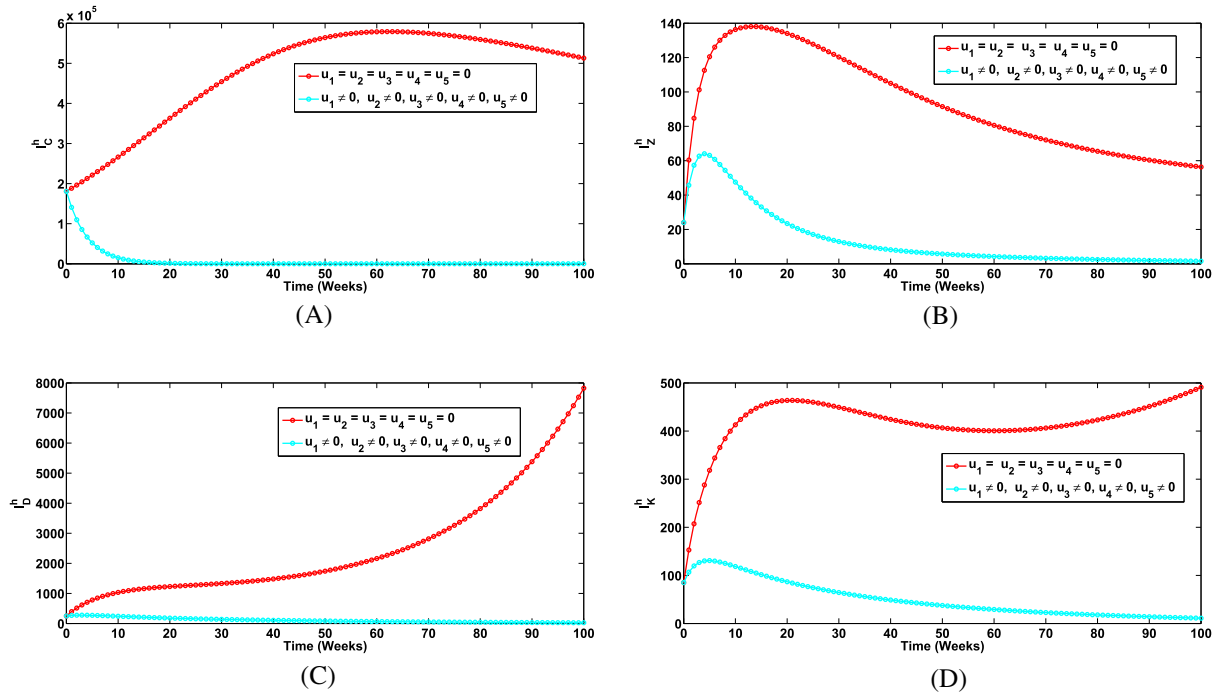


**FIGURE 11** Impact of universal control strategy on individuals in various epidemiological classes: (A)  $I_C^h$ , (B)  $I_Z^h$ , (C)  $I_D^h$ , and (D)  $I_K^h$ . Here,  $\beta_1 = 0.6150$ ,  $\beta_2 = 0.0866$ ,  $\beta_2^h = 0.0403$ ,  $\beta_3^h = 0.3029$ ,  $\beta_4^h = 0.1103$ ,  $\beta_2^v = 0.75$ ,  $\beta_3^v = 0.75$ ,  $\beta_4^v = 0.75$ , so that  $\mathcal{R}_0 = \max\{\mathcal{R}_{0C}, \mathcal{R}_{0Z}, \mathcal{R}_{0D}, \mathcal{R}_{0K}\} = 1.7693 > 1$ .

could avert, especially with respect to chikungunya-infected as well as co-infected populations. Applying this intervention strategy, for  $\beta_1 = 0.6150$ ,  $\beta_2 = 0.0866$ ,  $\beta_2^h = 0.0403$ ,  $\beta_3^h = 0.3029$ ,  $\beta_4^h = 0.1103$ ,  $\beta_2^v = 0.75$ ,  $\beta_3^v = 0.75$ ,  $\beta_4^v = 0.75$ , so that  $\mathcal{R}_0 = \max\{\mathcal{R}_{0C}, \mathcal{R}_{0Z}, \mathcal{R}_{0D}, \mathcal{R}_{0K}\} = 1.7693 > 1$ , shows a significant decrease in the total number of individuals infected with chikungunya virus, as expected (shown in Figure 9A). More so, this strategy has high positive population level impact on co-infected cases, seen in Figure 9B. It is also observed that, significant co-infected cases of COVID-19 and dengue are averted by this control strategy. Furthermore, this strategy caused great reduction in infected vector populations as observed in Figure 10C. The control profile for this strategy is depicted in Figure 10D. It is observed that, the control strategy against dengue transmission has significant impact.

**5.7 | Strategy E: Impact of universal control strategy ( $u_1 \neq 0, u_2 \neq 0, u_3 \neq 0, u_4 \neq 0, u_5 \neq 0$ )**

Simulations of the model (17) when all control strategies ( $u_1 \neq 0, u_2 \neq 0, u_3 \neq 0, u_4 \neq 0, u_5 \neq 0$ ) are implemented, are presented in Figures 11A–D, 12A–C, and 13A–C, respectively. This scenario, unlike the previous scenarios, focuses not only on COVID-19 prevention, but also on the elimination of the arboviruses: zika, dengue, and chikungunya. Applying this intervention strategy, for  $\beta_1 = 0.6150$ ,  $\beta_2 = 0.0866$ ,  $\beta_2^h = 0.0403$ ,  $\beta_3^h = 0.3029$ ,  $\beta_4^h = 0.1103$ ,  $\beta_2^v = 0.75$ ,  $\beta_3^v = 0.75$ ,  $\beta_4^v = 0.75$ , so that  $\mathcal{R}_0 = \max\{\mathcal{R}_{0C}, \mathcal{R}_{0Z}, \mathcal{R}_{0D}, \mathcal{R}_{0K}\} = 1.7693 > 1$ , shows very significant decrease in the total number of individuals infected with COVID-19, zika, chikungunya, and co-infections. This is not surprising. If efforts are stepped up against the co-circulation of all the diseases, then this would greatly lead to speedy elimination or reduction of new infections in the population. This strategy shows more significant reduction in new infections compared to the scenario when only the single control strategies are adopted. In addition, this strategy caused great reduction in infected vector populations as observed in Figure 13A–C. Thus, the strategy that combines and strictly implements preventive controls against COVID-19 and the arboviruses is the most effective in controlling the co-circulation of all the diseases in the population.

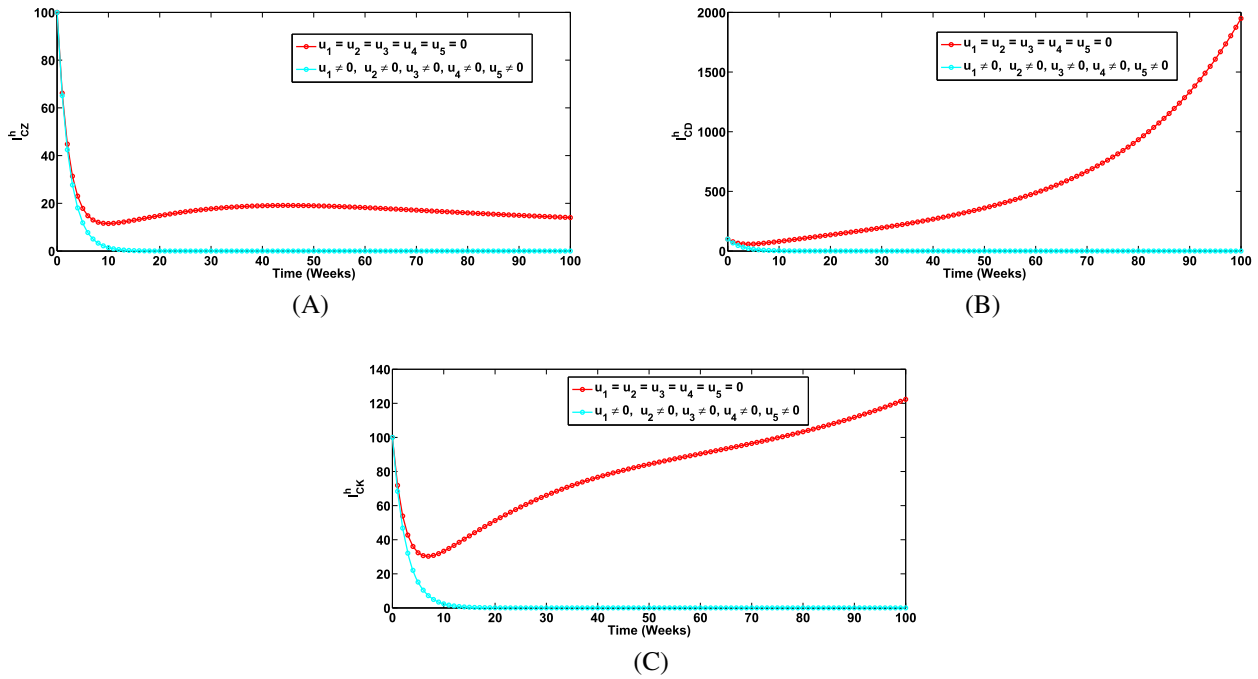


**FIGURE 12** Impact of universal control strategy on individuals in various epidemiological classes: (A)  $I_{CZ}^h$ , (B)  $I_{CD}^h$ , and (C)  $I_{CK}^h$ . Here,  $\beta_1 = 0.6150, \beta_2 = 0.0866, \beta_2^h = 0.0403, \beta_3^h = 0.3029, \beta_4^h = 0.1103, \beta_2^v = 0.75, \beta_3^v = 0.75, \beta_4^v = 0.75$ , so that  $\mathcal{R}_0 = \max\{\mathcal{R}_{0C}, \mathcal{R}_{0Z}, \mathcal{R}_{0D}, \mathcal{R}_{0K}\} = 1.7693 > 1$

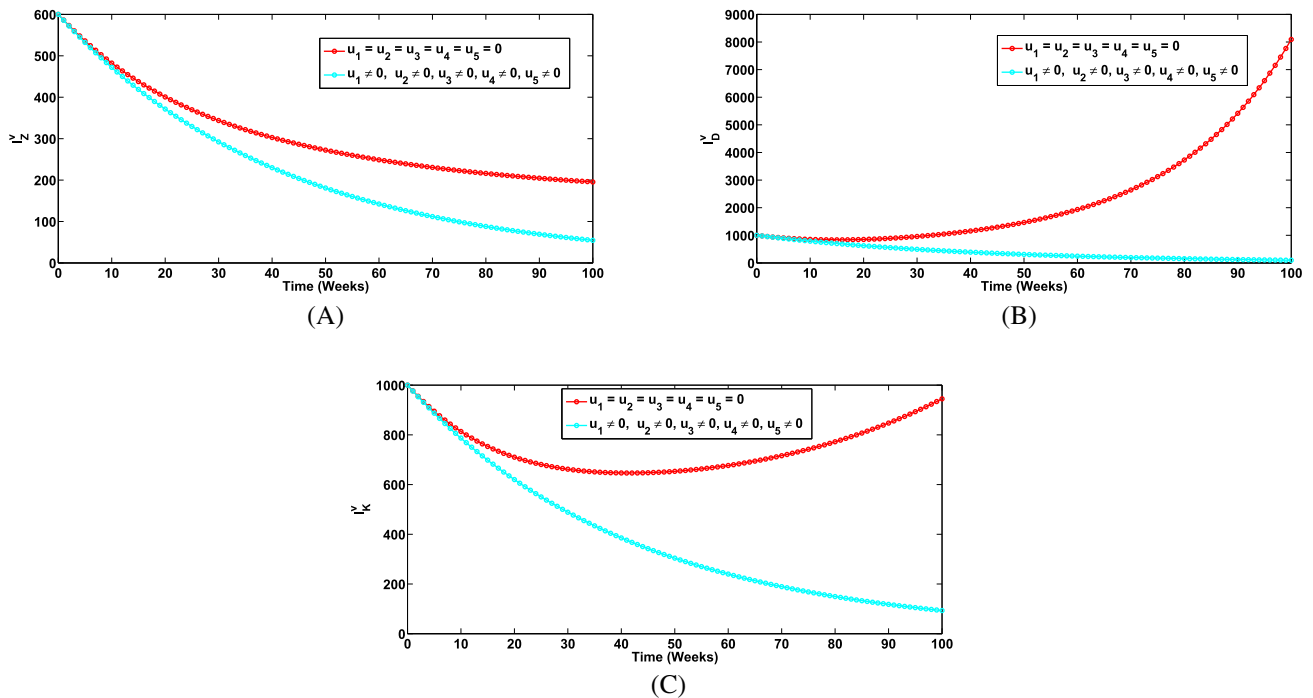


**FIGURE 13** Impact of universal control strategy on vectors in various epidemiological classes: (A)  $I_Z^v$ , (B)  $I_D^v$ , and (C)  $I_K^v$ . Here,  $\beta_1 = 0.6150, \beta_2 = 0.0866, \beta_2^h = 0.0403, \beta_3^h = 0.3029, \beta_4^h = 0.1103, \beta_2^v = 0.75, \beta_3^v = 0.75, \beta_4^v = 0.75$ , so that  $\mathcal{R}_0 = \max\{\mathcal{R}_{0C}, \mathcal{R}_{0Z}, \mathcal{R}_{0D}, \mathcal{R}_{0K}\} = 1.7693 > 1$

## 6 | CONCLUSION

A new mathematical model for COVID-19, zika, chikungunya, and dengue co-dynamics, with optimal control analysis is designed and studied to assess the impact of COVID-19 on zika, dengue, and chikungunya dynamics and vice-versa. The local and global stability analyses are carried out. Using the center manifold theory,<sup>34</sup> the model is shown to undergo backward bifurcation under a certain condition. To effectively manage the co-circulation of all the diseases under an endemic setting, time dependent controls in the form of COVID-19, zika, dengue, and chikungunya preventions are incorporated into the model. Global sensitivity analysis is also carried out on the parameters of the model to determine the most dominant terms with respect to each of the associated reproduction numbers and co-infected components of the model, respectively. For instance, using the zika-related reproduction number  $\mathcal{R}_{0Z}$ , as the response function, the important parameters are: the effective contact rate for vector-to-human transmission of zika ( $\beta_2^h$ , which is positively correlated), the human natural death rate ( $\vartheta^h$ , positively correlated), and the vector recruitment rate ( $\Psi^v$ ). Although the human-to-human transmission rate for zika ( $\beta_2$ ) is positively correlated, its impact is very negligible, as observed in Figure 2B. Also, using the class of individuals co-infected with COVID-19 and zika ( $\mathcal{I}_{CZ}^h$ ) as response function, the most dominant parameters are: the effective contact rate for COVID-19 transmission ( $\beta_1$ , positively correlated), the effective contact rate for vector-to-human transmission of zika ( $\beta_2^h$ , positively correlated). Other important parameters driving the dynamics of infections in this class are COVID-19 recovery rate ( $\zeta_C$ , negatively correlated) and the zika recovery rate ( $\zeta_Z$ ). Although the human-to-human transmission rate for zika ( $\beta_2$ ) is positively correlated, its impact on this epidemiological class is also very negligible, as observed in Figure 3A.

The simulations of the optimized system show that:

1. COVID-19 only prevention could greatly reduce the burden of COVID-19 and co-infections with zika, dengue, and chikungunya, respectively.
2. Focusing only on COVID-19 prevention strategies without any measure to control the arboviruses, could have marginal or detrimental impact on the arboviruses: zika, dengue, and chikungunya.
3. Preventive efforts against zika, dengue, and chikungunya, respectively, can significantly reduce the burden of co-infections with COVID-19.
4. Adopting an intervention strategy that focuses on the combined preventive controls against COVID-19, zika, dengue, and chikungunya was the most effective in reducing the co-circulation all the diseases within the population.

The current research has some limitations as well. In this article, to avoid model complexity, asymptomatic classes for COVID-19, zika, dengue, and chikungunya are not considered. These can be incorporated in a further work in this direction. In addition, less is known about infection acquired or vaccine-derived cross-immunity between COVID-19 and the arboviruses. No detailed information yet available to answer the question; whether the current available COVID-19 vaccines could have any impact on the dynamics of zika, dengue, and chikungunya. Thus, with more reliable data and detailed information about the interactions of the diseases, further study in this direction will be a matter of great interest. Mutations of viral and arboviral infections also invite further studies on their co-infections with other diseases. One could thus, consider a model for the co-dynamics of multi-strains of COVID-19, zika, dengue, and chikungunya. Also, the proposed model in this current work did not consider multiple co-infections or co-infection with two arboviral infections, which is quite possible. Future work with sufficient biological reports can also consider multiple co-infections and co-infections among the arboviruses. To the best of our knowledge, the work presented in this article is the first epidemiological study on COVID-19 and the three arboviral infections (zika, dengue, and chikungunya). However, more studies could be devoted to other mathematical (stochastic, agent based modeling, within/intra-host) and epidemiological dynamics of this co-interaction.

### ACKNOWLEDGMENTS

The authors specially thank the handling editor and anonymous reviewers for their constructive comments and queries which greatly helped improve the quality of the article.

### AUTHOR CONTRIBUTIONS

**Andrew Omame:** Conceptualization, Formal Analysis and Methodology, Writing Original Draft, Software; **Mary Ele Isah:** Writing Original Draft, Review & Editing; **Mujahid Abbas:** Writing Original Draft, Validation, Review & Editing, Supervision.

## DATA AVAILABILITY STATEMENT

The MATLAB codes written to run all the simulations presented in this work can be found on GitHub via the link: [https://github.com/andy-2727/Github\\_Omame](https://github.com/andy-2727/Github_Omame).

## ORCID

Andrew Omame  <https://orcid.org/0000-0002-1252-1650>

## REFERENCES

- Vicente CR, da Silva TCC, Pereira LDA, Miranda AE. Impact of concurrent epidemics of dengue, Chikungunya, Zika, and COVID-19. *J Braz Soc Trop Med*. 2021;54:e0837-e2020. doi:10.1590/0037-8682-0837-2020
- Ribeiro VST, Telles JP, Tuon FF. Arboviral diseases and COVID-19 in Brazil: concerns regarding climatic, sanitation, and endemic scenario. *J Med Virol*. 2020;92(11):2390-2391.
- Wilder-Smith A, Tissera H, Ooi EE, Coloma J, Scott TW, Gubler DJ. Preventing dengue epidemics during the COVID-19 pandemic. *Am J Trop Med Hyg*. 2020;103(2):570-571.
- do Rosário MS, de Siqueira IC. Concerns about COVID-19 and Arboviral (Chikungunya, Dengue, Zika) concurrent outbreaks. *Braz J Infect Dis*. 2020;24(6):583-584.
- Lorenz C, Azevedo TS, Chiaravalloti-Neto F. COVID-19 and dengue fever: a dangerous combination for the health system in Brazil. *Travel Med Infect Dis*. 2020;35:101659. doi:10.1016/j.tmaid.2020.101659
- Brito A, Machado L, Siconelli M, et al. MedRxiv; 2020. 10.1101/2020.08.10.20172247
- Ministerio da Saude. Monitoramento dos casos de arboviroses urbanas transmitidas pelo Aedes Aegypti (dengue, chikungunya e zika). *Semanas Epidemiol*. 2020;51:1-39. [https://www.gov.br/saude/ptbr/media/pdf/2020/outubro/23/boletim\\_epidemiologico\\_svs\\_41](https://www.gov.br/saude/ptbr/media/pdf/2020/outubro/23/boletim_epidemiologico_svs_41). Accessed May 3, 2022.
- MS/SVS. Monitoramento Dos Casos de Arboviroses Urbanas Transmitidas Pelo Aedes Aegypti (Dengue, Chikungunya e Zika). *Semanas Epidemiol*. 2020;51:1-26.
- Rodriguez-Morales AJ, Gallego V, Escalera-Antezana JP, et al. COVID-19 in Latin America: the implications of the first confirmed case in Brazil. *Travel Med Infect Dis*. 2020;35:101613. doi:10.1016/j.tmaid.2020.101613
- COVID-19: massive impact on lower-income countries threatens more disease outbreaks Gavi, the Vaccine Alliance; 2021. [gavi.org/news/media-room/covid-19-massive-impact-lower-income-countries-threatens-more-disease-outbreaks](https://www.gavi.org/news/media-room/covid-19-massive-impact-lower-income-countries-threatens-more-disease-outbreaks). Accessed 7 April 2022.
- Impact of COVID-19 on vaccine supplies. UNICEF Supply Division; 2020. <https://www.unicef.org/supply/stories/impact-covid-19-vaccine-supplies>. Accessed 7 April 2022.
- da Silva SJR, de Magalhaes JJF, Pena L. Simultaneous circulation of DENV, CHIKV, ZIKV and SARS-CoV-2 in Brazil: an inconvenient truth. *One Health*. 2021;12:100205.
- Nunez-Avellaneda D, Villagomez FR, Villegas-Pineda JC, et al. Evidence of coinfections between SARS-CoV-2 and select arboviruses in Guerrero, Mexico, 2020-2021. *Am J Trop Med Hyg*. 2022;106(3):896-899. doi:10.4269/ajtmh.21-1216
- Lokida D, Lukman N, Salim G, et al. Diagnosis of COVID-19 in a dengue-endemic area. *Am J Trop Med Hyg*. 2020;103:1220-1222.
- Asamoah JKK, Owusu MA, Jin Z, Oduro FT, Abidemi A, Gyasi EO. Global stability and cost-effectiveness analysis of COVID-19 considering the impact of the environment: using data from Ghana. *Chaos Soliton Fract*. 2020;140:110103. doi:10.1016/j.chaos.2020.110103
- Nkwayep CH, Bowong S, Tewa JJ, Kurths J. Short-term forecasts of the COVID-19 pandemic: study case of Cameroon. *Chaos, Solitons Fractals*. 2020;140:110106. doi:10.1016/j.chaos.2020.110106
- Wang H, Wang Z, Dong Y, et al. Phase-adjusted estimation of the number of coronavirus disease 2019 cases in Wuhan. *China Cell Discov*. 2020;6(1):1-8.
- Asamoah JKK, Okyere E, Abidemi A, et al. Optimal control and comprehensive cost-effectiveness analysis for COVID-19. *Results Phys*. 2022;33:105177. doi:10.1016/j.rinp.2022.105177
- Kucharski AJ, Russell TW, Diamond C, et al. Early dynamics of transmission and control of COVID-19: a mathematical modelling study. *Lancet Infect Dis*. 2020;20(5):553-558.
- Ferguson N, Laydon D, Gilani GN, et al. Report 9: impact of non-pharmaceutical interventions (NPIs) to reduce COVID-19. *Mortal Healthcare Demand*. 2020:1-20. doi:10.25561/77482
- Maier BF, Brockmann D. Effective containment explains subexponential growth in recent confirmed COVID-19 cases in China. *Science*. 2020;368(6492):742-746.
- Omame A, Abbas M, Onyenegecha CP. Backward bifurcation and optimal control in a co-infection model for SARS-CoV-2 and ZIKV. *Res Phys*. 2022;37:105481. doi:10.1016/j.rinp.2022.105481
- Omame A, Okuonghae D. A co-infection model for oncogenic human papillomavirus and tuberculosis with optimal control and cost-effectiveness analysis. *Optim Contr Appl Meth*. 2021;42(4):1081-1101. doi:10.1002/oca.2717
- Bonyah E, Khan MA, Okosun KO, Gómez-Aguilar JF. On the co-infection of dengue fever and Zika virus. *Optim Contr Appl Meth*. 2019;40(3):394-421.
- Omame A, Rwezaura H, Diagne ML, et al. COVID-19 and dengue co-infection in Brazil: optimal control and cost-effectiveness analysis. *Eur Phys J Plus*. 2021;136:1090. doi:10.1140/epjp/s13360-021-02030-6
- Hezam IM. COVID-19 and Chikungunya: an optimal control model with consideration of social and environmental factors. *J Ambient Intell Humaniz Comput*. 2022. doi:10.1007/s12652-022-03796-y

27. Okuneye KO, Velasco-Hernandez JX, Gumel AB. The eunholye Chikungunya-Dengue-Zika trinity: a theoretical analysis. *J Biol Syst.* 2017;25(4):545-585.
28. Nwankwo A, Okuonghae D. Mathematical analysis of the transmission dynamics of HIV syphilis Co-infection in the presence of treatment for syphilis. *Bull Math Biol.* 2018;80(3):437-492.
29. Garba SM, Gumel AB, Abu Bakar MR. Backward bifurcations in dengue transmission dynamics. *Math Biosci.* 2008;215:11-25.
30. <https://www.citypopulation.de/en/brazil/cities/espirtosanto/>. Accessed January 1, 2022.
31. [https://www.indexmundi.com/brazil/demographics\\_profile.html](https://www.indexmundi.com/brazil/demographics_profile.html). Accessed January 1, 2022.
32. van den Driessche P, Watmough J. Reproduction numbers and sub-threshold endemic equilibria for compartmental models of disease transmission. *Math Biosci.* 2002;180(1):29-48.
33. Castillo-Chavez C, Feng Z, Huang W. On the computation of  $R_0$  and its role on global stability. *Mathematical Approaches for Emerging and Reemerging Infectious Diseases: An Introduction.* Vol 125. Springer; 1999:229-250.
34. Castillo-Chavez C, Song B. Dynamical models of tuberculosis and their applications. *Math Biosci Eng.* 2004;2:361-404.
35. Villar L, Dayan GH, Arredondo-Garcia JL, et al. Efficacy of a tetravalent dengue vaccine in children in Latin America. *N Engl J Med.* 2015;372:113-123. doi:10.1056/NEJMoa1411037
36. Fleming WH, Rishel RW. *Deterministic and Stochastic Optimal Control.* Springer; 1975.
37. Olaniyi S, Okosun K, Adesanya S, Lebelo R. Modelling malaria dynamics with partial immunity and protected travellers: optimal control and cost-effectiveness analysis. *J Biol Dyn.* 2020;14(1):90-115.
38. Pontryagin L, Boltyanskii V, Gamkrelidze R, Mishchenko E. *The Mathematical Theory of Optimal Control Process.* Vol 4. John Wiley & Sons; 1963.
39. Lenhart S, Workman JT. *Optimal Control Applied to Biological Models.* Mathematical and Computational Biology Series. Chapman & Hall/CRC; 2007.
40. Blower SM, Dowlatabadi H. Sensitivity and uncertainty analysis of complex models of disease transmission: an HIV model, as an example. *Int Stat Rev.* 1994;2:229-243.
41. <https://www.es.gov.br/Noticia/sesa-divulga-36-boletim-da-dengue-zika-e-chikungunya>. Accessed January 1, 2022.
42. [https://coronalevel.com/Brazil/EspC3ADrito\\_Santo/](https://coronalevel.com/Brazil/EspC3ADrito_Santo/). Accessed January 1, 2022.
43. McCall J. Genetic algorithms for modelling and optimisation. *J Comput Appl Math.* 2005;184:205-222.
44. Martcheva M. *An Introduction to Mathematical Epidemiology.* Vol 61. Springer; 2015.

## SUPPORTING INFORMATION

Additional supporting information can be found online in the Supporting Information section at the end of this article.

**How to cite this article:** Omame A, Isah ME, Abbas M. An optimal control model for COVID-19, zika, dengue, and chikungunya co-dynamics with reinfection. *Optim Control Appl Meth.* 2022;1-35. doi: 10.1002/oca.2936

## APPENDIX A. THE NONZERO SECOND PARTIAL DERIVATIVES USED FOR THE BACKWARD BIFURCATION ANALYSIS

$$\begin{aligned} \frac{\partial^2 f_2}{\partial x_2^2} &= -\frac{2\beta_1 x_1^*}{\mathcal{N}^{h*2}}, \quad \frac{\partial^2 f_2}{\partial x_2 \partial x_3} = -\frac{\beta_1 x_1^*}{\mathcal{N}^{h*2}} - \frac{\beta_2}{\mathcal{N}^{h*2}}, \quad \frac{\partial^2 f_2}{\partial x_2 \partial x_4} = \frac{\partial^2 f_2}{\partial x_2 \partial x_5} = -\frac{\beta_1 x_1^*}{\mathcal{N}^{h*2}}, \\ \frac{\partial^2 f_2}{\partial x_2 \partial x_{14}} &= -\frac{\beta_2^h}{\mathcal{N}^{h*}}, \quad \frac{\partial^2 f_2}{\partial x_2 \partial x_{15}} = -\frac{\beta_3^h}{\mathcal{N}^{h*}}, \quad \frac{\partial^2 f_2}{\partial x_2 \partial x_{16}} = -\frac{\beta_4^h}{\mathcal{N}^{h*}}, \\ \frac{\partial^2 f_3}{\partial x_2 \partial x_3} &= -\frac{\beta_2 x_1^*}{\mathcal{N}^{h*2}} - \frac{\beta_1}{\mathcal{N}^{h*}}, \quad \frac{\partial^2 f_3}{\partial x_3^2} = -\frac{2\beta_2 x_1^*}{\mathcal{N}^{h*2}}, \quad \frac{\partial^2 f_3}{\partial x_3 \partial x_4} = \frac{\partial^2 f_3}{\partial x_3 \partial x_5} = -\frac{\beta_2 x_1^*}{\mathcal{N}^{h*2}}, \\ \frac{\partial^2 f_3}{\partial x_2 \partial x_{14}} &= -\frac{\beta_2^h x_1^*}{\mathcal{N}^{h*2}}, \quad \frac{\partial^2 f_3}{\partial x_3 \partial x_{14}} = -\frac{\beta_2^h x_1^*}{\mathcal{N}^{h*2}}, \quad \frac{\partial^2 f_3}{\partial x_4 \partial x_{14}} = \frac{\partial^2 f_3}{\partial x_5 \partial x_{14}} = -\frac{\beta_2^h x_1^*}{\mathcal{N}^{h*2}}, \\ \frac{\partial^2 f_4}{\partial x_2 \partial x_4} &= -\frac{\beta_1}{\mathcal{N}^{h*}}, \quad \frac{\partial^2 f_4}{\partial x_2 \partial x_{15}} = -\frac{\beta_3^h x_1^*}{\mathcal{N}^{h*2}}, \quad \frac{\partial^2 f_4}{\partial x_3 \partial x_{15}} = -\frac{\beta_3^h x_1^*}{\mathcal{N}^{h*2}}, \quad \frac{\partial^2 f_4}{\partial x_4 \partial x_{15}} = \frac{\partial^2 f_4}{\partial x_5 \partial x_{15}} = -\frac{\beta_3^h x_1^*}{\mathcal{N}^{h*2}}, \\ \frac{\partial^2 f_5}{\partial x_2 \partial x_5} &= -\frac{\beta_1}{\mathcal{N}^{h*}}, \quad \frac{\partial^2 f_5}{\partial x_2 \partial x_{16}} = -\frac{\beta_4^h x_1^*}{\mathcal{N}^{h*2}}, \quad \frac{\partial^2 f_5}{\partial x_3 \partial x_{16}} = -\frac{\beta_4^h x_1^*}{\mathcal{N}^{h*2}}, \quad \frac{\partial^2 f_5}{\partial x_4 \partial x_{16}} = \frac{\partial^2 f_5}{\partial x_5 \partial x_{16}} = -\frac{\beta_4^h x_1^*}{\mathcal{N}^{h*2}}, \end{aligned}$$

$$\begin{aligned} \frac{\partial^2 f_6}{\partial x_2 \partial x_3} &= \frac{\beta_1}{\mathcal{N}^{h*}} + \frac{\beta_2}{\mathcal{N}^{h*}}, \quad \frac{\partial^2 f_6}{\partial x_2 \partial x_{14}} = \frac{\beta_2^h}{\mathcal{N}^{h*}}, \quad \frac{\partial^2 f_7}{\partial x_2 \partial x_4} = \frac{\beta_1}{\mathcal{N}^{h*}}, \quad \frac{\partial^2 f_7}{\partial x_2 \partial x_{15}} = \frac{\beta_3^h}{\mathcal{N}^{h*}}, \quad \frac{\partial^2 f_8}{\partial x_2 \partial x_5} = \frac{\beta_1}{\mathcal{N}^{h*}}, \quad \frac{\partial^2 f_8}{\partial x_2 \partial x_{16}} = \frac{\beta_4^h}{\mathcal{N}^{h*}}, \\ \frac{\partial^2 f_{14}}{\partial x_1 \partial x_3} &= \frac{\partial^2 f_{14}}{\partial x_2 \partial x_3} = \frac{\partial^2 f_{14}}{\partial x_3 \partial x_4} = \frac{\partial^2 f_{14}}{\partial x_3 \partial x_5} = \frac{\partial^2 f_{14}}{\partial x_3 \partial x_9} = \frac{\partial^2 f_{14}}{\partial x_3 \partial x_{10}} = \frac{\partial^2 f_{14}}{\partial x_3 \partial x_{11}} = \frac{\partial^2 f_{14}}{\partial x_3 \partial x_{12}} = -\frac{\beta_2^v}{\mathcal{N}^{h*2}}, \\ \frac{\partial^2 f_{14}}{\partial x_3^2} &= -\frac{\beta_2^v}{\mathcal{N}^{h*2}}, \quad \frac{\partial^2 f_{14}}{\partial x_3 \partial x_{13}} = \frac{\beta_2^v}{\mathcal{N}^{h*}}, \\ \frac{\partial^2 f_{15}}{\partial x_1 \partial x_4} &= \frac{\partial^2 f_{15}}{\partial x_2 \partial x_4} = \frac{\partial^2 f_{15}}{\partial x_3 \partial x_4} = \frac{\partial^2 f_{15}}{\partial x_4 \partial x_5} = \frac{\partial^2 f_{15}}{\partial x_4 \partial x_9} = \frac{\partial^2 f_{15}}{\partial x_4 \partial x_{10}} = \frac{\partial^2 f_{15}}{\partial x_4 \partial x_{11}} = \frac{\partial^2 f_{15}}{\partial x_4 \partial x_{12}} = -\frac{\beta_3^v}{\mathcal{N}^{h*2}}, \\ \frac{\partial^2 f_{15}}{\partial x_4^2} &= -\frac{\beta_3^v}{\mathcal{N}^{h*2}}, \quad \frac{\partial^2 f_{15}}{\partial x_4 \partial x_{13}} = \frac{\beta_3^v}{\mathcal{N}^{h*}}, \\ \frac{\partial^2 f_{16}}{\partial x_1 \partial x_5} &= \frac{\partial^2 f_{16}}{\partial x_2 \partial x_5} = \frac{\partial^2 f_{16}}{\partial x_3 \partial x_5} = \frac{\partial^2 f_{16}}{\partial x_4 \partial x_5} = \frac{\partial^2 f_{16}}{\partial x_5 \partial x_9} = \frac{\partial^2 f_{16}}{\partial x_5 \partial x_{10}} = \frac{\partial^2 f_{16}}{\partial x_5 \partial x_{11}} = \frac{\partial^2 f_{16}}{\partial x_5 \partial x_{12}} = -\frac{\beta_4^v}{\mathcal{N}^{h*2}}, \\ \frac{\partial^2 f_{16}}{\partial x_5^2} &= -\frac{\beta_4^v}{\mathcal{N}^{h*2}}, \quad \frac{\partial^2 f_{16}}{\partial x_5 \partial x_{13}} = \frac{\beta_4^v}{\mathcal{N}^{h*}}. \end{aligned}$$

## APPENDIX B. PROOF OF THEOREM 6

Suppose the control set consisting of  $u = (u_1, u_2, u_3, u_4, u_5) \in [0, 1]^5$ ,  $x = (S^h, I_C^h, I_Z^h, I_D^h, I_K^h, I_{CZ}^h, I_{CD}^h, I_{CK}^h, R_C^h, R_Z^h, R_D^h, R_K^h, S^v, I_Z^v, I_D^v, I_K^v)$ , and  $f(t, x, u)$  the right hand of (17) which is given by

$$\begin{aligned} f(t, x, u) = & \left( \begin{aligned} & \Psi^h - \left( \frac{(1-u_1)\beta_1 I_C^h}{\mathcal{N}^h} + \frac{(1-u_2)\beta_2 (I_Z^h + I_{CZ}^h) + (1-u_3)\beta_2^h I_Z^v}{\mathcal{N}^h} + \frac{(1-u_4)\beta_3^h I_D^v}{\mathcal{N}^h} + \frac{(1-u_5)\beta_4^h I_K^v}{\mathcal{N}^h} + \vartheta^h \right) S^h \\ & \frac{(1-u_1)\beta_1 I_C^h}{\mathcal{N}^h} (S^h + R_C^h + R_Z^h + R_D^h + R_K^h) - (\eta_C + \zeta_C + \vartheta^h) I_C^h - \frac{(1-u_2)\beta_2 (I_Z^h + I_{CZ}^h) + (1-u_3)\beta_2^h I_Z^v}{\mathcal{N}^h} I_C^h \dots \\ & - \frac{(1-u_4)\beta_3^h I_D^v}{\mathcal{N}^h} I_C^h - \frac{(1-u_5)\beta_4^h I_K^v}{\mathcal{N}^h} I_C^h + \zeta_Z I_{CZ}^h + \zeta_D I_{CD}^h + \zeta_K I_{CK}^h \\ & \frac{(1-u_2)\beta_2 (I_Z^h + I_{CZ}^h) + (1-u_3)\beta_2^h I_Z^v}{\mathcal{N}^h} (S^h + R_C^h + R_Z^h + R_D^h + R_K^h) - (\eta_Z + \zeta_Z + \vartheta^h) I_Z^h - \frac{(1-u_1)\beta_1 I_C^h}{\mathcal{N}^h} I_Z^h + \zeta_C I_{CZ}^h \\ & \frac{(1-u_4)\beta_3^h I_D^v}{\mathcal{N}^h} (S^h + R_C^h + R_Z^h + R_D^h + R_K^h) - (\eta_D + \zeta_D + \vartheta^h) I_D^h - \frac{(1-u_1)\beta_1 I_C^h}{\mathcal{N}^h} I_D^h + \zeta_C I_{CD}^h \\ & \frac{(1-u_5)\beta_4^h I_K^v}{\mathcal{N}^h} (S^h + R_C^h + R_Z^h + R_D^h + R_K^h) - (\eta_K + \zeta_K + \vartheta^h) I_K^h - \frac{(1-u_1)\beta_1 I_C^h}{\mathcal{N}^h} I_K^h + \zeta_C I_{CK}^h \\ & \frac{(1-u_2)\beta_2 (I_Z^h + I_{CZ}^h) + (1-u_3)\beta_2^h I_Z^v}{\mathcal{N}^h} I_C^h + \frac{(1-u_1)\beta_1 I_C^h}{\mathcal{N}^h} I_Z^h - (\eta_C + \eta_Z + \zeta_C + \zeta_Z + \vartheta^h) I_{CZ}^h \\ & \frac{(1-u_4)\beta_3^h I_D^v}{\mathcal{N}^h} I_C^h + \frac{(1-u_1)\beta_1 I_C^h}{\mathcal{N}^h} I_D^h - (\eta_C + \eta_D + \zeta_C + \zeta_D + \vartheta^h) I_{CD}^h \\ & \frac{(1-u_5)\beta_4^h I_K^v}{\mathcal{N}^h} I_C^h + \frac{(1-u_1)\beta_1 I_C^h}{\mathcal{N}^h} I_K^h - (\eta_C + \eta_K + \zeta_C + \zeta_K + \vartheta^h) I_{CK}^h \\ & \zeta_C I_C^h - \left( \vartheta^h + \frac{(1-u_1)\beta_1 I_C^h}{\mathcal{N}^h} + \frac{(1-u_2)\beta_2 (I_Z^h + I_{CZ}^h) + (1-u_3)\beta_2^h I_Z^v}{\mathcal{N}^h} + \frac{(1-u_4)\beta_3^h I_D^v}{\mathcal{N}^h} + \frac{(1-u_5)\beta_4^h I_K^v}{\mathcal{N}^h} \right) R_C^h \\ & \zeta_Z I_Z^h - \left( \vartheta^h + \frac{(1-u_1)\beta_1 I_C^h}{\mathcal{N}^h} + \frac{(1-u_2)\beta_2 (I_Z^h + I_{CZ}^h) + (1-u_3)\beta_2^h I_Z^v}{\mathcal{N}^h} + \frac{(1-u_4)\beta_3^h I_D^v}{\mathcal{N}^h} + \frac{(1-u_5)\beta_4^h I_K^v}{\mathcal{N}^h} \right) R_Z^h \\ & \zeta_D I_D^h - \left( \vartheta^h + \frac{(1-u_1)\beta_1 I_C^h}{\mathcal{N}^h} + \frac{(1-u_2)\beta_2 (I_Z^h + I_{CZ}^h) + (1-u_3)\beta_2^h I_Z^v}{\mathcal{N}^h} + \frac{(1-u_4)\beta_3^h I_D^v}{\mathcal{N}^h} + \frac{(1-u_5)\beta_4^h I_K^v}{\mathcal{N}^h} \right) R_D^h \\ & \zeta_K I_K^h - \left( \vartheta^h + \frac{(1-u_1)\beta_1 I_C^h}{\mathcal{N}^h} + \frac{(1-u_2)\beta_2 (I_Z^h + I_{CZ}^h) + (1-u_3)\beta_2^h I_Z^v}{\mathcal{N}^h} + \frac{(1-u_4)\beta_3^h I_D^v}{\mathcal{N}^h} + \frac{(1-u_5)\beta_4^h I_K^v}{\mathcal{N}^h} \right) R_K^h \\ & \Psi^v - \left( \frac{(1-u_3)\beta_2^v (I_Z^h + I_{CZ}^h)}{\mathcal{N}^h} + \frac{(1-u_4)\beta_3^v (I_D^h + I_{CD}^h)}{\mathcal{N}^h} + \frac{(1-u_5)\beta_4^v (I_K^h + I_{CK}^h)}{\mathcal{N}^h} + \vartheta^v \right) S^v \\ & \frac{(1-u_3)\beta_2^v (I_Z^h + I_{CZ}^h)}{\mathcal{N}^h} S^v - \vartheta^v I_Z^v \\ & \frac{(1-u_4)\beta_3^v (I_D^h + I_{CD}^h)}{\mathcal{N}^h} S^v - \vartheta^v I_D^v \\ & \frac{(1-u_5)\beta_4^v (I_K^h + I_{CK}^h)}{\mathcal{N}^h} S^v - \vartheta^v I_K^v \end{aligned} \right). \quad (B1) \end{aligned}$$

To prove Theorem 6, we proceed as follows:

- (i) Note that  $U$  is convex. Consider any two arbitrary elements  $v, w \in U$ , where  $v = (v_1, v_2, v_3, v_4, v_5)$ ,  $w = (w_1, w_2, w_3, w_4, w_5)$ . Then,

$$\lambda v + (1 - \lambda)w \in U, \quad \forall \lambda \in [0, 1].$$

That is,  $\lambda v + (1 - \lambda)w \in U$ , and hence  $U$  is a convex set.

- (ii) The control system (17) can be expressed as a linear function of control variables  $(u_1, u_2, u_3, u_4, u_5)$  with the coefficients as functions of time and state variables:

$$f(t, x, u) = \vartheta(t, x) + \phi(t, x)u,$$

with

$$\vartheta(t, x) = \left( \begin{array}{l} \Psi^h - \left( \frac{\beta_1 I_C^h}{\mathcal{N}^h} + \frac{\beta_2(I_Z^h + I_{CZ}^h) + \beta_2^h I_Z^v}{\mathcal{N}^h} + \frac{\beta_3^h I_D^v}{\mathcal{N}^h} + \frac{\beta_4^h I_K^v}{\mathcal{N}^h} + \vartheta^h \right) S^h \\ \frac{\beta_1 I_C^h}{\mathcal{N}^h} (S^h + R_C^h + R_Z^h + R_D^h + R_K^h) - (\eta_C + \zeta_C + \vartheta^h) I_C^h - \frac{\beta_2(I_Z^h + I_{CZ}^h) + \beta_2^h I_Z^v}{\mathcal{N}^h} I_C^h \dots \\ - \frac{\beta_3^h I_D^v}{\mathcal{N}^h} I_C^h - \frac{\beta_4^h I_K^v}{\mathcal{N}^h} I_C^h + \zeta_Z I_{CZ}^h + \zeta_D I_{CD}^h + \zeta_K I_{CK}^h \\ \frac{\beta_2(I_Z^h + I_{CZ}^h) + \beta_2^h I_Z^v}{\mathcal{N}^h} (S^h + R_C^h + R_Z^h + R_D^h + R_K^h) - (\eta_Z + \zeta_Z + \vartheta^h) I_Z^h - \frac{\beta_1 I_C^h}{\mathcal{N}^h} I_Z^h + \zeta_C I_{CZ}^h \\ \frac{\beta_3^h I_D^v}{\mathcal{N}^h} (S^h + R_C^h + R_Z^h + R_D^h + R_K^h) - (\eta_D + \zeta_D + \vartheta^h) I_D^h - \frac{\beta_1 I_C^h}{\mathcal{N}^h} I_D^h + \zeta_C I_{CD}^h \\ \frac{\beta_4^h I_K^v}{\mathcal{N}^h} (S^h + R_C^h + R_Z^h + R_D^h + R_K^h) - (\eta_K + \zeta_K + \vartheta^h) I_K^h - \frac{\beta_1 I_C^h}{\mathcal{N}^h} I_K^h + \zeta_C I_{CK}^h \\ \frac{\beta_2(I_Z^h + I_{CZ}^h) + \beta_2^h I_Z^v}{\mathcal{N}^h} I_C^h + \frac{\beta_1 I_C^h}{\mathcal{N}^h} I_Z^h - (\eta_C + \eta_Z + \zeta_C + \zeta_Z + \vartheta^h) I_{CZ}^h \\ \frac{\beta_3^h I_D^v}{\mathcal{N}^h} I_C^h + \frac{\beta_1 I_C^h}{\mathcal{N}^h} I_D^h - (\eta_C + \eta_D + \zeta_C + \zeta_D + \vartheta^h) I_{CD}^h \\ \frac{\beta_4^h I_K^v}{\mathcal{N}^h} I_C^h + \frac{\beta_1 I_C^h}{\mathcal{N}^h} I_K^h - (\eta_C + \eta_K + \zeta_C + \zeta_K + \vartheta^h) I_{CK}^h \\ \zeta_C I_C^h - \left( \vartheta^h + \frac{\beta_1 I_C^h}{\mathcal{N}^h} + \frac{\beta_2(I_Z^h + I_{CZ}^h) + \beta_2^h I_Z^v}{\mathcal{N}^h} + \frac{\beta_3^h I_D^v}{\mathcal{N}^h} + \frac{\beta_4^h I_K^v}{\mathcal{N}^h} \right) R_C^h \\ \zeta_Z I_Z^h - \left( \vartheta^h + \frac{\beta_1 I_C^h}{\mathcal{N}^h} + \frac{\beta_2(I_Z^h + I_{CZ}^h) + \beta_2^h I_Z^v}{\mathcal{N}^h} + \frac{\beta_3^h I_D^v}{\mathcal{N}^h} + \frac{\beta_4^h I_K^v}{\mathcal{N}^h} \right) R_Z^h \\ \zeta_D I_D^h - \left( \vartheta^h + \frac{\beta_1 I_C^h}{\mathcal{N}^h} + \frac{\beta_2(I_Z^h + I_{CZ}^h) + \beta_2^h I_Z^v}{\mathcal{N}^h} + \frac{\beta_3^h I_D^v}{\mathcal{N}^h} + \frac{\beta_4^h I_K^v}{\mathcal{N}^h} \right) R_D^h \\ \zeta_K I_K^h - \left( \vartheta^h + \frac{\beta_1 I_C^h}{\mathcal{N}^h} + \frac{\beta_2(I_Z^h + I_{CZ}^h) + \beta_2^h I_Z^v}{\mathcal{N}^h} + \frac{\beta_3^h I_D^v}{\mathcal{N}^h} + \frac{\beta_4^h I_K^v}{\mathcal{N}^h} \right) R_K^h \\ \Psi^v - \left( \frac{\beta_2^v(I_Z^h + I_{CZ}^h)}{\mathcal{N}^h} + \frac{\beta_3^v(I_D^h + I_{CD}^h)}{\mathcal{N}^h} + \frac{\beta_4^v(I_K^h + I_{CK}^h)}{\mathcal{N}^h} + \vartheta^v \right) S^v \\ \frac{\beta_2^v(I_Z^h + I_{CZ}^h)}{\mathcal{N}^h} S^v - \vartheta^v I_Z^v \\ \frac{\beta_3^v(I_D^h + I_{CD}^h)}{\mathcal{N}^h} S^v - \vartheta^v I_D^v \\ \frac{\beta_4^v(I_K^h + I_{CK}^h)}{\mathcal{N}^h} S^v - \vartheta^v I_K^v \end{array} \right),$$

$$\phi(t, x) = \begin{pmatrix} \frac{\beta_1 I_C^h}{N^h} & \frac{\beta_2(I_Z^h + I_{CZ}^h)}{N^h} & \frac{\beta_2^h I_Z^v}{N^h} & \frac{\beta_3^h I_D^v}{N^h} & \frac{\beta_4^h I_K^v}{N^h} \\ -\frac{\beta_1 I_C^h}{N^h} \Psi & \frac{\beta_2(I_Z^h + I_{CZ}^h)}{N^h} & \frac{\beta_2^h I_Z^v}{N^h} I_C^h & \frac{\beta_3^h I_D^v}{N^h} I_C^h & \frac{\beta_4^h I_K^v}{N^h} I_C^h \\ \frac{\beta_1 I_C^h}{N^h} I_Z^h & -\frac{\beta_2(I_Z^h + I_{CZ}^h)}{N^h} \Psi & -\frac{\beta_2^h I_Z^v}{N^h} \Psi & 0 & 0 \\ \frac{\beta_1 I_C^h}{N^h} I_D^h & 0 & 0 & -\frac{\beta_3^h I_D^v}{N^h} \Psi & 0 \\ \frac{\beta_1 I_C^h}{N^h} I_K^h & 0 & 0 & 0 & -\frac{\beta_4^h I_K^v}{N^h} \Psi \\ -\frac{\beta_1 I_C^h}{N^h} I_Z^h & -\frac{\beta_2(I_Z^h + I_{CZ}^h)}{N^h} I_C^h & -\frac{\beta_2^h I_Z^v}{N^h} I_C^h & 0 & 0 \\ -\frac{\beta_1 I_C^h}{N^h} I_D^h & 0 & 0 & -\frac{\beta_3^h I_D^v}{N^h} I_C^h & 0 \\ -\frac{\beta_1 I_C^h}{N^h} I_K^h & 0 & 0 & 0 & -\frac{\beta_4^h I_K^v}{N^h} I_C^h \\ \frac{\beta_1 I_C^h}{N^h} R_C^h & \frac{\beta_2(I_Z^h + I_{CZ}^h)}{N^h} R_C^h & \frac{\beta_2^h I_Z^v}{N^h} R_C^h & \frac{\beta_3^h I_D^v}{N^h} R_C^h & \frac{\beta_4^h I_K^v}{N^h} R_C^h \\ \frac{\beta_1 I_C^h}{N^h} R_Z^h & \frac{\beta_2(I_Z^h + I_{CZ}^h)}{N^h} R_Z^h & \frac{\beta_2^h I_Z^v}{N^h} R_Z^h & \frac{\beta_3^h I_D^v}{N^h} R_Z^h & \frac{\beta_4^h I_K^v}{N^h} R_Z^h \\ \frac{\beta_1 I_C^h}{N^h} R_D^h & \frac{\beta_2(I_Z^h + I_{CZ}^h)}{N^h} R_D^h & \frac{\beta_2^h I_Z^v}{N^h} R_D^h & \frac{\beta_3^h I_D^v}{N^h} R_D^h & \frac{\beta_4^h I_K^v}{N^h} R_D^h \\ \frac{\beta_1 I_C^h}{N^h} R_K^h & \frac{\beta_2(I_Z^h + I_{CZ}^h)}{N^h} R_K^h & \frac{\beta_2^h I_Z^v}{N^h} R_K^h & \frac{\beta_3^h I_D^v}{N^h} R_K^h & \frac{\beta_4^h I_K^v}{N^h} R_K^h \\ 0 & 0 & \frac{\beta_2^v(I_Z^h + I_{CZ}^h)}{N^h} S^v & \frac{\beta_3^v(I_D^h + I_{CD}^h)}{N^h} S^v & \frac{\beta_4^v(I_K^h + I_{CK}^h)}{N^h} S^v \\ 0 & 0 & -\frac{\beta_2^v(I_Z^h + I_{CZ}^h)}{N^h} S^v & 0 & 0 \\ 0 & 0 & 0 & -\frac{\beta_3^v(I_D^h + I_{CD}^h)}{N^h} S^v & 0 \\ 0 & 0 & 0 & 0 & -\frac{\beta_4^v(I_K^h + I_{CK}^h)}{N^h} S^v \end{pmatrix},$$

where  $\Psi = (S^h + R_C^h + R_Z^h + R_D^h + R_K^h)$ .

As the parameters and variables of the model are positive, we have

$$\begin{aligned} \|f(t, x, u)\| &\leq \|\vartheta(t, x)\| + \|\phi(t, x)\| \|u\| \\ &\leq a + b\|u\|, \quad \text{where } a > 0, b > 0. \end{aligned}$$

(iii) The optimal control problem's Lagrangian is given by

$$\mathcal{L} = I_C^h(t) + I_Z^h(t) + I_D^h(t) + I_K^h(t) + I_{CZ}^h(t) + I_{CD}^h(t) + I_{CK}^h(t) + I_{CZ}^h(t) + I_Z^v(t) + I_D^v(t) + I_K^v(t) + \frac{1}{2} \sum_{i=1}^5 \xi_i u_i^2. \tag{B2}$$

Let us consider two arbitrary elements  $v, w \in U$ , with  $v = (v_1, v_2, v_3, v_4, v_5)$ ,  $w = (w_1, w_2, w_3, w_4, w_5)$ . and  $\lambda \in [0, 1]$ . We now show that

$$\mathcal{L}[t, x, (1 - \lambda)v + \lambda w] \leq (1 - \lambda)\mathcal{L}(t, x, v) + \lambda\mathcal{L}(t, x, w).$$

It follows from (B2) that,

$$\begin{aligned} \mathcal{L}[t, x, (1 - \lambda)v + \lambda w] &= I_C^h(t) + I_Z^h(t) + I_D^h(t) + I_K^h(t) + I_{CZ}^h(t) + I_{CD}^h(t) \\ &\quad + I_{CK}^h(t) + I_{CZ}^h(t) + I_Z^v(t) + I_D^v(t) + I_K^v(t) \\ &\quad + \frac{1}{2} \sum_{i=1}^5 \xi_i [(1 - \lambda)u_i + \lambda w_i]^2, \\ (1 - \lambda)\mathcal{L}(t, x, v) + \lambda\mathcal{L}(t, x, w) &= I_C^h(t) + I_Z^h(t) + I_D^h(t) + I_K^h(t) + I_{CZ}^h(t) + I_{CD}^h(t) \\ &\quad + I_{CK}^h(t) + I_{CZ}^h(t) + I_Z^v(t) + I_D^v(t) + I_K^v(t) \\ &\quad + \frac{1}{2} (1 - \lambda) \sum_{i=1}^5 \xi_i v_i^2 + \frac{1}{2} \lambda \sum_{i=1}^4 \xi_i w_i^2. \end{aligned} \tag{B3}$$

Taking the difference of the two equations given above, we have

$$\mathcal{L}[t, x, (1 - \lambda)v + \lambda w] - [(1 - \lambda)\mathcal{L}(t, x, v) + \lambda\mathcal{L}(t, x, w)] = \frac{1}{2}(\lambda^2 - \lambda)\sum_{i=1}^5 \xi_i (v_i - w_i)^2 \leq 0, \text{ since } \lambda \in [0, u_{\max}]. \quad (\text{B4})$$

Thus, we obtain that

$$\mathcal{L}[t, x, (1 - \lambda)v + \lambda w] \leq [(1 - \lambda)\mathcal{L}(t, x, v) + \lambda\mathcal{L}(t, x, w)],$$

which can be written as:

$$\mathcal{L}[t, x, (1 - \lambda)v + \lambda w] - [(1 - \lambda)\mathcal{L}(t, x, v) + \lambda\mathcal{L}(t, x, w)] \leq 0,$$

and hence the convexity of  $\mathcal{L}$  is proved.

- (iv) There exists constants  $\varpi_1, \varpi_2$  and  $\varpi_3$  such that,  $\mathcal{L} \geq \varpi_1 |u|^{\varpi_3} - \varpi_2$ ,  $\varpi_1 > 0$ ,  $\varpi_2 > 0$ ,  $\varpi_3 > 1$ . We now establish the bound on  $\mathcal{L}$ . Note that  $\zeta_5 u_5^2 \leq \zeta_5$ . As  $u_5 \in [0, 1]$ ,  $\frac{1}{2}\zeta_5 u_5^2 \leq \frac{1}{2}\zeta_5$ . So,

$$\begin{aligned} \mathcal{L} &> \frac{\xi_1}{2} u_1^2 + \frac{\xi_2}{2} u_2^2 + \frac{\xi_3}{2} u_3^2 + \frac{\xi_4}{2} u_4^2 + \frac{\xi_5}{2} u_5^2 \\ &\geq \frac{\xi_1}{2} u_1^2 + \frac{\xi_2}{2} u_2^2 + \frac{\xi_3}{2} u_3^2 + \frac{\xi_4}{2} u_4^2 + \frac{\xi_5}{2} u_5^2 - \frac{\xi_5}{2} \\ &\geq \min \left( \frac{\xi_1}{2}, \frac{\xi_2}{2}, \frac{\xi_3}{2}, \frac{\xi_4}{2}, \frac{\xi_5}{2} \right) (u_1^2 + u_2^2 + u_3^2 + u_4^2 + u_5^2) - \frac{\xi_5}{2} \\ &\geq \min \left( \frac{\xi_1}{2}, \frac{\xi_2}{2}, \frac{\xi_3}{2}, \frac{\xi_4}{2}, \frac{\xi_5}{2} \right) |u_1, u_2, u_3, u_4, u_5|^2 - \frac{\xi_5}{2}. \end{aligned}$$

Hence,

$$\mathcal{L} \geq \varpi_1 |u|^{\varpi_3} - \varpi_2, \quad \text{where } \varpi_1 = \min \left( \frac{\xi_1}{2}, \frac{\xi_2}{2}, \frac{\xi_3}{2}, \frac{\xi_4}{2}, \frac{\xi_5}{2} \right) > 0, \quad \varpi_2 = \frac{\xi_5}{2} > 0, \quad \text{and } \varpi_3 = 2 > 1.$$

### APPENDIX C. MATLAB CODE FOR PARAMETER ESTIMATION

For the MATLAB code used for the model fitting and parameter estimation, see the supplementary document.